VNIVERSITAT DE VALÈNCIA

PhD program in Biomedicine and Biotechnology

Bioengineering strategies of the uterus towards improving current investigative models and female reproductive health

Author:

Hannes Marcus Jeff Campo

Supervised by:

Dr. Irene Cervelló Alcaraz

Prof. Antonio Pellicer Martínez

Valencia, September 2018

VNIVERSITAT DE VALÈNCIA

Dra. Irene Cervelló Alcaraz, Doctora en Biología, Investigadora principal del área de Células Madre y Bioingeniería en Fundación IVI (FIVI) y Coordinadora del laboratorio de FIVI.

CERTIFICA:

Que el trabajo de investigación titulado: "**Bioengineering strategies of the uterus towards improving current investigative models and female reproductive health**" ha sido realizado íntegramente por Hannes Marcus Jeff Campo bajo mi dirección. Dicha memoria está concluida y reúne todos los requisitos para su presentación y defensa como TESIS DOCTORAL ante un tribunal.

Y para que así conste a los efectos oportunos, firmo la presente certificación en Valencia a 18 de septiembre de 2018.

Fdo. Dra. Irene Cervelló Alcaraz

VNIVERSITAT DE VALÈNCIA

Prof. Antonio Pellicer Martínez, Catedrático en Ginecología, Doctor en Medicina y Cirugía, Profesor titular del Departamento de Pediatría, Obstetricia y Ginecología de la Facultad de Medicina de la Universidad de Valencia, fundador del Instituto Valenciano de Infertilidad y presidente de la Fundación IVI.

CERTIFICO:

Que el trabajo de investigación titulado: "**Bioengineering strategies of the uterus towards improving current investigative models and female reproductive health**" ha sido realizado íntegramente por Hannes Marcus Jeff Campo bajo mi dirección. Dicha memoria está concluida y reúne todos los requisitos para su presentación y defensa como TESIS DOCTORAL ante un tribunal.

Y para que así conste a los efectos oportunos, firmo la presente certificación en Valencia a 18 de septiembre de 2018.

Fdo. Dr. Antonio Pellicer Martínez

ACKNOWLEDGEMENTS

At long last I find myself here, on the verge of concluding a chapter in my life that I never thought I would experience. These years flew by in a heartbeat. I initially arrived in Valencia for a short internship, to breathe in new air and to learn new things in a highly regarded laboratory. That was 5 years ago.

Writing a thesis is, in the first place, an exercise in sustained suffering; being plagued by insecurity, doubt, endlessly repeating experiments thinking you did it right only to be proven otherwise, growing through the frustrations, learning from it and continue. This made me grow on both a scientific and personal level. Not only did I learn a lot inside the lab but also outside, picking up a new language, culture and way of life, making friends from all around the world and incorporating all this into my personality.

While attempting the ungrateful and impossible task of thanking everyone that helped making this an experience I will never forget, I will try to recreate the headache-inducing mixtures of languages that was part of this multinational/multilingual thesis experience. I hope that the readers of these agradecimientos will have a taste of what this implies and even maybe get as confused as I was in the beginning of this adventure.

It goes without saying that this thesis wouldn't have been possible without my directors: Premièrement Irene, je te remercie avec tout mon coeur de croire en moi, et de croire en mes capacités plus que je faisais moi. C'était une grande aventure avec des hauts et des bas mais chaque moment valait la peine. Je suis fier de voir en rétrospective notre trajet, où on a commencé et où on est maintenant. Merci beaucoup de me montrer ce domaine scientifique passionnant et de me guider dans cette thèse. También me gustaría agradecer a mi antiguo director de tesis Dr. Carlos Simón, por tener la visión científica de ver el valor en este campo de investigación dentro de la medicina reproductiva, y por supuesto, por su ayuda y sus consejos. Me hubiera gustado ver el resultado de este estudio contigo, pero es una pena que esto no haya sido posible. Por último, me gustaría dar la gracias a Dr. Antonio Pellicer por recibir a este estudiante huérfano, y darme la posibilidad de seguir y reenfocar este estudio tan prometedor.

La mayoría del trabajo se ha realizado en los laboratorios de fundación IVI, donde he tenido el placer de trabajar con los compañeros más increíbles que he visto en mi vida. Tras todas las dificultades siempre ha sido un lugar agradable para venir a trabajar y esto es solo gracias a vosotros. Habéis españolizado a este guiri, sois los mejores.

Gracias Nuria, Mi esposa andalu y compañera de grupo por compartir muchas de las preocupaciones diarias del laboratorio. Vendré a visitarte pronto para que me enseñes las cosas maravillosas de tu país. Grazie alle mie bellissime e pazze ragazze italiane Alessia e Stefania per essere le mie complici straniere in laboratorio. Stefy, grazie per essere la persona con la quale posso parlare sempre quando ho bisogno, noi due vediamo la vita e la scienza nello stesso modo e io sono sicuro che le nostre strade si incroceranno di nuovo in futuro. Gracias a Amparo por enseñarme tantas cosas. Gracias a los del laboratorio que ya llevan mucho tiempo: Silvia mi africana favorita, Ana Corachan y Ana Buigues. Pero también a los que conocemos desde hace poco: Sara, Lucia, Roberto, Luismi y Mª Jose. Gracias a mis amigos frikis por las discusiones interesantes durante la comida: Marcos, Jose, Alejandro, Alfredo, Pablo, Almudena y los demás, gracias por no dejarme comer solo, aun sabiendo que era demasiado temprano para los españoles.

Aunque ya no está en FIVI, gracias a Sebas, mi primer profesor de español, por enseñarme los principios importantes del idioma y detalles esenciales de la cultura española, desde carajillos hasta el futbol. Gràcies a les meues profesores de valencià Amparo i Patricia per ensenyar-me el valencià tradicional i vocabulari que mai podria utilitzar en aquestos agraïments per raons obvies (excepte “senyor piroctècnic” i “pot començar la mascletà”).

También gracias al restos de fundación que no quiero olvidar de mencionar: Mi hermana Sonia, Horten, Paco, Patricia, Alicia.

This thesis would be only a fraction of what it has become without the fruitful collaborations and constructive interactions with other experts and labs. Obrigada Pedro, por nos guiares com a tua experiência e conhecimento no campo da engenharia de tecidos, e por teres sido uma mão amiga desde o princípio. Não só apenas aprendi muito no teu laboratório, como também da tua visão e conselhos. É com alegria que te considero como um amigo.

En segon lloc, m’agradaria donar les gràcies al laboratori de Biotecnologia de la Reproducció de la UPV. Especialment, a Francisco Jiménez, qui a més d’haver-me donat l’oportunitat d’apendre moltes coses al seu laboratori, ha contribuït de forma relevant en aquesta investigació. Ximo, moltes gràcies pel teu incondicional suport. Després de tant de

temps i esforç per fi podem estar orgullosos dels resultats. Ha sigut un gran plaer treballar mà a mà amb un amic.

To all my friends outside of the lab, thanks for the necessary distractions for this overthinking mind of mine. Paco, you are the Turk to my J.D. and we had more fun and adventures than I can remember. I didn't know it was possible to have so much in common with someone who grew up at the other side of the planet. For all my life, I thought I have only one sibling, but here in Valencia I found my brother. Also special thanks to Ivan, Ester, Nick and Sara and the rest of the Pla family, without you guys I wouldn't have had half as much fun as it was. I will feel as an honorary Pla forever and will hopefully crash your family parties for a long time to come. Bob, ouwe rakker, ook al ben je de nieuwste additie in onze illustere Valenciaanse groep, ben je in korte tijd een van mijn beste vrienden hier geworden.

Köszönöm szépen Boginak, az én magyar hercegnőmnek, hogy végigküzdötted velem ezt az időszakot. Amióta megismertelek itt Valenciában, az életem fenekestül felfordult. A támogatásod, szereteted és törődésed sokat számított, nélküled nem tudtam volna végigcsinálni.

Gracias a Felix, Irving, Fabricio, Yuku y Cristian, que conozco desde mi primer año en valencia por las ideas malas y buenos momentos compartidos. También un grand merci aan mijn Belgische Valencianen Germain en Leti.

Ik ben ook enorm dankbaar aan al mijn vrienden uit België om de ±1700 km tussen ons niet onze vriendschap te laten aantasten. Jullie zijn me elk minstens 2 keer komen bezoeken. Ik heb geluk om jullie als vrienden te hebben. Furie, Harald, Reinout en Geert, merci voor de toffe trips. Dank u Boone en Basic voor de slaapplaats in Leuven en de steunberichtjes op tijd en stond. Free, om de Belgische scientific liason te zijn alsook de tweelingsbroer dat ik nooit heb gehad. Dank u Stabel voor de motivation Mondays, ik had ze vaker nodig dan ik dacht.

Last but not least moet ik mijn familie bedanken en voornamelijk mijn zus, mama en papa. Zonder jullie was niets van dit mogelijk. Mama, dank u om de beste moeder en meest zorgzame persoon te zijn die ik ken. Pa, zonder jou had ik nooit de stap naar Valencia gezet, en zonder jouw advies zou ik nergens staan. Charly, thanks for being my partner in crime. Samen kunnen we elke tegenslag aan en er zelfs bovenuit stijgen. Jullie allemaal hebben mij stap voor stap gedragen tot waar ik nu sta en ervoor gezorgd dat ik de persoon ben geworden dat ik nu ben. Jullie raad, advies, crisisoplossend vermogen hebben dit bewerkstelligd. Het is onmoglijk om jullie aandeel in dit hele gebeuren recht aan te doen in zulke korte tekst.

Een lange tijd geleden zeiden jullie tegen mij “plus est en vous”, maar dat was enkel mogelijk dankzij jullie drie. This was 100% a team effort.

Sadly, it is impossible to name everyone that helped making these last 5 years the craziest and most fulfilling years in my life. Therefore, I will just end by saying for one last time to you all: dank u, merci, gracias, köszönöm, gràcies, grazie, thank you.

Hannes

El presente trabajo de tesis doctoral ha sido realizado en parte en los laboratorios de la Fundación IVI, el laboratorio de Bioingeniería de Órganos y Medicina Regenerativa del Instituto de Investigación Sanitaria de Aragón y también en el laboratorio de Biotecnología de la Reproducción de la Universitat Politècnica de València.

Gracias a la ayuda de un proyecto de investigación con la Universidad de Valencia en la Facultad de Medicina, Departamento de Pediatría, Obstetricia y Ginecología que ha sido financiado por la ayuda PROMETEO de la Generalitat Valenciana para la realización de proyectos I+D para grupos de investigación (PROMETEOII/2013/018), por el programa Santiago Grisolía de la Generalitat Valenciana para la formación de personal investigador, en centros de investigación de la Comunitat Valenciana (GRISOLIA/2015/002).

RESUMEN

INTRODUCCIÓN

Sistema reproductor femenino: el útero y el endometrio

El desarrollo completo de la producción de células germinales femeninas, la fecundación, la implantación de embriones y el embarazo hasta el parto tiene lugar dentro del sistema reproductor femenino. Los principales órganos responsables de estos procesos se encuentran en los genitales internos, que están constituidos por los ovarios, las trompas de Falopio, el útero y la vagina.

El útero es el órgano más grande del sistema reproductor femenino. Este órgano hueco, muscular, con forma de pera, evacuará el óvulo no fecundado durante el ciclo menstrual o proporcionará nutrición y soporte al embrión en crecimiento (en caso de fecundación) hasta el nacimiento. El útero humano es de forma simple, lo que significa que está fusionado en un solo órgano. Otras formas de útero de mamífero incluyen diferentes morfologías como la anatomía dúplex (conejo, ratón y rata) y la anatomía bicorne (perro y cerdo). La pared uterina consta de tres capas: el perimetrio externo, el miometrio medio y el endometrio luminal. El endometrio es la capa mucosa que recubre el interior del útero crucial para la implantación y desarrollo del embrión. A nivel celular, se puede distinguir un compartimento de células epiteliales, estromales, vasculares e inmunes dentro del endometrio. Estas células están situadas en las dos capas principales del endometrio, denominadas estrato basal y estrato funcional. La capa funcional, que es la parte más gruesa del endometrio, abarca dos tercios de este tejido y es extremadamente sensible a los esteroides. Esta capa transitoria se prepara para la implantación del blastocisto y en cada ciclo menstrual sufre proliferación, secreción y degeneración en respuesta a señales hormonales. Sin embargo, la capa basal es la única parte del endometrio que permanece intacta después de la menstruación, a partir de la cual se regenera la capa funcional. Esta capa no sufre cambios significativos y contiene la base de las glándulas y la vasculatura, a partir de la cual el ciclo de regeneración endometrial puede comenzar de nuevo.

En humanos y primates superiores, este tejido altamente dinámico se desprende y se regenera en respuesta a las hormonas sexuales femeninas durante cada ciclo menstrual. El ciclo menstrual es el resultado de una interacción compleja y sincronizada entre el hipotálamo, la glándula pituitaria anterior y el ovario y endometrio, repitiéndose de 400 a 500 veces durante toda la vida reproductiva. El hipotálamo estimula las células glandulares de la hipófisis anterior al producir la hormona liberadora de gonadotropinas. A su vez, produce la hormona luteinizante y la hormona foliculoestimulante. Estas hormonas permiten que el ovario produzca los esteroides sexuales responsables de las 3 principales fases de desarrollo del endometrio: menstrual, proliferativa y secretora. El primer día del ciclo menstrual coincide con el primer día de la menstruación. Después del desprendimiento o descamación del endometrio acompañado de hemorragia, se produce la reepitelización. A esta fase le sigue la fase proliferativa, la cual corresponde a la fase folicular ovárica hasta la ovulación. Esta fase se caracteriza por la remodelación tisular, por la presencia de los procesos proliferativos y antiapoptóticos, y la angiogénesis. La fase secretora coincide con la fase lútea ovárica, que dura aproximadamente 14 días. El endometrio continúa engrosándose; la transformación celular principal tiene lugar en las células del estroma donde ocurre la decidualización para preparar el endometrio para la posible implantación embrionaria. Si la fecundación e implantación no se producen, el cuerpo lúteo se degrada, lo que produce diferentes procesos celulares y vasoconstricción de las arterias espirales que conducen a la menstruación.

Estos extensos cambios endometriales también se llevan a cabo en la matriz extracelular (MEC) del endometrio. El colágeno tipo I es la principal proteína estructural y con mayor abundancia. Además, está presente de manera constante durante todo el ciclo menstrual. Del mismo modo, los tipos III y IV también se distribuyen ampliamente durante todas las fases. También ha sido observado que la expresión del colágeno tipo III disminuye en relación al colágeno tipo I, especialmente durante la fase secretora media o tardía. El colágeno tipo V es un importante regulador de la fibrilogénesis del colágeno y está interactuando fuertemente con el colágeno tipo I durante la fase proliferativa. Por otro lado, está presente la fibronectina, una glicoproteína, también abundante en el endometrio humano. La Tenascina C es una glicoproteína con un alto número de tipos de ligandos diferentes; y se expresa en el estroma subepitelial durante la fase proliferativa y alrededor de las paredes de los vasos sanguíneos durante todo el ciclo, pero curiosamente está ausente durante la fase secretora media. La laminina, el colágeno tipo IV y el proteoglicano heparán sulfato son componentes importantes de la membrana basal. Éstos muestran una

localización limitada bajo las células endoteliales y epiteliales, aumentando gradualmente hasta una expresión generalizada alrededor de las células epitelioides circundantes a lo largo de la decidua madura. Otros estudios realizados en mamíferos también demuestran la naturaleza dinámica de la MEC endometrial.

Patologías uterinas que afectan al éxito reproductivo humano

Existen varias patologías uterinas que podrían solucionarse gracias a los avances realizados en el campo de ingeniería tisular en los últimos años. Y parte de esto se investiga en el presente estudio.

La infertilidad total por factor uterino (AUFI, Absolute uterine factor infertility) afecta a 1 de cada 500 mujeres durante su etapa reproductiva, aumentando este dato hasta 1,5 millones de mujeres en todo el mundo. AUFI puede provenir de orígenes congénitos o ser adquirida. La AUFI adquirida es causada entre otros por tumores uterinos malignos, miomas uterinos, adenomiosis, hemorragias postparto y adhesiones intrauterinas (Sindrome de Asherman). Las causas congénitas incluyen el síndrome de Mayer-Rokitansky-Kuster-Hauser (MRKH), la hipoplasia uterina y las malformaciones uterinas. El Síndrome de MRKH o aplasia Mulleriana afecta a 1 de cada 4000 mujeres y está descrito como la agenesia del útero y los dos tercios superiores de la vagina. La única manera de reestablecer la fertilidad en este tipo de patologías es con un trasplante uterino. La prueba de concepto fue realizada recientemente por el grupo de Brännström, estos investigadores lograron por primera vez el nacimiento de un bebé después del trasplante de útero.

La atrofia endometrial es una patología en la cual el endometrio nunca crece más de 7 mm y está íntimamente relacionada con una disminución en la probabilidad de embarazo. Se caracteriza por un bajo crecimiento del epitelio glandular, falta de flujo sanguíneo uterino, disminución de la expresión del factor de crecimiento endotelial vascular y un desarrollo vascular deficiente. Los diferentes tratamientos proporcionados a estas pacientes pueden incluir la administración oral o vaginal de estradiol, a veces suplementado con inyección de gonadotropina coriónica humana, tamoxifeno, óxido nítrico, factor estimulante de colonias de granulocitos e incluso la terapia con células madre. En el caso del Síndrome de Asherman, el endometrio funcional está destruido debido a adhesiones intrauterinas. Dependiendo de la gravedad de las adhesiones existen posibles tratamientos, aunque ninguno de ellos altamente efectivo que incluyen la histerotomía, la dilatación y curetaje, y la cirugía histeroscópica. Una opción interesante para estas pacientes podría ser la terapia celular. En un trabajo reciente se inyectaron células madre autólogas derivadas de

la médula ósea en las arteriolas espirales del endometrio de estas pacientes y se pudo observar una mejora en el grosor del endometrio para ambas patologías endometriales (atrofia endometrial y Síndrome de Asherman).

Biomateriales e ingeniería de tejidos en reproducción

La Ingeniería de tejidos (IT) representa un prometedor campo interdisciplinario de investigación, donde se combinan aspectos que van desde el trasplante celular, la ciencia de materiales y la bioingeniería. El objetivo original de la IT, definido primeramente por Langer y Vacanti, fue restaurar, mantener o mejorar la función de los tejidos o de los órganos completos. Sin embargo, la ingeniería tisular también se ha convertido en una opción viable para las pruebas con diferentes agentes terapéuticos, el control y conocimiento de enfermedades y la medicina de precisión (aplicaciones *in vitro*). Lo que distingue a la IT es el posible uso de biomateriales, que pueden implantarse directamente en el paciente con o sin células, o incubarse en biorreactores donde se someten a estímulos mecánicos o químicos que dan como resultado una réplica del órgano *in vitro*. Estos biomateriales o biomoldes son dispositivos o construcciones con complejas y específicas funciones físicas y biológicas que interactúan a través de señales bioquímicas y físicas con las células y, una vez implantados, con el ambiente corporal.

Estas funciones deben servir como un entorno físico para que las células tengan propiedades mecánicas similares a las que ocurre *in vivo*, como la rigidez y elasticidad, para proporcionar señales bioactivas que regulen la actividad celular, para secuestrar factores de crecimiento y, por último, ser degradables, de tal forma que puedan ser reemplazados por MEC nativas. Las características de estos biomateriales o biomoldes es que se pueden adaptar dependiendo de su fuente de origen y de los métodos de fabricación correspondientes, y pueden ser de origen sintético o natural. Por último, se puede obtener un tipo especial de biomolde natural a través de un proceso llamado descelularización (DC), donde las células se eliminan de su compleja MEC natural.

Los biomateriales o biomoldes sintéticos son muy valiosos en biomedicina; tienen una composición exacta conocida, una vida útil larga y se pueden producir grandes cantidades bajo condiciones controladas con muy poca variabilidad, haciéndolos más baratos y seguros que los polímeros naturales. Las desventajas que presentan son una bioactividad reducida y la posible toxicidad ocasionada por el propio biomaterial o sus productos de degradación. Los biomateriales procedentes de orígenes naturales se consideran los primeros biomateriales utilizados clínicamente y tienen varias ventajas inherentes, ya que contienen unión del ligando a receptores presentes en la MEC que dan como resultado excelentes

interacciones celulares, además de adhesión, buen crecimiento y biocompatibilidad. Además, son biodegradables y pueden ser remodelados por las células de forma nativa. Sin embargo, existen diferentes especulaciones relacionadas con una posible respuesta inmunológica y/o la transmisión de patógenos. La extracción y purificación de estos diversos compuestos también puede ser complicada, por lo que crear un biomolde homogéneo de una manera reproducible puede resultar difícil, especialmente en comparación con sus homólogos sintéticos. Además, tienen una estabilidad mecánica limitada, lo que los hace menos ideales para aplicaciones de carga. Los polímeros derivados naturalmente pueden originarse a partir de proteínas, polisacáridos o ambos.

Los biomateriales o biomoldes sólidos se fabrican a través de procesos que pueden resultar incompatibles con las células; por esta razón, la topografía superficial, la porosidad y el tamaño de los poros resulta muy importante, puesto que influye en la penetración celular, el crecimiento y las conexiones entre células. Para los modelos *in vitro* y los ensayos *in vivo* se han considerado materiales de tipo sintéticos porosos tales como la malla de vicryl, el poliéteruretano y tubos de ácido poli-L-láctico. Además, los biomateriales (nano-) fibrosos se pueden fabricar usando el método de electrospinning o electrohilado para crear un modelo 3D *in vitro* de endometrio bovino utilizando cultivos primarios de células epiteliales y estromales. La construcción resultante presentaría células estromales que liberarían fibronectina y con epitelio polarizado, siendo reactivo a la oxitocina y al ácido araquidónico o lipopolisacárido. Las esponjas de colágeno se han utilizado para estudiar la regeneración en varios modelos animales con daño uterino severo. Para ello, se incubaron con el factor de crecimiento de fibroblastos recombinante o se incubaron *in vitro* brevemente con células madre mesenquimales derivadas de médula o con células similares a las endometriales. En este sentido, se observó una mejora en la regeneración, la fertilidad y una menor formación de cicatrices, aunque se desconoce si la placentación tuvo lugar, lo que podría indicar una vascularización y anastomosis subóptimas.

Estos estudios *in vivo* muestran que es posible regenerar la pared uterina por completo empleando la ingeniería tisular, aunque de manera incorrecta. Los inconvenientes más difíciles de superar consisten en mejorar la vascularización, la placentación y la implantación de los embriones en el injerto generado a través de estos estudios. Los tejidos descelularizados, que consisten en una compleja mezcla de componentes moleculares de la MEC del útero, donde incluso se pueden obtener biomoldes acelulares vascularizados, pueden resultar realmente prometedores.

Descelularización de tejidos uterinos

El proceso de DC permite obtener la MEC nativa y utilizarla como un molde natural para la IT. Hasta hace unos años, se pensaba que la MEC actuaba únicamente como soporte celular, sin embargo, en la actualidad queda claro que se trata de una compleja mezcla no solo formada por proteínas fibrosas estructurales sino además por proteínas funcionales, glicosaminoglicanos y proteoglicanos que juegan un papel clave y fundamental en la migración, proliferación y diferenciación de las células que la envuelven. Para cada tejido y órgano, existe un intercambio bidireccional entre las células y la MEC circundante. Esta relación mutua resulta en un remodelamiento dinámico y constante de la MEC durante el estado de homeostasis o de daño en el tejido, que se denomina "reciprocidad dinámica". Esta reciprocidad dinámica conlleva la elaboración de una MEC con una composición y organización tridimensional única y dinámica para cada tejido, que permite llevar a cabo las funciones celulares tejido específicas, haciéndola un molde bioactivo ideal.

El concepto de DC se basa en la eliminación de todo el material celular de un tejido u órgano mientras se minimiza cualquier efecto adverso sobre la complejidad, la composición y la ultraestructura tridimensional de la MEC. Al eliminarse los antígenos celulares, las reacciones inflamatorias e inmunológicas perjudiciales se atenúan. Esto permite la utilización de biomateriales procedentes de fuentes alogénicas y xenogénicas.

Hasta hoy, la DC ha sido aplicada con éxito prácticamente en todos los tejidos y órganos que se han sometido a esta técnica. Esto incluye desde tejidos simples tales como vasos sanguíneos, submucosa intestinal, nervios, córnea, tendón y membrana amniótica hasta órganos complejos completos como riñón, hígado y corazón. En el ámbito de la medicina reproductiva, también se han establecido protocolos de DC para la mayor parte de los tejidos y órganos reproductivos incluido los ovarios, testículos, endometrio, útero y placenta.

El miometrio fue el primer tejido uterino a partir del cual se crearon construcciones de ingeniería de tejidos, con el fin de cultivar miocitos *in vitro* sobre un molde descelularizado miometrial. Su objetivo a largo plazo era crear un molde capaz de regenerar defectos uterinos antes de un posible embarazo de riesgo. Otros estudios compararon diferentes protocolos de DC de fragmentos uterinos usando detergentes como SDS (dodecilsulfato sódico), alta presión hidrostática (APP) o Tritón X-100. El uso de APP dió una menor cantidad de fibras de colágeno desnaturalizadas comparado con el protocolo basado en SDS, mientras que el tercer protocolo no consiguió una DC completa. Usando los fragmentos endometriales tratados con SDS, se logró dilucidar el papel de STAT3 (transductor de señal y activador de la transcripción 3) en la reconstrucción epitelial. Este proceso de regeneración

luminal demostrado aquí muestra importantes similitudes con la reparación epitelial durante la fase menstrual en humanos.

El endometrio descelularizado fue utilizado en un modelo endometrial en 3D *in vitro* que dio lugar a la proliferación endometrial celular, la expresión de receptores hormonales y la producción de factores de secreción. Sin embargo, el uso más innovador de fragmentos DC fue llevado a cabo con una nueva plataforma de microfluidos llamada EVATAR. En esta, modelos 3D de varios tejidos descelularizados fueron conectados a través de microfluidos, recreando el sistema anatómico completo del tracto reproductor femenino (ovario murino, oviducto humano, endometrio y ectocérvix) y también incluyeron hígado. Esta investigación demostró el potencial de los denominados "organs-on-a-chip" (órganos en un chip) y permitió posiblemente obtener una potente herramienta para la investigación básica y traslacional en medicina reproductiva.

Descelularización de órganos

La última y principal ventaja de los biomoldes descelularizados es la habilidad de descelularizar órganos completos por perfusión. Mediante el uso del propio sistema vascular nativo de los órganos, los agentes descelularizantes son liberados hacia todas las capas del órgano, donde las células son lisadas y eliminadas. El debris celular es entonces retirado, dejando un biomolde tridimensional acelular vascularizado. El biomolde puede entonces ser depositado en un biorreactor, donde células madre autólogas pueden ser introducidas para recrear nuevos órganos completos. Este enfoque podría ser una respuesta a los principales problemas que afectan a los trasplantes: escasez de órganos de donantes, rechazo de órganos y efectos secundarios relacionados con inmunosupresores.

El primer estudio que describe DC en órganos reproductivos completos fue publicado en 2014 y su objetivo fue el útero. La arquitectura y microvascularura de úteros proveniente de ratas fue preservado tras perfundir la arteria aorta con detergentes aniónicos (SDS), dando lugar a un molde acelular vascularizado tridimensional. Asimismo, se logró la recelularización (RC) *in vitro* tras sembrar células endometriales en esta nueva estructura y el estudio *in vivo* sugirió el prometedor uso de este biomaterial en la regeneración uterina. Otros estudios investigaron el efecto de diferentes tipos de protocolos de DC por perfusión en mayor detalle y los optimizaron para su uso en órganos reproductivos provenientes de especies de gran tamaño.

A pesar de estos esfuerzos, la RC de órganos completos y la recuperación de alguna funcionalidad *in vitro*, ya reportada en otros órganos, no ha sido aún logradas. La

bioingeniería uterina se encuentra todavía en su infancia y se requieren más estudios para poder aplicar estas técnicas para la medicina reproductiva humana. Una alternativa interesante y versátil para el uso de estos biomoldes sólidos son los hidrogeles (derivados de las propias MEC), los cuales tienen el potencial de mejorar muchos modelos actuales de investigación e incluso, de proveer opciones innovadoras para el tratamiento en pacientes.

Hidrogeles en medicina reproductiva

Los hidrogeles están constituidos por una red insoluble de polímeros hidrofílicos entrecruzados, siendo capaces de absorber miles de veces su peso seco en agua o fluidos biológicos a través de fuerzas capilares, osmóticas o de hidratación. Por este motivo, los hidrogeles se hinchan en vez de disolverse y presentan una consistencia blanda y gomosa, mimetizando la del tejido biológico y, por lo tanto, minimizando la reacción inflamatoria por parte de las células circundantes. Esta red polimérica hidratada y tridimensional es mecánicamente estable y porosa, permitiendo el transporte de nutrientes, oxígeno y productos metabólicos de desecho. Además, en función de su modo de entrecruzamiento, las células pueden incorporarse uniformemente en el entorno 3D durante la solidificación. Los hidrogeles pueden dividirse en sólidos, semisólidos y líquidos. Cuando los hidrogeles líquidos son inyectados en el sitio de interés, se forma un gel que se adapta perfectamente a su entorno. La distinción aquí se hará principalmente en base a la fuente polimérica sintética, natural o híbrida.

Los tres hidrogeles más frecuentemente empleados en bioingeniería uterina son el Matrigel, derivado de polímeros naturales, el colágeno I y el polímero sintético polietilenglicol. Estos hidrogeles se estudian *in vivo* como nuevo tratamiento para patologías uterinas o como modelo *in vitro* de cultivo celular 3D con el objetivo de convertirse en plataformas para el testeo de fármacos, la investigación de interacciones célula-célula, los modelos de implantación y el estudio de la fisiopatología.

Además, el cultivo *in vitro* de embriones desempeña un papel esencial en las tecnologías de reproducción asistida. Los avances realizados en este aspecto acontecen al medio de cultivo, a las plataformas de cultivo estáticas y dinámicas y, por último, a la superficie del cultivo. En referencia a este último elemento, generalmente se emplean superficies inertes como el poliestireno, el vidrio y el polidimetilsiloxano. Muchos de los polímeros derivados de la MEC se usan como revestimiento o suspendidos en el medio de cultivo, tales como el

Matrigel y el ácido hialurónico. Otros sistemas de cultivo bidimensionales investigados usaron el co-cultivo de embriones con distintos tipos de células.

Una aproximación innovadora e interesante podría ser el uso de hidrogeles derivados de la DC de órganos reproductivos lo que permitiría el siguiente paso en el cultivo de embriones, el cultivo organotípico en 3D e innovadores futuros tratamientos.

Una nueva era en reproducción y medicina regenerativa: hidrogeles de matriz extracelular

La mezcla compleja de proteínas extracelulares obtenidas mediante DC puede ser procesada de distintas maneras y servir con diferentes propósitos. Por ejemplo, se pueden obtener secciones o bloques de tejidos descelularizados y sembrarse con células de cultivo primario, células progenitoras o células madre para crear sistemas de cultivo celular tridimensionales. Además, estos biomoldes acelulares pueden ser convertidos en polvos de MEC, liofilizados, solubilizados y usados como hidrogeles o revestimientos para cultivos *in vitro*. Mediante la conversión de los tejidos en sustratos como hidrogeles o revestimientos, la organización espacial de las proteínas de la MEC podría perderse, pero los elementos bioquímicos específicos y relevantes permanecen intactos. El mejor ejemplo del potencial terapéutico de este tipo de hidrogeles lo encontramos en un hidrogel de MEC miocárdico de origen porcino desarrollado por el laboratorio de Christman, el cual está actualmente en ensayos clínicos para tratar pacientes que han sufrido infartos de miocardio.

En otras palabras, los hidrogeles de MEC son una plataforma interesante para aplicaciones reproductivas *in vitro* e *in vivo*. Estos geles no sólo son compatibles con células, sino que también pueden ser mejorados o adaptados con factores de crecimiento. Para futuras aplicaciones en medicina reproductiva, también se ha demostrado que los hidrogeles de MEC pueden utilizarse como base de materiales híbridos para la impresión tisular en 3D. Hasta la fecha no hay estudios que describan el desarrollo de un hidrogel de MEC constituido por tejido endometrial.

OBJETIVOS

Objetivo principal

El objetivo principal de la presente tesis doctoral es desarrollar aproximaciones de ingeniería tisular basadas en la descelularización de tejidos uterinos obtenidos a partir de órganos completos con el fin de mejorar la medicina reproductiva. Se investigarán diferentes alternativas que no sólo mejorarán los modelos *in vitro* empleados actualmente en investigación, sino que también tienen el potencial de poder emplearse, en el futuro, como

nuevos tratamientos para las patologías femeninas endometriales que llevan a disfunciones reproductivas.

Objetivos específicos

- Establecer un protocolo de descelularización basado en la perfusión de agentes desnaturalizantes de órganos reproductores grandes, concretamente útero porcino y cunicular.
- Comprobar la biocompatibilidad de este biomolde natural por lo que se pretende recelularizar discos de endometrio porcino acelular con células madre endometriales humanas (Side Population) y crear estructuras similares a organoides.
- Desarrollar un protocolo basado en la microdisección para separar el endometrio de conejo desde órganos enteros y descelularizados y convertir estas secciones endometriales descelularizadas en hidrogeles y futuros soportes para cultivos *in vitro*.
- Comprobar el posible uso de estos hidrogeles para cultivar embriones de conejo *in vitro*.
- Investigar los efectos de estos sustratos hechos de endometrio estimulado y no estimulado descelularizado en un modelo de cultivo embrionario.

METODOLOGÍA

Modelo porcino: descelularización del útero completo y recelularización del endometrio acelular

Descelularización del útero completo

El objetivo principal de este estudio fue desarrollar un protocolo de DC basado en la perfusión de órganos reproductivos de gran tamaño (en comparación con lo publicado hasta la fecha), dando como resultado un biomolde biocompatible.

Un total de seis úteros fueron seleccionados, en función de su morfología y prestando especial atención a su sistema vascular, tres úteros fueron congelados-descongelados, y tres úteros fueron descelularizados inmediatamente tras la recolección (en fresco). La arteria uterina de un único cuerno fue canulada (cuerno descelularizado), dejando el otro sin perfundir. A continuación, se procedió cuidadosamente a la conexión a una bomba peristáltica y, se realizó una perfusión inicial de una hora con PBS para eliminar los restos de sangre y células. La velocidad de la perfusión para todos los protocolos fue establecida de acuerdo a un caudal fisiológico de 15mL/min.

- Protocolo 1: Muestras congeladas/descongeladas (P1). Los úteros (n = 3) fueron congelados tras la canulación, descongelados después de varios días y, posteriormente se llevaron a cabo dos ciclos idénticos de DC después de la perfusión inicial con PBS. Cada ciclo duró 24 horas y consistió en cuatro pasos de perfusión: primero 18 horas con una solución al 0,1% SDS, seguido de 30 minutos con dH_2O, 30 minutos con 1% Triton X-100 y finalmente, cinco horas con PBS.
- Protocolo 2: Muestras frescas (P2). En el segundo protocolo también se llevó a cabo el mismo ciclo dos veces tal y como se detalla arriba, pero al contrario que en el primer protocolo, el paso de congelación/descongelación tras la canulación no se realizó (n = 3).

La eficiencia de la DC fue evaluada mediante técnicas histológicas: tinción con hematoxilina y eosina (H&E), tinciones de Masson y azul alcián. Para la detección del ADN nuclear, se utilizó medio de montaje con DAPI. También se llevó a cabo la cuantificación de ADN y proteínas.

Seguidamente se analizó la composición e integridad de la MEC en las muestras control y descelularizadas. Se llevó a cabo inmunofluorescencia de cinco proteínas mayoritariamente constitutivas de la MEC: fibronectina, elastina, colágeno tipo I y IV, y laminina. Esto fue realizado en muestras descelularizadas procedentes de ambos protocolos y comparado con un útero fresco no tratado para evaluar la conservación de la MEC. Para evaluar la integridad de la vasculatura se utilizó "Batson's No.17 plastic replica and corrosion kit". Se realizaron cortes circulares del molde uterino obtenido por DC y se abrieron; estas muestras se fotografiaron bajo un microscopio estereoscópico y se sometieron a pulverización de oro y paladio para microscopia electrónica.

Recelularización de discos de matriz extracelular

Finalmente, para evaluar la biocompatibilidad de los moldes acelulares se realiza la RC, para ello se utilizaron líneas de células madre endometriales humanas de origen epitelial (ICE6) y estromal (ICE7) para recelularizar los discos endometriales. Biopsias obtenidas de órganos descelularizados del P2 se orientaron con el endometrio hacia arriba. A partir de estas muestras se realizaron biopsias de punción de 5 mm las cuales fueron lavadas y esterilizadas. Los discos obtenidos fueron cubiertos con un pellet viscoso que contenía una combinación de 0,5 millones de células madre (4/5 de ICE6 y 1/5 ICE7) y fueron incubados en condiciones de hipoxia. El medio de cultivo endometrial fue cambiado cada 3, 6 y 9 días de cultivo. Tras esto, la estructura tipo organoide resultante fue embebida en parafina y se

realizaron cortes seriados. La RC y la correcta diferenciación celular fue analizada con tinción H&E e inmunofluorescencia contra vimentina y citoqueratina humana.

Modelo de conejo: descelularización de útero completo, solubilización del endometrio acelular y cultivo embrionario sobre soportes generados mediante ingeniería de tejidos

El objetivo de este estudio fue crear revestimientos e hidrogeles a partir de diferentes tejidos endometriales descelularizados y comparar el desarrollo embrionario *in vitro* entre estos sustratos y, con sustratos comerciales en diferentes condiciones de cultivo. En total 8 condiciones diferentes de cultivo fueron evaluadas: revestimientos derivados de hidrogeles (C de inglés "coatings") e hidrogeles puros (H) hechos a partir de endometrio acelular no-sincrónico (NSC y NSH), sincrónico (SC y SH) y Matrigel (MC y MH), y además se incluyeron dos condiciones estándar de cultivo usando pocillos sin revestimiento con medio de cultivo suplementado con y sin un 10 % de Suero Bovino Fetal (SBF), C+SBF y C-SBF respectivamente. A continuación, se evaluó y comparó las tasas de eclosión ("hatching"), la morfometría de los embriones y la expresión de 3 marcadores de pluripotencia.

Descelularización de úteros enteros

Cuatro úteros enteros fueron descelularizados, 2 de ellos procedentes de conejos no estimulados, y 2 de conejos 72 horas después de ser sometidos a estimulación ovárica. Este último tipo será nombrado desde ahora como sincrónico (S) debido a la sincronización o ajuste temporal de eventos entre el embrión y el tejido endometrial después del tratamiento hormonal (ambos a día 3). El protocolo de DC de cerdo fue adaptado con el fin de adecuarlo al modelo de conejo, tras un lavado inicial con PBS se realizaron dos ciclos consistentes en cuatro pasos de perfusión: primero con 0,1% de SDS durante 18 horas, seguido de 30 minutos con H_2O destilada, 30 minutos con Tritón X-100 y de cinco horas con PBS. Del mismo modo que en el modelo porcino, la eficiencia de la DC fue evaluada mediante técnicas histológicas: tinción con H&E, tinciones de Masson y azul alcián. Para la detección del ADN nuclear, se utilizó medio de montaje con DAPI. También se llevó a cabo la cuantificación de ADN y proteínas.

Preparación y propiedades del hidrogel de matriz extracelular no-sincrónico y sincrónico

El endometrio acelular se separó mediante microdisección, se liofilizó y se molió. Este polvo enriquecido en proteínas complejas de la MEC se puso en suspensión mediante una digestión parcial con pepsina, alicuotando la solución pre-gel y almacenándola a -80ºC. Se incubó cada hidrogel durante 1 hora a 37ºC. Tras ello, dichos hidrogeles fueron completamente caracterizados. Para analizar la densidad y grosor de las fibras se empleó

microscopía electrónica de barrido, midiéndose el diámetro de las mismas con el software ImageJ.

La cinética de gelificación se analizó mediante turbidimetría. Se añadieron 100 µl de cada solución por triplicado en placas de 96 pocillos a 37ºC y se analizaron espectrofotométricamente midiendo la absorbancia cada 2 min y normalizándose los valoras obtenidos. Se calcularon dos parámetros cinéticos de gelificación: el tiempo medio de gelificación ($t_{1/2}$), definido como el tiempo necesario para alcanzar el 50% de la absorbancia máxima, y el tiempo lag (t_{lag}), definido como el momento en el que la curva de gelificación supera el 0% de la absorbancia normalizada.

Además, para testar la estabilidad y esterilidad estructural, los hidrogeles (NSH, SH y MH) se dejaron en medio DMEM/F12 con 10% de SBF y 0,1% de antibióticos durante 7 días.

Características biológicas y aplicaciones de los hidrogeles

Como se ha descrito anteriormente, se cultivaron embriones en día 3 durante 48 horas en 8 condiciones comparando sincrónico, no-sincrónico y Matrigel versus condiciones control. La capacidad de desarrollo *in vitro* de los embriones fue evaluada basándose en la tasa de hatching/hatched (proporción de blastocistos realizando la eclosión y eclosionados a las 48 horas del cultivo respecto al total de embriones cultivados). A continuación, se realizó un análisis morfométrico de los embriones eclosionados. Este y los siguientes análisis fueron realizados solo en las tandas de embriones cultivados en condiciones control y en pocillos con revestimiento (condición que incluye incubación de los hidrogeles toda la noche y realización de lavados antes del cultivo), pues tras comparar las tasas de hatching quedó claro que todos los grupos de hidrogeles (NSH, SH y MH) tenían un desarrollo muy inferior. Finalmente, se evaluó el perfil de expresión génica de tres factores clave de pluripotencialidad (*OCT4, NANOG and SOX2*) tras las 48 horas de cultivo *in vitro* en los grupos experimentales C-SBF, C+SBF, MC, NSC y SC. Las condiciones de revestimiento o soporte (C, coatings) NSC, SC y MC corresponden a pocillos recubiertos con endometrio descelularizado no-sincrónico, sincrónico y Matrigel.

RESULTADOS

Descelularización de úteros de cerdo y conejo

Ambos protocolos, tanto de cerdo como de conejo, dieron lugar a DC completa: las tinciones H&E y tricrómica de Masson mostraron la eliminación del material celular y los núcleos en todo el órgano, pero preservando la arquitectura de la MEC compuesta

predominantemente por colágenos. Además, la tinción con DAPI confirmó una completa destrucción de los núcleos en todas las capas uterinas. Estos resultados fueron corroborados por la cuantificación de ADN y proteínas. Así, en el modelo de cerdo la cuantificación de ADN residual mostró una caída del 90,94% y 97,35% para los protocolos P1 y P2, respectivamente. La cuantificación de la fracción remanente de proteína mostró un descenso del 61,02% y 70,03%, respectivamente. Para el útero de conejo se registró una reducción del 95,3% y 93,2% en el ADN de doble cadena para el útero descelularizado no-sincrónico y sincrónico, y una disminución de la concentración de proteínas en ambos tejidos (del 45,9% y del 38,2%, respectivamente).

El modelo porcino: efecto del protocolo de descelularización sobre la matriz extracelular

El análisis cuantitativo de Glucosaminoglucanos (GAGs) sulfatados mediante tinción con azul alcián muestra una distribución generalizada que se mantiene con ambos protocolos, con una señal notoriamente inferior en el epitelio.

Mediante inmunofluorescencia se observa que el colágeno I, el tipo de colágeno más abundante, permanece uniformemente disperso en la MEC antes y después de la DC. La elastina, otro de los principales constituyentes estructurales de la MEC, se encontró fundamentalmente en el miometrio, la capa basal del endometrio y alrededor de las arterias. Tras la DC hubo una señal notablemente más débil en el epitelio intersticial, mientras que el miometrio y las arterias no se vieron afectados. La fibronectina no se vio afectada y se encontró uniformemente dispersa antes y después de ambos protocolos. Dos de los componentes principales de la membrana basal, el colágeno IV y la laminina, fueron detectados antes y después de la DC en las capas endoteliales alrededor de los vasos sanguíneos y en las estructuras glandulares de ambas capas. También se observó colágeno IV en el miometrio.

Mediante el uso del microscopio electrónico de barrido a baja magnificación se apreciaron elementos del lumen endometrial, la superficie epitelial y las estructuras glandulares permaneciendo intactas y no se observaron diferencias estadísticamente significativas entre todas las condiciones, tanto antes como después de la DC. A mayor magnificación se observa claramente que las fibras y su topografía mantienen su apariencia en ambos protocolos y los conductos vasculares mantienen su conformación. La microscopia electrónica de transmisión muestra fibras de colágeno, que mantienen su patrón estriado y se encuentran de forma abundante en todas las orientaciones a lo largo del tejido. No se observaron diferencias destacables a nivel estructural entre los protocolos probados.

Se investigó la vasculatura empleando un molde de corrosión vascular, tras ambos protocolos de DC se observó una disminución de la integridad vascular tanto macroscópicamente como a mayor magnificación. Esto probablemente se deba al protocolo, que se basa en la penetración de una solución de un monómero viscoso. La región correspondiente al plexo capilar subepitelial se encontró en todos los casos. Cuando se estudió empleando microscopía electrónica en todos los casos se encontraron capilares con el grosor adecuado.

Recelularización de discos acelulares de endometrio porcino

Para estos experimentos se empleó tejido procedente del protocolo P2, ya que este proporciona la MEC más uniforme. Tras sembrar células madre endometriales humanas (Side Population), los biomoldes utilizados recubiertos con estas células se enrollaron y comprimieron, formando una estructura similar a un organoide. La tinción de H&E mostró que las células se encapsularon en el en el biomolde descelularizado, mostrando que las células se adherían e interactuaban estrechamente con la MEC endometrial.

Para demostrar el comportamiento específico del tejido generado por las células madre SP, se realizaron tinciones de inmunofluorescencia de marcadores típicamente endometriales. Se observaron células con señal positiva para vimentina, filamento intermedio expresado por las células mesenquimales, a lo largo de toda la estructura. Y también se observó la presencia de células que expresaban citoqueratina, marcador de células epiteliales.

Caracterización de los hidrogeles de MEC en el modelo de conejo

La microdisección nos permitió obtener tejido endometrial puro tanto de los tejidos control como descelularizados. Este endometrio acelular no-sincrónico (NS) y sincrónico (S) fue liofilizado y molido con hielo seco en una ultracentrífuga hasta alcanzar un tamaño de grano inferior a 0,0625mm^2. Este polvo fue digerido en pepsina hasta disolver totalmente el tejido. Después se dejó a 37ºC durante una hora, las soluciones resultantes de pre-gel viscoso formaron hidrogeles estables que requirieron un delicado manejo. Se demostró la estabilidad estructural a largo plazo y la esterilidad de estos geles derivados de MEC mediante su incubación a 37ºC en medio de cultivo standard durante 7 días. El hidrogel permaneció intacto durante este periodo y no se observó crecimiento bacteriano.

La cinética de gelificación fue medida espectrofotométricamente, lo que nos permitió calcular parámetros importantes (t_{lag} y $t_{1/2}$). En ambos geles, la cinética de gelificación siguió una curva sigmoidea, pero se observaron diferencias significativas en los parámetros. La

gelificación del hidrogel S comenzó casi inmediatamente y tendió a tener un menor tiempo lag que el hidrogel NS (t_{lag} =2,98 ± 0,86 min vs 4,9 ± 0,33 min). El tiempo para alcanzar el 50% de la gelificación máxima no mostró diferencias estadísticamente significativas, aunque el gel S necesitó aproximadamente 5 min menos que el hidrogel NS ($t_{1/2}$ = 10,43 ± 0,74 min y 15,46 ± 0,29 min respectivamente).

El análisis mediante microscopia electrónica de barrido de la superficie del hidrogel mostró que tanto los geles NS como S presentaban una estructura fibrilar homogénea, entrelazada aleatoriamente, de densidad similar. El diámetro de las fibras de los hidrogeles NS y S fue analizado a partir de imágenes tomadas a resolución 60.000X (>30 medidas por gel). El diámetro de las nanofibras re-ensambladas de ambos geles mostraron un rango entre 50 y 149nm, con un promedio de 70,04 ± 9,15 nm versus 102,90 ± 22,66 nm para los hidrogeles no-sincrónicos y sincrónicos respectivamente. Ambos diámetros de fibra resultaron ser significativamente diferentes. Es posible que estas diferencias se deban a que las fibrillas de colágeno, con un grosor medio de 50nm, permanecieran más empaquetadas en el hidrogel S o que persistieran componentes que interaccionan con estas.

Características biológicas de los hidrogeles: cultivo embrionario

El desarrollo de los embriones *in vitro* se ha visto afectado significativamente tras el cultivo con hidrogeles, el promedio de la tasa de eclosión en estas condiciones es 27,64±26,38%. Sin embargo, no era el caso en los controles y en los pocillos con los diferentes revestimientos, con promedio de 89,4±3,13%. Después de 48 horas de cultivos *in vitro* se encontraron diferencias significativas en el diámetro medio de los embriones en los grupos SC y C+SBFcomparado con los grupos NSC, C-SBF and MC.

No obstante, los blastocistos del grupo NSC mostraban niveles más altos de expresión de *OCT4* que en el grupo C-FBS, mientras que la expresión de *SOX2* era más alta en los grupos de SC, NSC y C+SBF comparado con los grupos de MC y C-SBF

DISCUSIÓN

Con más de 70 millones de parejas afectadas, la infertilidad se considera un problema de salud pública a nivel mundial. Una de las principales causas en medicina reproductiva es la infertilidad total por factor uterino. El trasplante de útero es la única cura hasta ahora conocida, tal y como lo ha demostrado el grupo del Dr. Brännström.

En la actualidad se están desarrollando muchas aproximaciones y tecnologías con el fin de resolver los problemas que afectan a los trasplantes de órganos. Una línea de

investigación basada en la des- y recelularización de órganos completos, ha mostrado resultados prometedores para posiblemente algún día lograr órganos trasplantables. En la primera parte de esta tesis, se realizó una comparación entre úteros porcinos congelados/descongelados (P1) versus frescos (P2), usando un protocolo consistente en ciclos de SDS y Tritón X-100. Después de dos ciclos idénticos de 24 horas, se obtuvo una matriz macroscópicamente acelular con aspecto semitransparente y blanco. El SDS es un detergente iónico que se usa ampliamente para descelularizar y que, a bajas concentraciones, puede eliminar efectivamente los residuos celulares causando un mínimo daño a la MEC. Además, el paso de congelación/descongelación no afectó notablemente a la arquitectura de MEC, según nuestra experiencia. También, hay estudios que afirman que un solo ciclo de congelación/descongelación puede reducir las respuestas inmunológicas de los tejidos descelularizados, lo que sugiere que este paso inicial podría ser una opción interesante y muy conveniente para preservar y descelularizar los órganos de los donantes.

La ausencia de constituyentes celulares vitales muestra que se eliminó una cantidad suficiente de material celular nativo como para considerar el órgano como " descelularizado". Además, las propiedades físicas y posibles propiedades mecánicas de la MEC se demostraron por la presencia de fibras de colágeno nativas visualizadas con las tinciones de azul alcián y tricrómica de Masson. Los principales componentes de la MEC, como los colágenos tipo I y IV, elastina, laminina y fibronectina, se conservaron. Estos resultados y los de la microscopía electrónica implican que las proteínas intersticiales de la MEC y la membrana basal permanecieron intactas en ambas condiciones de DC. El mantenimiento de la composición proteínica de la MEC es importante en los procesos de RC contribuyendo en la adhesión celular, la integración tisular, el desarrollo y las funciones fenotípicas celulares normales.

La preservación de la red vascular también es crítica, primero para una perfusión eficiente de los detergentes y, en segundo lugar, para una futura RC del órgano. Se demostró que los protocolos solo comprometían ligeramente la integridad vascular, lo que abre la posibilidad de recelularizar el órgano completo mediante la adición de células vía perfusión o inyección y la creación de un sistema capaz de intercambiar nutrientes y gases en el nuevo órgano generado.

El paso final fue verificar la biocompatibilidad y evaluar las propiedades bioinductivas de los biomoldes xenogénicos generados *in vitro*. Después de 3-4 días de cultivo celular en condiciones hipóxicas, las estructuras derivadas de los úteros descelularizados porcinos fueron cultivadas en presencia de células madre endometriales humanas (Side Population);

tras lo cual se contrajeron y enrollaron, y tras 9-12 días se observaron estructuras similares a organoides. Esta estructura tipo organoide se investigó más a fondo con el fin de determinar si las células humanas podían recapitular *in vitro* la arquitectura que tiene el tejido *in vivo*. La histología mostró una interacción estrecha entre las células y los biomoldes naturales utilizados. Además, las células endometriales de ambas fracciones epiteliales (citoqueratina positiva) y estromales (vimentina positiva) se identificaron en la nueva estructura.

En la segunda parte de la tesis, demostramos la DC del útero entero de conejo y el aislamiento del tejido endometrial acelular. El endometrio sufre, bajo la influencia de los esteroides sexuales femeninos diferentes ciclos de crecimiento y reorganización. La MEC del tejido endometrial sigue este ciclo mediante la expresión diferencial de proteínas tanto intersticiales como de la membrana basal, muchas de las cuales permanecen tras la DC. Las células endometriales producen diferentes compuestos de secreción y factores de crecimiento durante las diferentes fases del ciclo endometrial que podrían ser secuestradas por la MEC nativa y retenidas después de la DC.

Aunque solo se observaron ligeras diferencias entre los tejidos, este no fue el caso cuando se compararon las ultraestructuras de los hidrogeles NSH y SH. En el hidrogel SH se observan fibras significativamente más gruesas. Sin embargo, cuando los embriones se cultivaron en estos hidrogeles NSH, SH o Matrigel (MH), su desarrollo se vio gravemente afectado, en contraste con el uso del pocillo con revestimiento proteíco derivado del hidrogel (NSC, SC y MC). Una posible explicación podría ser que la densidad y la rigidez del hidrogel desempeñan un papel en el desarrollo, o que algún factor inhibidor aún permanece dentro del hidrogel como resultado del procesamiento del tejido. Cuando el revestimiento se realizó a partir del endometrio estimulado o sincrónico (SC), el efecto positivo produjo blastocistos con mayores tasas de eclosión o hatching, con tamaño similar a las condiciones positivas estándar en estos ensayos, compensando efectivamente la ausencia de proteínas de adhesión y factores de crecimiento del suero en el medio de cultivo.

Nuestros resultados mostraron patrones de expresión similares de los genes *OCT4* y *SOX2*, tanto en el grupo de endometrio sincrónico como en el de suero. El complejo regulador SOX2-OCT4-NANOG controla la expresión de genes pluripotentes, incluyendo estos tres genes en un circuito auto-regulatorio. Podría ser que la expresión inadecuada de estos estuviera desencadenando fallos en el desarrollo e implantación de los embriones. Este hecho resalta el papel tan importante que juega SOX2 durante el periodo preimplantatorio. De modo que nuestros resultados parecen demostrar que el revestimiento con endometrio

sincrónico retendría y liberaría componentes que permitirían, al menos en parte, mimetizar *in vitro* el ambiente endometrial.

Los hidrogeles y revestimientos procedentes de la MEC endometrial derivada de conejo tienen el potencial de convertirse en plataformas para el cultivo de células madre o progenitoras y de células procedentes de cultivo primario, con la finalidad de mantener mejor su fenotipo específico correspondiente al tejido de origen, mejorando así los modelos *in vitro*. Esto también podría tener aplicaciones *in vivo*, como en el tratamiento del Síndrome de Asherman o la atrofia endometrial.

Para concluir podemos decir que la IT supone un campo de investigación multidisciplinario incipiente y prometedor, dispuesto a transformar la medicina traslacional y la investigación. Si bien estamos solo ante sus inicios en cuanto a su aplicación en la medicina reproductiva, algunas técnicas como la des- y recelularización de tejidos y el cultivo *in vitro* con el uso de hidrogeles ya han mostrado resultados prometedores en el área de la reproducción.

CONCLUSIONES

De esta tesis pueden extraerse las siguientes conclusiones:

1. Se ha logrado establecer un protocolo de descelularización por perfusión utilizando ciclos de detergentes iónicos y no iónicos, protocolo capaz de eliminar eficazmente todo el material celular en órganos reproductores de gran tamaño (porcino), sin comprometer la morfología de la matriz extracelular.
2. Las proteínas vitales de la matriz extracelular como elastina, laminina, fibronectina o colágeno tipo I permanecen en el biomolde descelularizado generado tras aplicar el protocolo de descelularización anteriormente mencionado; asimismo se demuestra que un ciclo de congelación-descongelación tiene pocas consecuencias negativas, o ninguna, en la composición o en la ultraestructura del mismo.
3. El biomolde resultante es biocompatible ya que las células madre endometriales de origen humano (Side Population) crecen en él y forman estructuras de tipo organoide; estos organoides expresan marcadores típicos de células humanas endometriales epiteliales y estromales.
4. Tan solo es necesario hacer unas ligeras modificaciones para poder aplicar este protocolo de descelularización a úteros de otras especies (en nuestro caso conejo); siendo un candidato prometedor para la descelularización de úteros humanos.

5. El tejido endometrial descelularizado en conejos y en diferentes etapas del ciclo endometrial se puede separar por microdisección. Además, este tejido puede ser convertido en hidrogeles y usarse como revestimientos/soportes específicos para cultivos *in vitro*.
6. Cuando los embriones en día 3 crecen en los revestimientos de matriz extracelular de endometrio estimulado o sincrónico, su desarrollo es similar al que se produce aplicando las condiciones de cultivo positivas; indicando que la especificidad del tejido se conserva tras la descelularización.

CONTENTS

LIST OF FIGURES

LIST OF TABLES

ABBREVIATIONS

3D	Three-dimensional
ART	Artificial reproductive technologies
AS	Asherman's syndrome
AUFI	Absolute uterine factor infertility
bFGF	Basic fibroblast growth factor
BM	Basement membrane
BMDSCs	Bone-marrow derived stem cells
BM-MSC	Bone marrow-derived mesenchymal stem cells
BRL	Buffalo rat liver
BSA	Bovine serum albumin
CBD	Collagen binding domain
cDNA	Complementary DNA
CK	Cytokeratin
COL1	Collagen I
COL4	Collagen IV
DAPI	4',6-diamidino-2-phenylindole
DC	Decellularization
DMEM	Dulbecco's modified eagle medium
DNA	Deoxyribonucleic acid
DNase	Deoxyribonuclease
E_2	Estradiol
EA	Endometrial atrophy
ECM	Extracellular matrix
EDTA	Ethylenediaminetetraacetic acid
EEC	Endometrial epithelial cells
ELN	Elastin
ER	Estrogen receptor
ESC	Endometrial stromal cells
FBS	Fetal bovine serum
FDA	Food and Drug Administration
FN	Fibronectin
FSH	Follicle-stimulating hormone
GAGs	Glycosaminoglycans
GAPDH	Glyceraldehyde-3-phosphate dehydrogenase
G-CSF	Granulocyte colony stimulating factor
GFP	Green fluorescent protein
GnRH	Gonadotropin-releasing hormone
H&E	Hematoxylin and eosin
H2AFZ	H2A histone family member Z
HA	Hyaluronic acid
hCG	Human chorionic gonadotropin
hESC	Human embryonic stem cells
HPP	High hydrostatic pressure
hUC	Human umbilical cord-derived matrix

ICE6	Epithelial SP-derived cell line
ICE7	Stromal SP-derived cell line
IUA	Intra-uterine adhesion
IVF	*In vitro* fertilization
LH	Luteinizing hormone
LIF	Leukemia inhibitory factor
LM	Laminin
LPS	Lipopolysaccharide
M	Matrigel
MC	Matrigel coating
MH	Matrigel hydrogel
MI	Myocardial infarction
MMPs	Matrix metalloproteases
MRKH	Mayer-Rokitansky-Kuster-Hauser
MSC	Mesenchymal stem cells
MT	Masson's trichrome
NA	Normalized absorbance
NGS	Normal goat serum
NO	Nitric oxide
NS	Non-synchronous
NSC	Non-synchronous coating
NSH	Non-synchronous hydrogel
OCT4	Octamer-binding transcription factor 4
P_4	Progesterone
PBS	Phosphate buffered saline
PCR	Polymerase chain reaction
PDMS	Polydimethylsiloxane
PEG	Poly-(ethylene glycol)
PEGLA	Polyethylene glycated leukemia inhibitory factor antagonist
PFA	Paraformaldehyde
PGs	Proteoglycans
PHEMA	Poly-(2-hydroxyethyl methacrylate)
PLLA	Poly-L-lactic acid
PR	Progesterone receptor
PU	Polyetherurethane
PVA	Poly-(vinyl alcohol)
RC	Recellularization
REPROTEN	Reproductive tissue engineering
S	Synchronous
SC	Synchronous coating
SCSIE	Servicio Central de Apoyo a la Investigación experimental
SDS	Sodium dodecyl sulfate
SEM	Scanning electron microscopy
SH	Synchronous hydrogel
SIS	Small intestinal submucosa
SKM	Skeletal muscle
SOX2	Sex-determining region Y-box 2
SP	Side population
SrtA	Sortase A
TCM 199	Tissue culture medium 199
TE	Tissue engineering
TEM	Transmission electron microscopy
UC-MSCs	Umbilical cord derived mesenchymal stem cells
VEGF	Vascular endothelial growth factor
Vit c	Vitamin C

Chapter

I

INTRODUCTION

I. INTRODUCTION

1 The basis for tissue engineering: the female reproductive tract

1.1 Anatomy of the female reproductive system

The entire course from female germ cell production, fertilization, embryo implantation and pregnancy until the partum takes place within the female reproductive system. Anatomically we can first make a division between the external and internal genitals. The external genitalia comprise the perineum and what is collectively referred to as the vulva, consist of mons pubis, labia majora and minora, clitoris, vestibule, urethral meatus, greater vestibular (Bartholin's) glands, Skene's glands, and the periurethral area. The internal genitalia are located deep within the pelvic cavity; this is where the main organs responsible for the reproductive process are harbored. These are the ovaries, fallopian tubes or oviducts, the uterus and the vagina (Ramírez-González et al., 2016; Simón et al., 2009). The detailed anatomy of these internal organs can be found in figure 1.

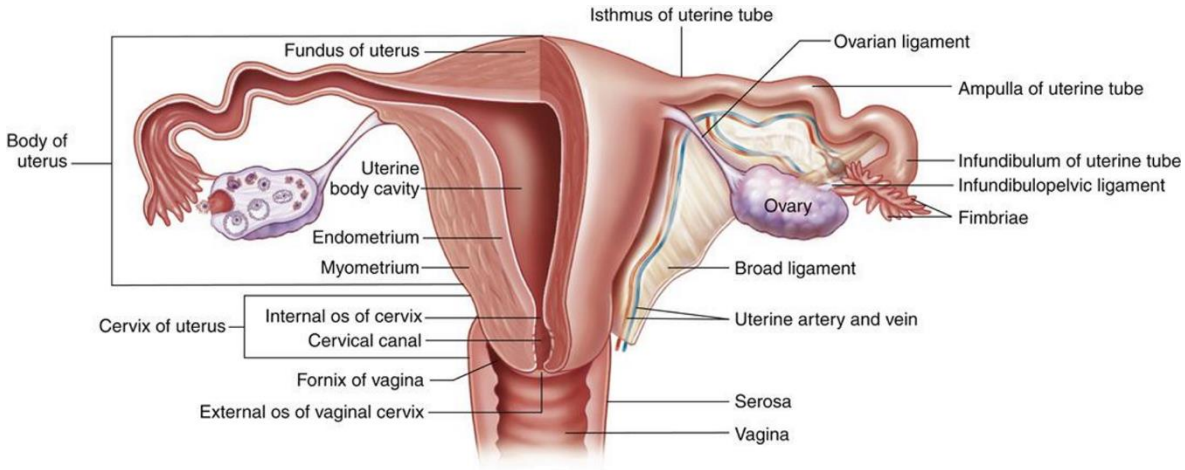

Figure 1. A comprehensive depiction of the internal organs of the female reproductive tract. *This consist of the ovaries, kept into place by the ovarian ligaments, followed by the fallopian tubes with the fimbria, infundibulum, ampulla and isthmus. Both arrive to the body of the uterus. The uterus consists of the fundus, corpus and cervix. The last internal organ, the vagina, connects the entire gestational tract to the outside. Image adapted from basicmedicalkey.com.*

The ovaries or female gonads are paired, almond shaped organs measuring about 3.5 cm long and 1.5 cm thick; they are situated in the ovarian fossa of the abdominal cavity. The ovary exists out of a central medullary zone and a peripheral cortex, in which the follicles reside and develop. These organs have two central functions, namely the production of female gametes called oocytes (oogenesis), and to serve as endocrine glands producing the

female sex hormones such as estrogens and progesterone (steroidogenesis). During the female reproductive life about 400 oocyte-containing follicles successfully go through the developmental stages from primordial follicles to growing, and finally, mature or Graafian follicles from which secondary oocytes are released during ovulation; the remaining follicular wall collapses and forms the highly vascularized corpus luteum or luteal gland. This ovarian cycle is regulated by hormones secreted from the adenohypophysis and lasts about 28 days.

The fallopian/uterine tubes or oviducts act as the conduits that transports the oocytes from the ovaries to the uterus. This is done by the coordinated contractions of the smooth muscle layer and the beating of the cilia lining the outside and lumen of the uterine tube. This is also where both male and female gametes interact during fertilization; this typically takes place in the middle section of the fallopian tubes called the ampulla.

Following the isthmus and intramural part of the oviduct, we arrive to the uterus. This hollow, muscular, inverted pear-shaped organ will evacuate the unfertilized egg with the menstrual period, or provide nourishment and support for the growing embryo until birth. This organ is the largest organ of the system, measuring 7cm high, 5cm wide and 2cm deep and can be divided into the fundus (superior to the fallopian tubes), corpus and cervix. The human uterus is of the simplex form, meaning that it is fused into one single organ, other forms of mammalian uteri include duplex (rabbit, mouse, rat) and bicornuate (dog, pig) anatomy (Figure 2).

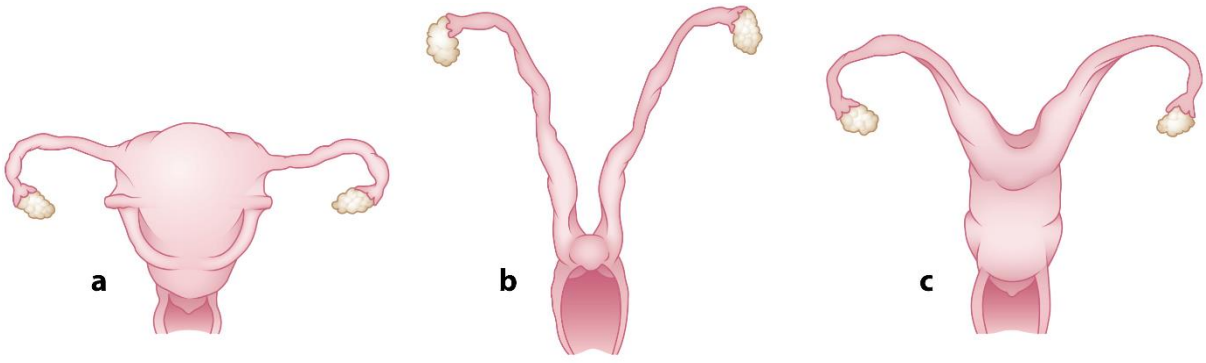

Figure 2. The anatomy of mammalian uteri. *These forms can be (a) simplex, (b) duplex, or (c) bicornuate. Reprinted from (Kabagambe et al., 2018) with permission of Annual Reviews.*

The uterine wall itself consists of three layers: the outer perimetrium, middle myometrium and inner or luminal endometrium. The myometrium is the thickest layer and is composed of 3 layers of smooth muscle cells; these are an inner and outer layer with longitudinally oriented fibrillar bundles and a middle layer that is highly vascularized with arcuate arteries. The cells here are circularly or spirally organized, allowing for the

elongation and distention of the uterus during the pregnancy. The third and most complex layer lining the inner surface of the uterus is the endometrium; this is the mucosal layer crucial for embryo implantation and development. In humans and higher primates this highly dynamic tissue constantly changes during the menstrual cycle in reaction to female sex hormones (Simón et al., 2009; Speroff and Fritz, 2005). These changes, both at physiological, cellular and extracellular level will be discussed in detail in the following sections.

The lowest part of the internal female genitalia is the vagina; this fibromuscular tube connects the cervix with the outer genitals and is the tract through which uterine secretions are expelled, receives the penis and acts as the passage of the full-term foetus.

1.2 The human endometrium: cellular composition, structure and function

On a cellular level, an epithelial, stromal, vascular and immune cell compartment can be distinguished within the endometrium. These cells are situated in the two main layers of the endometrium, namely the *stratum basalis* and the *stratum functionalis* (Dallenbach-Hellweg, 1971; Simón et al., 2009); these two layers are detailed in figure 3. Both play vital roles during the menstrual cycle; the functional layer is the thickest part of the endometrium, spanning two-thirds of the endometrium and is extremely responsive to steroids. This transient layer prepares for the implantation of the blastocyst and during every menstrual cycle it is the site of proliferation, secretion, and degeneration in response to hormonal cues. Predecidual transformation formed a compact layer in the upper part, followed by a lower less dense spongiosa that extends to the basalis (Speroff and Fritz, 2005). This basal layer is the only part of the endometrium that remains intact after menstruation, from which the functional layer regenerates. This layer does not undergo significant changes and contains the base of the glands and supportive vasculature from which the cycle can start anew (Dallenbach-Hellweg, 1971; Speroff and Fritz, 2005). This high regenerative capacity suggests that the endometrium has a stem cell population residing in the basalis layer that supports tissue maintenance and regrowth (Cervelló et al., 2010, 2011a, 2017; Gargett and Masuda, 2010; López-Pérez et al., 2018).

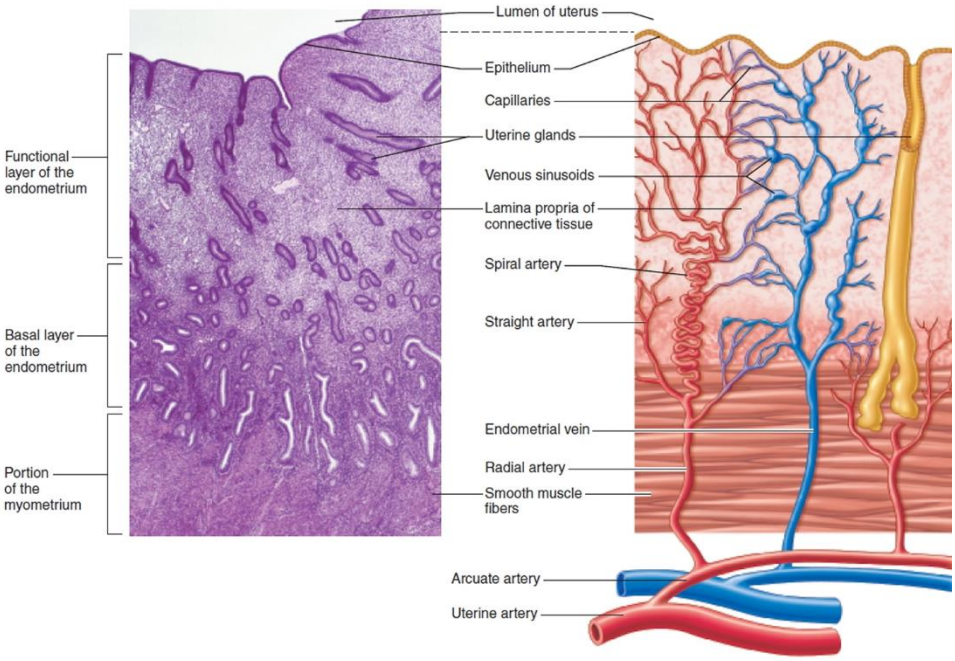

Figure 3. Histology and organization of the human endometrium. *Histological image (left) and corresponding detailed figure (right) of the human endometrium showing all important structures such as glandular and luminal epithelium, stroma and vasculature and their distribution within the different layers. The basal layer borders the myometrium, where the spiral arteries and base of the glands reside. Above this is the functional layer, note in the lower, less dense zone and upper dense zone of the functionalis are well visible in the histology. Image from healthjade.com.*

The endometrial epithelium is a monolayer of cuboidal and polarized cells and is responsible for creating the microenvironment for the first interactions with the embryo while also acting as a barrier against pathogens. For this, the luminal epithelium adapts the morphology of the plasma membrane and cytoskeleton to the menstrual cycle while the cells of the glandular epithelium secrete the necessary molecules for the implantation and nourishment of the blastocyst. This epithelium is regulated by the hormones coming directly from the ovaries or those from the stromal cells. The stroma consists of extracellular matrix (ECM) and pluripotential mesenchymal cells, mainly fibroblasts. Major changes take place during the menstrual cycle, a process also referred as decidualization. Here, ECM remodeling and cellular morphological, biochemical and genetic changes occur starting from day 6 or 7 of the cycle. The endometrial vasculature starts from the middle myometrium, which is highly vascularized by the arcuate arteries. Coming from the uterine artery, the arcuate arteries turn into the radial arteries when reaching the endometrium. From here straight arteries and spiral arties branch. The former irrigates the basal layer and the latter branches out in capillaries that in turn irrigate the superficial functionalis layer.

Finally, the last important fraction of the endometrium is the immune cell population, whose role is to ward off infectious diseases and invasion of aberrant cells, as well as to avoid immune reactions caused by the embryo during implantation. The distribution and

proportion of the major leukocytes such as T cells, B cells, natural killer cells, macrophages and dendritic cells and even the amount of lymphoid aggregates vary depending on the phase of the menstrual cycle (Dallenbach-Hellweg, 1971; Kämmerer et al., 2004; Simón et al., 2009).

The female reproductive tract has surface epithelial cells with a complex mixture of glycosaminoglycans and (fibrous) glycoproteins that interact with the embryo. When the embryo arrives at the endometrium during the window of implantation successful apposition, attachment and invasion of the embryo is possible. Implantation failure can happen when there are abnormalities of embryonic or uterine origin or when there is loss of synchrony between embryo development, endometrial receptivity and/or the immune system response (Simon and Laufer, 2012). For this, artificial reproductive technologies (ART) have been developed to improve the reproductive outcome. One of the pillars of ART is *in vitro* fertilization (IVF), which had its first milestone in 1978, with the birth of the first 'IVF baby' Louise Joy Brown. Here, fertilization takes place outside of the body and the formed zygote is cultured for 2-6 days.

1.3 Dynamic morphology of the endometrium

1.3.1 The menstrual cycle.

The menstrual cycle is the result of a complex and synchronized interplay between hypothalamus, anterior pituitary, ovary, and endometrium that first takes place with the menarche and ends with menopause. This cycle of endometrial de- and regeneration takes on average 28 days but can fluctuate between 24-36 days in 90% of the women and is repeated from 400 to 500 times during their reproductive life. A summary of this is given in figure 4.

The menstrual cycle is influenced by the events of folliculogenesis of the ovarian cycle; here we can distinguish two phases: the follicular phase and luteal phase with ovulation marking the transition between them. The hypothalamus stimulates the glandular cells of the anterior pituitary by producing gonadotropin-releasing hormone (GnRH). They in turn produce luteinizing hormone (LH) and follicle-stimulating hormone (FSH). In the first 14 days of the menstrual cycle (the first day of the menstrual bleed is considered as day 1), during the follicular phase, many primordial follicles start to develop until usually only one dominant follicle matures and reaches ovulation. During this period the granulosa and developing theca cells are stimulated to produce increasing amounts of estradiol (E_2), leading to a spike in LH and FSH and finally resulting in ovulation. The remaining follicular

cells in the ovary become luteinized as part of the corpus luteum, and increase progesterone secretion, marking the start the luteal phase. If there is no embryo implantation, the LH concentrations trigger luteal degeneration and decreasing progesterone (P_4) and E_2 levels which in turn causes the FSH and LH levels to rise, starting the cycle once again (Hawkins and Matzuk, 2008; Ramírez-González et al., 2016)

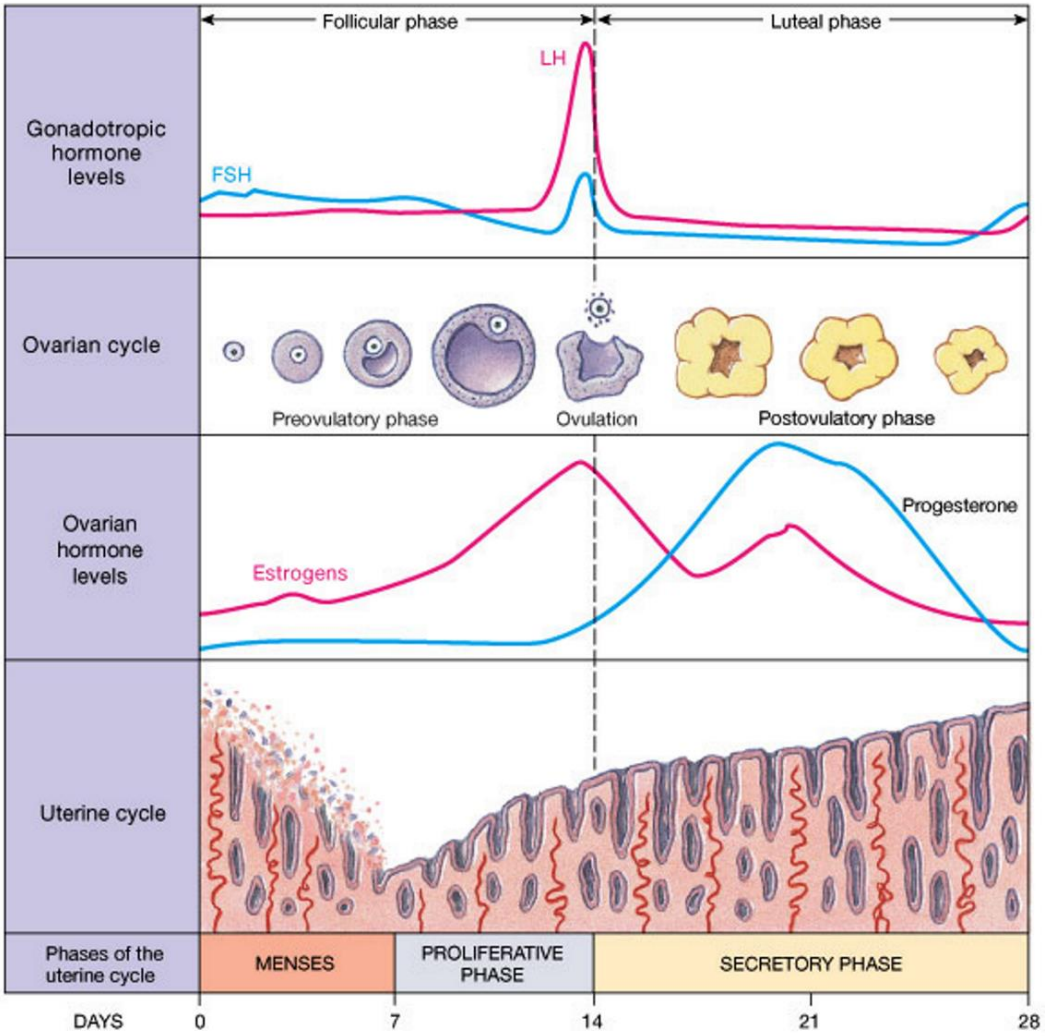

Figure 4. The ovarian and endometrial cycle during the menstrual cycle. *The ovarian cycle is influenced by luteinizing (LH) and follicle-stimulating hormone (FSH) secreted by the anterior pituitary gland; during the folliculogenesis the ovary produces female sex steroids that affect the endometrial development. Ovulation separates the follicular phase, which corresponds to the menses and proliferative phase of the uterine cycle and the luteal phase, which overlaps with the endometrial secretory phase. When fertilization or implantation does not occur, progesterone concentrations fall rapidly, resulting in the sloughing of the endometrium and resetting the cycle. Image from quara.com.*

The endometrium is extremely sensitive to the female sex steroids; because of this the endometrial cycle goes synchronized with the ovarian cycle. Throughout the cycle, the thickness of the endometrial lining will vary from 0.5mm to 7mm and even up to 10mm

(Mclennan and Rydell, 1965) when going through the 3 main developmental phases: the menstrual, proliferative and secretory phases.

The first day of the menstrual cycle coincides with the first day of menstruation; in the menstrual phase the functionalis layer of the endometrium is shed due to a sharp decline of P_4 levels. After shedding, torn surfaces with gland openings without epithelial layer are left and during this phase the re-epithelization occurs (Maybin and Critchley, 2015). This is followed by the proliferative phase whose duration can vary between 10-20 days but corresponds with the follicular phase until ovulation. This phase is characterized by tissue remodeling, proliferative and anti-apoptotic processes, and stimulated angiogenesis. An early, middle and late proliferative stage can be distinguished (Dallenbach-Hellweg, 1971; Strowitzki et al., 2006). In the early proliferative stage (days 4-7) a low and recently re-epithelialized basalis with fewer glands is present. With the rising estrogen levels, the functionalis grows markedly resulting in stromal edema and glands become more tortuous, all of which is characteristic for the mid proliferative phase (day 8-10). The late phase (day 11-14) is characterized by even more tortuous glands with a denser epithelium; this is because of a temporary decreased growth rate and regression of the edema. The secretory phase coincides with the luteal phase, lasting for approximately 14 days. The endometrium continues to thicken, the main cellular transformation takes place in the stromal cells and decidualization occurs in order to prepare the endometrium for implantation. Here we also find the window of implantation, during the mid-luteal phase between days 20 and 24 (Domínguez et al., 2003). If fecundation does not occur, the corpus luteum degrades and P_4 and E_2 levels drop, resulting in cellular processes and vasoconstriction of the spiral arteries leading to menstruation.

1.3.2 Evolution of the extracellular matrix during the menstrual cycle

The extracellular matrix is the connective tissue material found between cells, not only providing physical support, but also interacting with cells via biochemical cues that are vital for cell adhesion, survival, differentiation and migration. Two main classes of macromolecules can be distinguished within this highly dynamic structure: proteoglycans (PGs) and fibrous proteins (Frantz et al., 2010). Fibrous ECM proteins constitute most of the weight of the ECM: collagens, elastin, tenascins, fibronectin and laminin are the most prevalent components. Proteoglycans are made out of glycosaminoglycan (GAG) chains that are covalently linked to a specific protein core (hyaluronic acid (HA) being the exception here); they have unique buffering, hydration, binding and force-resistance properties (Järveläinen et al., 2009). The major structures within the ECM are the interstitium and

basement membrane. Examples of the interstitial ECM proteins in the mesenchyme are collagens (I, III, V, VI and XIII), fibrillin, fibronectin, tenascin C and several PGs and GAGs such as versican, decorin and HA. These ECM proteins are anchored to those of the basement membrane (BM). The BM are sheets of specialized ECM found at the basal surfaces of endothelial and epithelial cells, serving as filters and anchors for signaling. Laminin, collagen IV, nidogen and sulphated PGs such as perlecan, agrin and collagen XVIII are also part of this (Miner, 2011).

The examples provided here are only part of the proteins comprising the complex ECM, with the advent of "-omics" analysis the term "matrisome" was introduced by Hynes and Naba as "the larger list of all the proteins that can contribute to matrices in different situations"(Hynes and Naba, 2012). From here, a robust list of the central proteins defining any specific mammalian ECM has been proposed, called the core matrisome. Recently, this core matrisome has been published for the ovaries (Ouni et al., 2018). Another way to describe this concept is to say that every tissue has its unique, heterogenous mixture of these components to provide the correct environment for their intended use, as is the case for the endometrium. Throughout the menstrual cycle the endometrium goes through extensive changes in its composition, size and organization. Even more, it is the only adult tissue that is able to repair itself time and again without scar formation which is in part due to the specific composition of the ECM (Aplin et al., 2008; Evans et al., 2011; Hawkins and Matzuk, 2008).

Table 1 summarizes the changes of ECM protein levels in the most pertinent publications concerning the human endometrium. The data used were abstracted from histological samples and do not entail a true quantifiable result. Depending on the protocol, antibody used, and the interpretation of the researcher results can vary widely. For example, there is no consensus on the expression of collagen VI in the stroma during the menstrual cycle, while Aplin *et al.* suggest that the onset of desmin (a decidualization marker) is correlated with the disappearance of collagen VI signal; this was not stated by Oefner *et al.* (Aplin et al., 2008; Oefner et al., 2015).

Of all the collagens, type I is the most abundant and is consistently present during the menstrual cycle. This is not surprising since they are the major structural proteins of the ECM and make up for 20-30% of the total dry weight of mammals (Law et al., 2017; Parenteau-Bareil et al., 2010). Likewise, type III and VI are also widely distributed during all phases; it was reported that expression of type III does diminish relatively to collagen I, especially during the mid to late secretory phase. Collagen V is an important regulator of

collagen fibrillogenesis; its epitopes were cryptic during the proliferative phase, possibly because of a strong interaction with collagen I (Aplin et al., 1988; Sun et al., 2011). Fibronectin, a glycoprotein, was also abundant in the human endometrium, as is the case for rat and pig (Aplin et al., 2008; Campo et al., 2017; Glasser et al., 1987). Tenascin C is a glycoprotein with a high number of different ligand types, it is involved in cell proliferation and even interacts with pathogens, possibly as barrier or conduit (Midwood et al., 2016). In the human endometrium it is expressed in subepithelial stroma during proliferative phase and around the blood vessel walls during the entire cycle, interestingly becoming absent in the mid secretory phase (Harrington et al., 1999; Yamanaka et al., 1996). It has been postulated that it plays a role in endometriosis because of its correlation with proliferating cells (Tan et al., 2008).

			Secretory		**Decidua**		
		Proliferative	Mid	Late	basalis	parietalis	**References**
Collagen I	S	+/++	+/++		++/++	++/++	(Oefner et al., 2015)/ (Iwahashi et al., 1996)
	Bm	-	-				
	Vw	+	+		+	+	
Collagen III	S	+/+++	+/++	+/++	++/++/++	++/++/++	(Oefner et al., 2015)/ (Aplin et al., 1988)/ (Iwahashi et al., 1996)
	Bm	-/-/-	-/-/-	-/-/-			
	Vw	+/+	+/+		+/+	+/+	
Collagen IV	S	-/-	+		+++/ - to +++	+/ - to +++	(Oefner et al., 2015)/ (Aplin et al., 1988)
	Bm	+/+++	+/+++	+/+++	/+++		
	Vw	+/+++	++/+++	++/+++	++/+++	+/+++	
Collagen V	S	+++ (largly cryptic)	+(partially cryptic)	+	+		(Aplin et al., 1988)
Collagen VI	S	+/+++/+	++/++ to +- /+	++/+ to - /+	++/-	++/-	(Oefner et al., 2015)/ (Aplin et al., 1988)/ (Iwahashi et al., 1996)
	Bm	-/-/-	-/-/-				
	Vw	+/+	+/+	+/+	+/+	+/+	
Laminin	S	-	-	- to +-	- to +++		(Aplin et al., 1988)/ (Harrington et al., 1999)
	Bm	+++	+++	+++	+++		
	Vw	+++	+++	+++	+++		
Fibronectin	S	++	+++	++	++		(Aplin et al., 1988)
	Bm	-	-	-	-		
	Vw	+	+	+	+		
Vitronectin	S	+	-	-	-		(Aplin et al., 1988)/ (Harrington et al., 1999)
	Bm	-	+				
	Vw	-	+				
heparan sulphate PG	S	-	-	- to +	- to +++		(Aplin et al., 1988)
	Bm	+++	+++	+++	+++		
	Vw	+++	+++	+++	+++		
Tenascin	S	++/++	+/+	-/+			(Harrington et al., 1999; Yamanaka et al., 1996)/ (Tan et al., 2008)
	Bm	-	-/+				
	Vw	+	+				

Table 1.Presence of main ECM components in the human endometrium during menstrual cycle. *If no information was given, an empty space was left. + present, ++ strong, +++ very strong, - absent. S: stroma, Bm: basement membrane, PG: proteoglycan, Vw: vascular wall.*

Laminin and collagen IV are the most important components of the basement membrane and present a very similar evolution during the cycle, as is the case with heparan sulphate proteoglycan. First, limited localization beneath endo- and epithelial cells is observed, gradually augmenting until a widespread expression around the surrounding epithelioid cells throughout the mature decidua (Aplin et al., 1988; Oefner et al., 2015). Other and newly discovered members of the BM, peroxidasin and Goodpasture antigen-binding protein, have a distinct spatial and temporal localization and it has been proposed that they could play an important role in the dynamic reorganization and functional changes of the endometrium (Jones-Paris et al., 2017). Other studies investigating the same proteins and several others, have been also done with other mammals, demonstrating the dynamic nature of the endometrium (Guillomot, 1999; Salgado et al., 2009; Scolari et al., 2017).

1.4 Uterine pathologies affecting the human reproductive outcome.

Infertility is defined as "the failure to achieve a clinical pregnancy after 12 months or more of regular unprotected sexual intercourse" and has been recognized as a worldwide public health issue by the World Health Organization (Zegers-Hochschild et al., 2009). It is estimated that worldwide 8-12% of reproductive-aged couples suffer from some degree of infertility and it was reported that 1.9% of child-seeking women aged 20–44 years were unable to have a first live birth (Mascarenhas et al., 2012; Ombelet et al., 2008). Nowadays many pathologies continue resulting in reproductive dysfunction and reproductive tissue engineering could play a transformative role for many of these. Here we will discuss some of the uterine pathologies that could benefit from TE in general and by extension, the investigation done in this thesis.

1.4.1 The uterine factor: absolute uterine factor infertility

Absolute uterine factor infertility (AUFI) affects 1 in every 500 women of fertile age, which translates to possibly up to 1.5 million women worldwide. AUFI can come from congenital origins or be acquired. Acquired AUFI is caused by hysterectomy due to malignant uterine tumor, benign diseases (including leiomyoma and adenomyosis), postpartum hemorrhage, and loss of fertility due to intrauterine adhesions (Asherman's syndrome). The congenital types include Mayer-Rokitansky-Kuster-Hauser (MRKH) syndrome, uterine hypoplasia, and uterine malformation. MRKH syndrome, also referred to as Müllerian agenesis or Müllerian aplasia, afflicts 1 in 4000 to 5000 females and can be described as the agenesis of the uterus and upper two thirds of the vagina (Bombard and Shaker, 2014). Treatment options here were mainly limited to creating neovaginas allowing

the patients to have normal sexual interaction. To this scope, vaginal dilators (Frank's and Ingram's method) and surgical options such as Creatsas vaginoplasty and the Vecchietti procedure were developed. Interestingly, this is also one of the first examples of the successful use of engineered reproductive tissues. In 2014 autologous cells of the patient were incubated *in vitro* for 5 to 6 weeks on a 50:50 poly-(DL-lactide-co-glycolide) scaffold to create an engineered vaginal organ. These were transplanted and reported to be functional in a clinical setting up to 8 years after surgery; its functional variables were in the normal range for desire or arousal, lubrication, orgasm, satisfaction, and absence of pain (Raya-Rivera et al., 2014). Until recently the only viable way for these women to have offspring was gestational surrogacy, having its own set of economic, legal, and ethical challenges (Shenfield et al., 2005). The only true way to restore fertility is by uterine transplantation, the proof-of-concept was recently provided by the Brännström group, where the first successful live birth after uterus transplantation was achieved (Brännström et al., 2015).

1.4.2 The endometrial factor: endometrial atrophy and Asherman's syndrome

Endometrial atrophy (EA) is a pathology where the endometrium never grows thicker than around 7 mm, which is correlated with a decreased probability of pregnancy and is considered as suboptimal for embryo transfer (Mahajan and Sharma, 2016; Senturk and Erel, 2008). It is relatively uncommon among patients treated by assisted reproduction cycles (2.4%) and is encountered more frequently in women older than 40 with non-stimulated cycles (25%)(Mahajan and Sharma, 2016). Miwa et al. characterized this pathology by poor growth of glandular epithelium, high uterine blood flow impedance, decreased vascular endothelial growth factor (VEGF) expression, and poor vascular development (Miwa et al., 2009). In other words, low perfusion and angiogenesis are important factors in EA. In addition, other factors that could lead to a thin endometrium could be of inflammatory, iatrogenic or idiopathic origin. Remarkably, Asherman's syndrome (AS) is also frequently stated as a cause (Mahajan and Sharma, 2016; Senturk and Erel, 2008). Treatment options for this syndrome include oral or vaginal administration of estradiol, sometimes supplemented with human chorionic gonadotropin (hCG) injection, tamoxifen, nitric oxide (NO), granulocyte colony stimulating factor (G-CSF) and regenerative medicine by stem cell therapy (Eftekhar et al., 2018). In a study of Santamaria et al. a 1.5mm improvement was observed after the administration of autologous CD133+ bone-marrow derived stem cells (BMDSCs) through the spiral arterioles by non-invasive radiological procedures.

Furthermore, three out of seven patients treated in this study obtained spontaneous pregnancy (Santamaria et al., 2016).

First described by Joseph G. Asherman (Asherman, 1948), AS is also an uncommon gynaecological disorder, affecting 1.5% in women of reproductive age, and has a prevalence of 19.1% in women after miscarriage, and up to 50% in those with recurrent curettage (Hooker et al., 2014). In AS the functional endometrium is destroyed due to intrauterine adhesions (figure 5). March et al. were one of the first to classify AS patients based on involvement of adhesions, morphology and menstrual pattern. This hysteroscopic classification can be mild, moderate or severe (March et al., 1978). This corresponds to stage I, II and II respectively in the classification used by the American Fertility Association. This can be assessed by ultrasound, sonohysterography, hysterosalpingography and the golden standard, hysteroscopic imaging (Conforti et al., 2013). Hysterotomy, dilatation and curettage, and hysteroscopic surgery are possible treatment options depending on the severity of intrauterine adhesions. In the previously mentioned study of Santamaria et al. the treatment with CD133+ BMDSCs corresponded to a 2.4 mm improvement of the endometrial thickness (Santamaria et al., 2016).

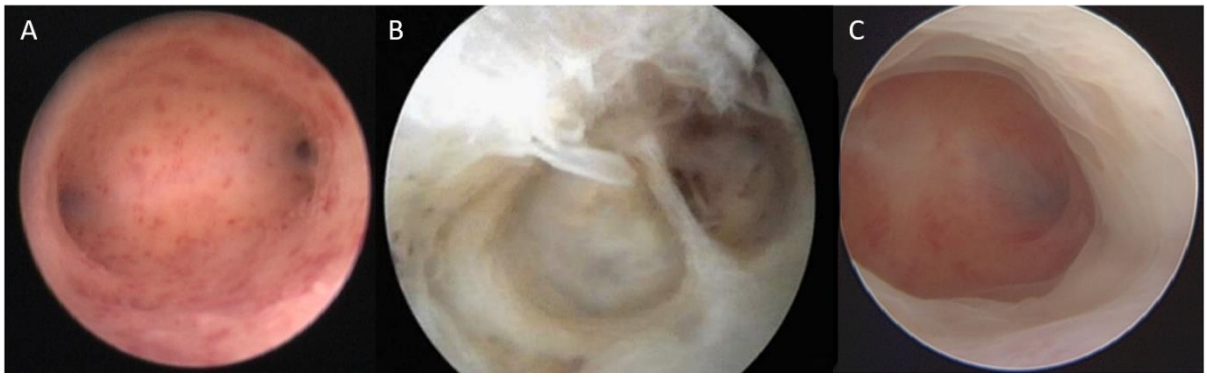

Figure 5. Hysteroscopic view of uterine synechiae. *Hysteroscopic image of healthy cavity (A), total obliteration of uterine cavity by adhesion formation (Asherman's syndrome, B) and post-operative view two months after hysteroscopic surgery for full AS (C). Images by courtesy of dr. Rudi Campo.*

2 Uterine bioengineering: emulating native tissues

2.1 Biomaterials and tissue engineering

Certain pathologies leading to reproductive dysfunction such as AUFI, AS, EA and others are still not or insufficiently treatable. Regenerative medicine seeks to resolve this issue using various tactics and two different, but complementary approaches can be distinguished: cell therapy and tissue engineering. Tissue engineering (TE), represents a promising interdisciplinary field of investigation, combining aspects of cell transplantation,

materials science, and bioengineering. What sets TE apart is the use of biomaterials, which can be implanted directly with or without cells in the patient, or incubated in a bioreactor where they are subjected to mechanical or chemical stimuli resulting in a tissue engineered construct (figure 6) (O'Brien, 2011). These biomaterials or scaffolds are devices or constructions with specific and complex physical and biological functions that interact through biochemical and physical signals with cells and, when implanted, with the body environment. A biomaterial needs to be biocompatible, biodegradable and must possess the right mechanical properties and architecture for its intended use (O'Brien, 2011). The characteristics of these scaffolds can be adapted depending on the source of the scaffold and its corresponding manufacturing methods.

The original aim of TE was first defined by Langer and Vacanti, which is to restore, maintain, or improve function of tissues or whole organs (regenerative medicine, *in vivo* application) (Langer and Vacanti, 1993). However, these engineered tissues have also evolved into a viable option for drug testing, disease modeling, and precision medicine (*In vitro* applications, figure 6) (Wobma and Vunjak-Novakovic, 2016).

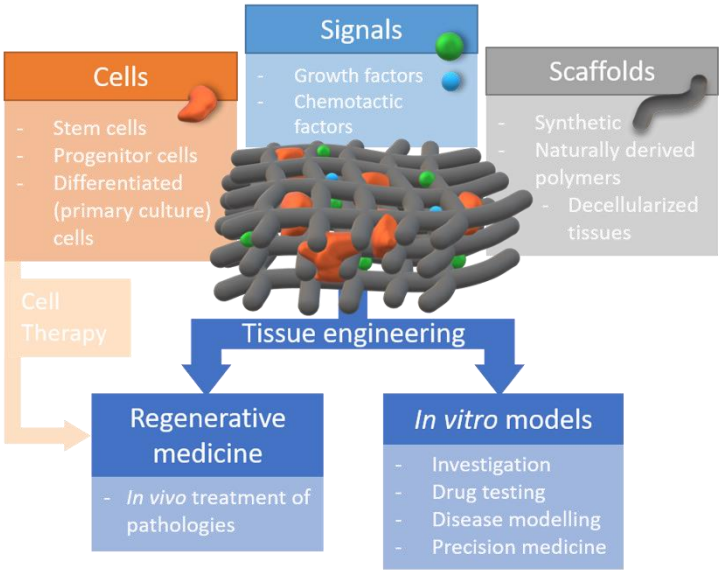

Figure 6. The "tissue engineering triad" for the creation of engineered tissues and their applications. *Cells adhere, proliferate and migrate on and in the scaffolding material, while signals from growth factors (chemical) and bioreactor (biophysical) provide together with the scaffold the correct template for the cell reorganization. These constructs can then be implanted in the patient to treat pathologies or used in vitro as a model that better recapitulates in vivo behavior. Cell therapy, on the other hand, attempts the former by only using cells.*

2.2 Taking design cues from the ideal scaffold: the natural extracellular matrix

The molecular organization of the ECM was already discussed in detail in section 1.3.2 "Evolution of the extracellular matrix during the menstrual cycle". The ECM was once thought to act mainly as structural support for the cells (Bornstein et al., 1978), but now it is clear that this complex mixture of fibrous structural proteins, specialized proteins, GAGs and proteoglycans (PGs) plays an important role in cell migration, proliferation and

differentiation (Beattie et al., 2008; Turner and Badylak, 2013). The central role of the ECM is apparent when looking at the first stages of developing embryo, where it is synthesized and secreted by the cells in the earliest phases of development and has vital roles in germ line separation, morphogenesis and organogenesis (Daley et al., 2008; Tsang et al., 2010). Also, the effects of the physical properties of the ECM such as stiffness play an important role in stem cell lineage specification (Lv et al., 2017). There is ample evidence that there is an active interaction between the cell and its ECM with its surroundings and stress, regulating protein turnover and remodeling (Swift and Discher, 2014).

For every tissue and organ, there is a bidirectional interchange between the cell and its surrounding ECM. This mutual instructional relationship results in a dynamic and constant remodeling of the ECM during homeostasis or injury. Cells do this by the production of ECM (precursor) proteins and secretion of matrix metalloproteases (MMPs), which is influenced by the information provided by mechanotransduction or (cryptic) biochemical signals from the ECM. This state is called "dynamic reciprocity" (figure 7); a good example for this are the astronauts suffering from microgravity-induced osteoporosis after prolonged stays in outer space (Vico et al., 2000). This also means that the dynamic composition and three-dimensional organization of the ECM is unique and for each tissue, in order for them to preform tissue-specific cellular functions, making it a potentially ideal biological scaffolding material (Nelson and Bissell, 2006; Schultz et al., 2011; Thorne et al., 2015).

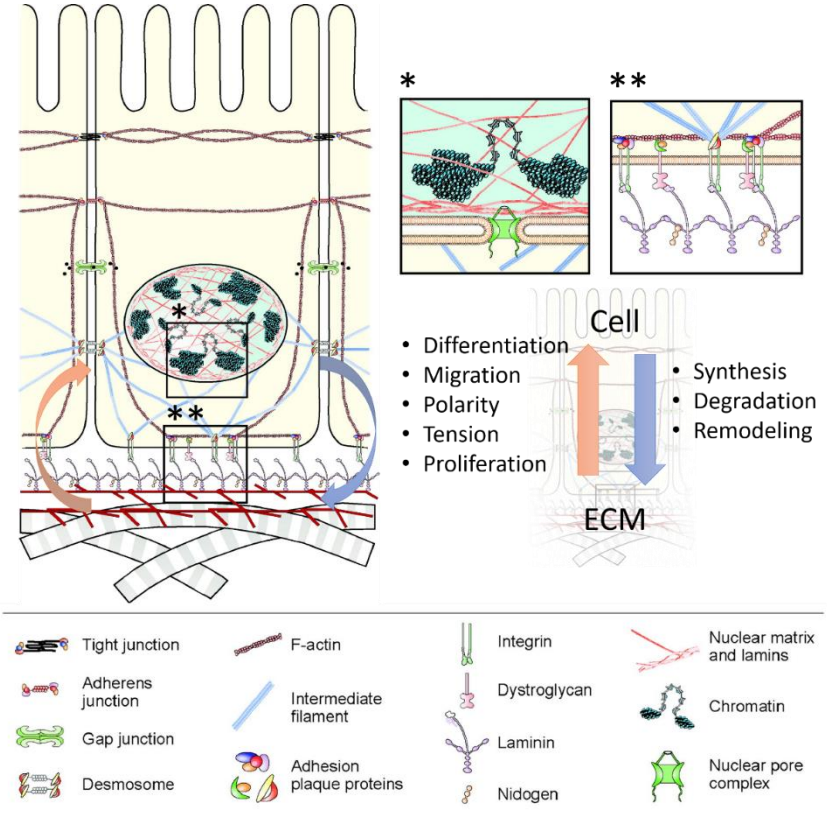

Figure 7. The dynamic reciprocity of cells and ECM. *A relatively complete view of the interactions between cells and the ECM constituting the reciprocal interactions and contributing to the "original" reorganization. Adapted from (Nelson and Bissell, 2006) with permission from Annual reviews.*

Table 2 summarizes what encompasses an ideal biomaterial/scaffold by comparing it to the functions of the ECM. These functions are to serve as a physical environment that will support cells, to have similar mechanical properties such as rigidity and elasticity, to provide bioactive cues to regulate the cellular activity, to able to sequester growth factors and lastly to be degradable (Chan and Leong, 2008). This last one is important, so that the cells can replace the scaffold with their own ECM over time, converting the tissue engineered construct into true native tissue. This artificial extracellular matrix can be produced from synthetic materials, naturally derived polymers or obtained via a process called decellularization, where cells are removed from their natural complex ECM.

	Functions of ECM in native tissues	Analogous functions of scaffolds in engineered tissues	Architectural, biological, and mechanical features of scaffolds
1	Provides structural support for cells to reside	Provides structural support for exogenously applied cells to attach, grow, migrate and differentiate *in vitro* and *in vivo*	Biomaterials with binding sites for cells; porous structure with interconnectivity for cell migration and for nutrients diffusion; temporary resistance to biodegradation upon implantation
2	Contributes to the mechanical properties of tissues	Provides the shape and mechanical stability to the tissue defect and gives rigidity and stiffness to the engineered tissues	Biomaterials with sufficient mechanical properties filling up the void space of the defect and simulating that of the native tissue
3	Provides bioactive cues for cells to respond to their microenvironment	Interacts with cells actively to facilitate functions such as proliferation and differentiation	Biological cues such as cell-adhesive binding sites; physical cues such as surface topography
4	Acts as the reservoirs of growth factors and potentiates their actions	Serves as delivery vehicle and reservoir for exogenously applied growth-stimulating factors	Microstructures and other matrix factors retaining bioactive agents in scaffold
5	Provides a flexible physical environment to allow remodeling in response to tissue dynamic processes such as wound healing	Provides an empty volume for vascularization and new tissue formation during remodeling	Porous microstructures for nutrients and metabolites diffusion; matrix design with controllable degradation mechanisms and rates; biomaterials and their degraded products with acceptable tissue compatibility

Table 2. The design cues from the native ECM. *Functions of the natural ECM, the manner of which the scaffolds mimic these and the various features necessary to copy these functions. Reprinted from (Chan and Leong, 2008) with permission from Springer-Verlag.*

Advances in biomaterials, stem cells, cellular microenvironment and differentiation factors have created unique opportunities for tissue engineering in reproductive medicine. Recently a definition for "reproductive tissue engineering" or REPROTEN has been coined as follows: "An interdisciplinary field that applies tissue engineering strategies to restore fertility and/or improve the quality of life of patients affected by reproductive dysfunction through creation, replacement or regeneration of cells, tissues or organs of the reproductive

system."(Amorim, 2017). This exceedingly rapid progress using bioengineered constructs *in vitro* and in small animal models for REPROTEN purposes shows the increasing interest in this field. More research must be done however using different scaffolds (synthetic/natural), growth factors and cell combinations before starting clinical trials in humans. Within this chapter the most prominent and representable publications will be discussed. Firstly, we will evaluate the most relevant synthetic and naturally derived polymer scaffolds used in uterine bioengineering, followed by the rationale for decellularized bioscaffolds and the relevance to convert them into hydrogels. Figure 8 gives an overview of all biomaterials currently used for uterine tissue engineering.

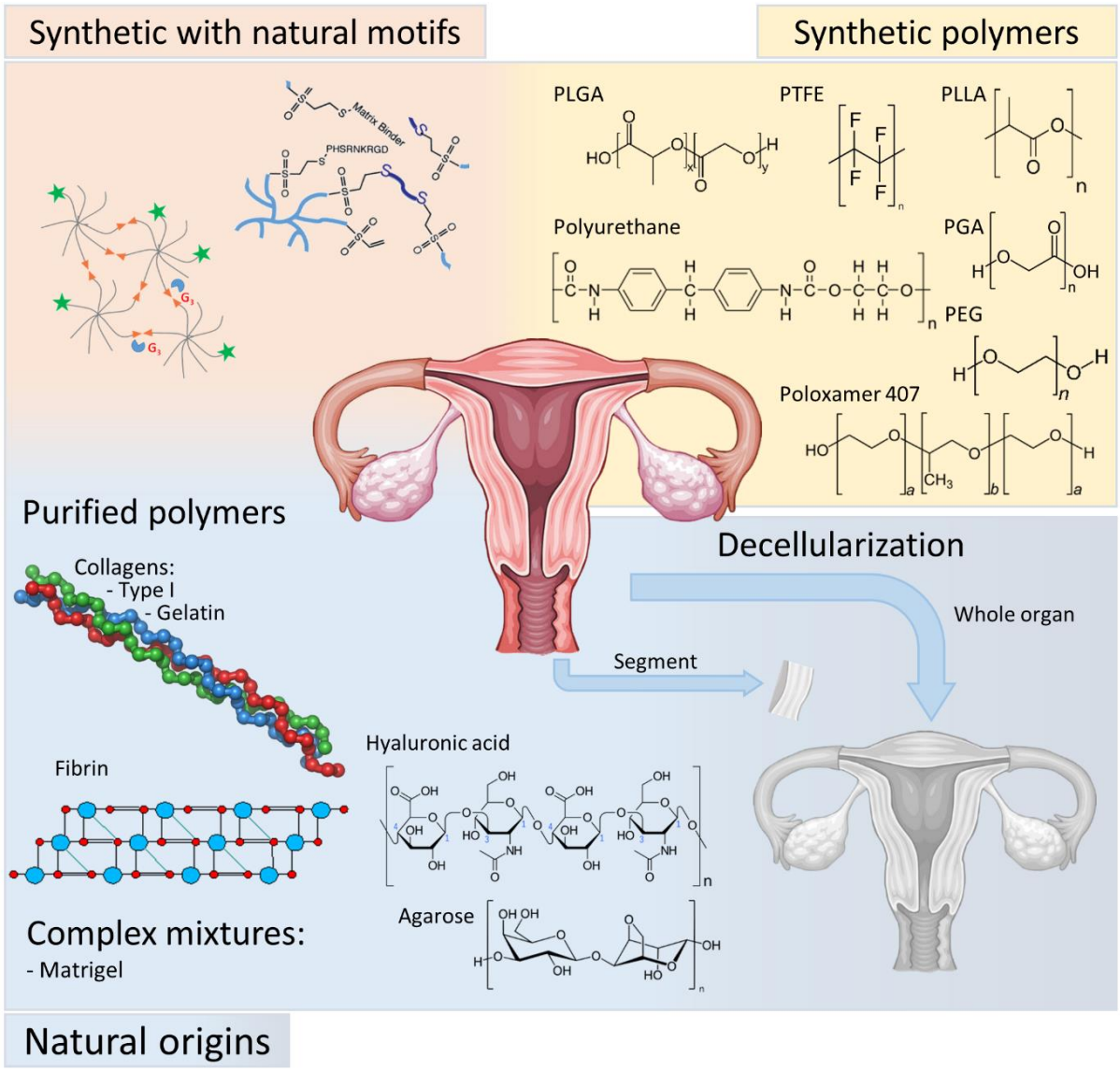

Figure 8. The various biomaterials used in uterine bioengineering. *The biomaterials can be divided in: solid or hydrogels; and come from natural and/or synthetic origins and/or a combination of both.*

2.3 Solid biomaterials for reproductive medicine: synthetic and naturally derived polymers

Synthetic scaffolds are very valuable in biomedicine; they have a known exact composition, long shelf lives, and large quantities can be produced under controlled conditions with very little variability, making them cheaper and more reliable than natural polymers. Downsides are a reduced bioactivity and possible toxicity from the scaffold or its degradation products (Place et al., 2009). Two main groups within synthetic scaffolds are ceramics and synthetic polymers; the latter can be divided further into solid scaffolds or hydrogels, each with their own advantages and downsides for uterine bioengineering. Solid scaffolds use manufacturing processes that are incompatible with cells; this is why surface topography, porosity and pore size are very important, influencing cell penetration, growth and attachment, moreover different cell types have specific ideal pore diameters and porosity (Wei and Ma, 2004). In reproductive medicine, porous scaffolding material such as vicryl mesh and polyetherurethane and poly-L-lactic acid (PU/PLLA) tubes have been considered for *in vitro* modelling and *in vivo* testing (Jonkman et al., 1986; Young et al., 2003). Furthermore, (nano-) fibrous scaffolds can be made using electrospinning as done by MacKintosh *et al*. to create an *in vitro* 3D model of bovine endometrium using primary epithelial and stromal cells. The resulting construct had stromal cells depositing fibronectin and a polarized epithelium and was reactive to oxytocin plus arachidonic acid or lipopolysaccharide (LPS) (MacKintosh et al., 2015).

Biomaterials derived from natural origins are regarded as the first biomaterials used clinically and have several inherent advantages; they already contain receptor-binding ligands present in the ECM that results in excellent cell interactions, adhesion, growth and biocompatibility (Nair and Laurencin, 2007). Furthermore, they are biodegradable and can be remodeled natively by the cells. However, there are concerns considering a possible immunogenic response and/or pathogen transmission (Hortensius and Harley, 2016). The extraction and purification of these diverse compounds can also be complicated, hence creating a homogenous scaffold in a reproducible fashion can be difficult, especially compared to their synthetic counterparts. They also have limited mechanical stability what makes them less ideal for load bearing applications (Alaribe et al., 2016). Naturally derived polymers can originate from proteins, polysaccharides or both (composites) (Alaribe et al., 2016; Ige et al., 2012; Willerth and Sakiyama-Elbert, 2008). Protein based biomaterials include collagen, gelatin, elastin, fibrin and silk while hyaluronan, chitosan, alginate and agarose are examples of polysaccharide-based biomaterials.

Collagen is by far the most widely used naturally derived polymer for uterine bioengineering. It is very versatile, promotes cell adhesion, migration and differentiation and can be used as solid porous scaffolds (sponges) fabricated by freeze drying (Oh et al., 2012), nanofibrous material (Law et al., 2017) and hydrogels (Xu et al., 2017) among others. Furthermore, it has been demonstrated that human fibroblasts are attracted chemotactically by their degradation products, possibly assisting in regeneration (Postlethwaite et al., 1978). Its usability and versatility were demonstrated in various *in vivo* animal models, mainly by the groups of Jianwu Dai and Yali Hu: Li et al. used a collagen scaffold loaded with a recombinant angiogenic growth factor (basic fibroblast growth factor, bFGF). Attempting to decrease the diffusion out of the scaffold, this was fused with collagen binding domain (CBD) derived from mammalian collagenase to create a collagen/CBD-bFGF scaffold. When grafted in a severe uterine horn damage model, the scaffold yielded a higher reconstruction rate of both myo- and endometrium compared to collagen/phosphate buffered saline (PBS) and collagen/natural bFG. In addition, , embryos were present in the grafted site but at a lower rate than the sham group (Li et al., 2011). Following this, the same base collagen scaffold was incubated *in vitro* with different types of stem cells before transplantation (Ding et al., 2014; Song et al., 2015). For its study, Ding et al. used bone marrow-derived mesenchymal stem cells (BM-MSC). After transplantation, a higher expression of growth factors, bFGF included, was measured in the implanted collagen/BM-MSC scaffold and showed improved regeneration and neovascularisation. The graft sites supported implantation, but it is unclear if actual placentation took place, as commented by others (Hellström et al., 2017). Similarly, Song et al differentiated human embryonic stem cells (hESC) to endometrium-like cells using a co-culture system with cytokines and human endometrial stromal cells and seeded these on a collagen scaffold (Song et al., 2015). As with previous investigations, less scar formation, an improved recovery and fertility was observed. Interestingly, very little hESC derived cells were present in the regenerated tissue, suggesting that via auto- or paracrine signaling endogenous cell migration, proliferation and differentiation takes place. In these examples, the bioreactor used was an *in vitro* setup; Campbell *et al.* on the other hand, used an unique kind of bioreactor by transplanting a molded blood clot autologously in the rat (Campbell et al., 2008). This activates the foreign body response and after 2-3 weeks myofibroblast-rich tissue encapsulating the mold was created, expressing genes indicating the capacity to further differentiate smooth muscle and possibly other cells (Le et al., 2010). This tissue was removed from the blood clot and used to regenerate excised segments of the uterine horn. Over a 12-week period, an increasingly

structurally complex tissue was formed, showing the main structural components of the uterus: simple columnar epithelium and glands within the endometrium and two distinct muscle layers of the myometrium. Full placentation on the grafting site did not take place, possibly because of insufficient vascularization. Nonetheless, it demonstrates the feasibility of a creative way to create implantable tissue using the host as a bioreactor instead of *in vitro* culture.

These *in vivo* studies show that it is possible to regenerate the entire uterine wall using tissue engineering, albeit imperfectly. The most challenging issues to overcome are improving vascularization, placentation and implantation of embryos on the graft. Much promise can be found in decellularized tissues that consist out of a complex mixture of the component molecules of the ECM of the uterus, where even vascularized acellular scaffolds can be obtained.

2.4 Decellularization of tissues and organs

Decellularization (DC) intends to use the tissue-specific and complex ECM and utilize it as a bioscaffold for tissue engineering. The concept of DC is to remove all the cells or cellular material from a tissue or organ, while minimizing any adverse effect on the hierarchical complexity, composition and the three-dimensional ultrastructure of the ECM (Gilbert et al., 2006). The origins of DC can be found in de late 40's, where Poel *et al.* found that homogenizing muscle tissue at – 70 °C, followed by centrifugation resulted in the removal of cells from the tissue (Poel, 1948). Real clinical approaches only came 50 years later by the likes of Badylak *et al.*; here they used decellularized small intestinal submucosa (SIS) of xenogeneic origin to repair injuries of the Achilles tendon. They demonstrated that SIS-remodeled neotendons were stronger than their controls and that over time the bioscaffold started to be absorbed by the body and replaced by native connective tissue (Badylak et al., 2004). This is also a good example of one of the biggest advantages of decellularized tissue: by removing the cellular antigens, detrimental immunological or inflammatory reactions are attenuated. This means that biomaterials from all allogeneic origins can be used, independent of the source. This can be for example from donations after circulatory death or from previously immunological incompatible sources, expanding the possible donor pool. Furthermore, the main constituents of the ECM are well conserved between species, and decellularized xenogeneic scaffolds have been approved by the Food and Drug Administration (FDA) and are now full-fledged commercial products (Table 3)

(Badylak, 2004). Interestingly, in some *in vitro* studies using xenogeneic ECM yielded better results than their allogeneic counterpart (Young and Goloman, 2013).

Commercial brand/name	Scaffolding materials
AlloDerm®	Freeze-dried human acellular dermal matrix with preserved basement membrane
AlloPatch HD™, FlexHD®	Acellular human dermis derived from human allograft skin
Epic™, SJM Biocor®	Acellular porcine heart valve leaflets
Prima™ Plus	Porcine acellular valve
Perimount®	Bovine acellular pericardium valve leaflets
MatriStem®, Acell Vet	Porcine acellular urinary bladder matrix
Oasis®, SurgiSIS®	Porcine small intestine submucosa (SIS) acellular grafts
Strattice™	Acellular porcine dermis
TissueMend®	Fetal collagen scaffold from acellular fetal bovine dermis
CorMatrix ECM™	Acellular scaffold from porcine small intestine
Meso BioMatrix™	Acellular tissue graft derived from porcine peritoneum
IOPatch™	Acellular human sclera graft
SureDerm	Human acellular lyophilized dermis
Permacol Surgical Implant	Acellular porcine dermal implant
Synergraft®	Decellularized porcine heart valves

Table 3. Some examples of commercial solutions made from decellularized tissues. *Adapted from (Rana et al., 2017) with permission from John Wiley and Sons.*

There are three main methods used to decellularize tissues or organs: these are physical, biological and chemical (figure 9) (Crapo et al., 2011; Keane et al., 2015).

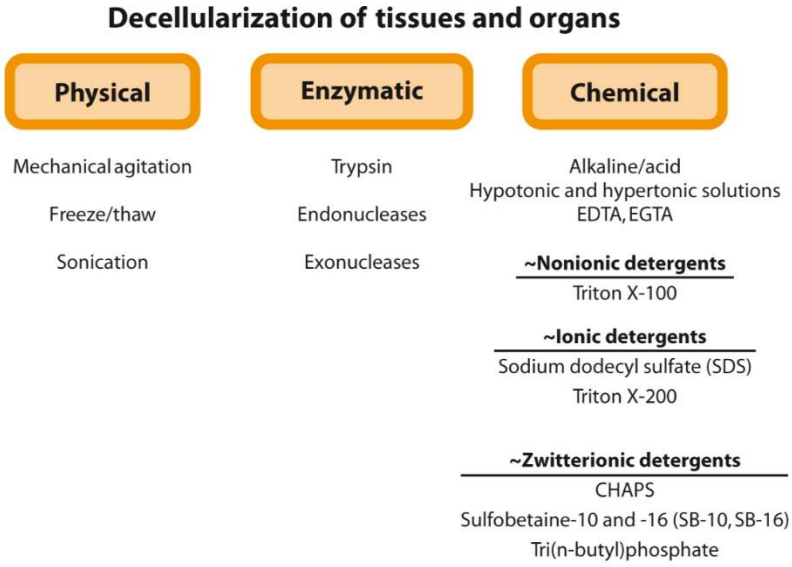

Figure 9. The various ways of decellularizing tissues and organs. *The main physical, biological and chemical techniques and components are also presented. Reprinted from (Badylak et al., 2011) with permission from annual review of biomedical engineering.*

Usually a combination of these techniques is used; the first being most commonly combined with the others since physical methods usually result in insufficient DC. These include freeze–thaw cycles, agitation, pressure gradients or using supercritical fluids. Biological methods include the use of chelating agents and enzymes such as nucleases,

trypsin and dispase that cleave specific peptides and (deoxy)ribonucleotide chains. Finally, the most popular methods include the use of various chemical agents. These can be acids and bases, hypo/hypertonic solutions, (non/zwitter-) ionic detergents, alcohols and other types of solvents. The goal is to remove the cellular material as efficiently as possible; if not inflammation can occur. Other causes for inflammation include: altered tissue matrix biochemistry and residual detergents or endotoxins. For now, there are no official guidelines to define successful DC, mainly because of the heterogeneity between tissues and their corresponding DC protocols. Crapo et al postulated a three-part criteria: (1) <50 ng dsDNA per mg ECM dry weight, (2) <200 bp DNA fragment length and (3) lack of visible nuclear material in tissue sections stained with 4′,6-diamidino-2-phenylindole (DAPI) or hematoxylin and eosin stain (H&E) (Crapo et al., 2011).

Decellularization has been successfully applied to virtually all tissues and organs. This goes from singular tissues such as blood vessels (Pashneh-Tala et al., 2016; Quint et al., 2011), small intestinal submucosa (SIS) (Badylak, 2007; Badylak et al., 1989), nerve (Hudson et al., 2004; Hundepool et al., 2017), cornea (Hashimoto et al., 2010; Shafiq et al., 2012), tendon (Pridgen et al., 2011), amniotic membrane (Wilshaw et al., 2006, 2008) to entire complex organs like the kidney (Nakayama et al., 2010; Sullivan et al., 2012), liver (Baptista et al., 2013; Uygun et al., 2010) and heart (Ott et al., 2008).

DC protocols for the major reproductive tissues and organs such as ovaries (Laronda et al., 2015), testis (Baert et al., 2015), endometrium (Olalekan et al., 2017), uterus (Campo et al., 2017; Hellström et al., 2016; Miyazaki and Maruyama, 2014) and the placenta (Kakabadze et al., 2018) have also been established. A summary of all studies using decellularized whole uteri and fragments is given in table 4.

2.4.1 Decellularization of uterine tissues

The optimal DC methodologies and applications depend on the organ characteristics and the final objective (*in vitro* models, aiding regeneration of tissues or organs, regenerating entire organs etc.). Correctly decellularized tissues represents the ideal biological support for the development and homeostasis of cells, tissues and organs (Badylak, 2007; Crapo et al., 2011). The studies that decellularized only fragments of the uterus, not using perfusion-based techniques, are discussed here.

The myometrium was the first uterine tissue from which tissue engineered constructs (neo-myometrial tissue patches) were created by *in vitro* culturing myocytes on a myometrial decellularized scaffold (Young and Goloman, 2013). The long-term goal of the

study is to create a scaffold capable of restoring uterine defects before pregnancy and for this reason, both autologous and non-autologous tissue was used and evaluated. This approach yielded 2 types of myometrium: allo-neo myometrium (components from the same species) and xeno-neo-myometrium (human and rat components). When artificial defects were introduced in rat allo-neo myometrium extensive scaffold remodeling would occur over time. A general observation was that cells much better preferred the second type of myometrium, providing an adequate three-dimensional (3D) environment for *in vitro* cell culture, forming typical myometrial-bundles structures that showed coordinated contractions. It would be interesting to see how this model would be improved when the construct is exposed to an external (pulling) force during cultivation, possibly aiding cell alignment.

In order to better mimic the *in vivo* setting, an innovative and inclusive 3D *in vitro* culture system was created throughout 2017. Here, 3D models of various decellularized tissues were connected via microfluidics, recreating entire anatomical systems (Xiao et al., 2017). For this, they integrated female reproductive tract tissues (murine ovary, human fallopian tube, endometrium, ectocervix) and liver in a new platform called EVATAR. This system allows to study the organ-organ interactions beyond the female reproductive tract during the human menstrual cycle. Specifically, endometrial cells were grown in decellularized uterine scaffolds (pieces of human DC endometrium) and placed in microfluidic cultures simulating 28-day menstrual cycle. Stromal and epithelial cells expressed, typical hormonal (ER and PR, estrogen and progesterone receptor respectively) and proliferative markers (Ki-67) at the end of 28-day culture, indicative of active cell proliferation and uterine cell characteristics. This investigation demonstrated the potential of organs-on-a-chip and can possibly provide a potent tool for basic and translational research in reproductive medicine (Nawroth et al., 2018).

Table 4. A summary of studies using biomaterials from decellularized uterine tissues. *Abbreviations used: DC: decellularized; GFP-MSCs: Green Fluorescent Protein-Mesenchymal Stem Cells; SDS: sodium dodecyl sulfate.*

Decellularized tissues	Species	Description	Cells used	*In vivo* transplant?	Results	Ref.
Myometrial segments	Rat and human	Proof of principle creating allo- and xeno-neo-myometrium *in vitro* using tissue-engineering techniques.	Human and rat myocytes	No	Allo-neo myometrium from rats: poor surface overgrowth, no bundle formation. Xeno-neo-myometrium: good cellularity, cell viability and showed coordinated contractions.	(Young and Goloman, 2013)
Uterine segments (myo- and endometrium)	Rat	Assessment of 3 different DC methods with *in vivo* evaluation (transplant + fertility evaluation).	/	Yes (up to 51 days)	Optimization of the protocol depends of the type of samples. Demonstration of a functional uteri after partial reconstruction in Sprague Dawley rats.	(Santoso et al., 2014)
Whole uterus	Rat	First whole uterus DC through perfusion and assessment of regeneration and reconstruction of uterine tissues *in vitro* and *in vivo*.	Neonatal + adult uterine cells, and rat mesenchymal stem cells	Yes (up to 90 days)	Aortic perfusion with anionic detergents (SDS) preserved tissue architecture and microvasculature in the rat uterus. *In vitro* recellularization was achieved after reseeding with endometrial cells, the *in vivo* approach suggested the promising use of this scaffold to partially regenerate the uterus	(Miyazaki and Maruyama, 2014)
Whole uterus	rat	Quantitatively biochemical and mechanical comparison of three different DC protocols.	/	No	Triton X-100/dimethyl sulfoxide/H2O yielded a compact, weaker scaffold. A sodium deoxycholate/dH2O protocol resulted in a porous scaffold resembling the native uterus more.	(Hellström et al., 2014)
Whole uterus	rat	Creation of bioengineered uterine constructs derived from whole organ DC in female rats.	Rat uterine primary cells and GFP-MSCs	Yes (3 days static *in vitro* culture + 9 weeks)	They reached *in vitro* cell culture with uterine primary cells and GFP-MSCs and partial transplantation *in vivo* demonstrating the ability to give support during pregnancy.	(Hellström et al., 2017)
Uterine segments (myo- and endometrium)	Mouse	Establishment of mouse model of decellularized uterine matrix (DUM) transplantation.	/	Yes (up to 7 weeks)	Regeneration in all layers was observed, starting with epithelium. STAT3 is suggested as an important player for uterine epithelial regeneration.	(Hiraoka et al., 2016)
Mouse ovary + human fallopian tube, endometrium, ectocervix and liver	Mouse + human	Creation of a new *in vitro* organs-on-a-chip model using 3D cultures of reproductive tract tissues and peripheral organs connected by	Endometrial primary culture	No	A microphysiologic and dynamic culture system that is reconfigurable was established. Murine ovarian follicles survived and recapitulate a complete 28-day human menstrual cycle.	(Xiao et al., 2017)
Endometrial tissue	Human	Development of novel 3D model using the decellularized human endometrium reconstructed with primary cells.	Human endometrial prim. culture	No	The recellularized scaffold contained viable proliferating cells reacting to 28-day ovarian steroid hormone regimen.	(Olalekan et al., 2017)
Whole uterus	Pig	Establishment of a decellularization protocol usable for large reproductive organs that preserves components ECM, ultrastructure and vasculature and is compatible for recellularization.	Human endometrial SP stem cell lines	No	Using an SDS and Triton X-100 based protocol they demonstrated the removal of cells and DNA content, the preservation of most important ECM components, 3D architecture and vascular integrity and the successful recellularization preserving	(Campo et al., 2017)
Uterus ECM powder (65 vol%) + PLGA polymer (35 vol%)	Bovine	The development of "tissue papers" using native porcine tissues/organs and assessing their mechanical properties, cell compatibility and manageability.	Human MSCs	No	Large surface tissue papers were created that were structurally stable with adhesion, proliferation and infiltration of MSCs shown.	(Jakus et al., 2017)

Moreover, Olalekan *et al.* described a novel 3D *in vitro* model from decellularized human endometrium supporting endometrial cell proliferation, hormone receptor expression and production of secretory factors (Olalekan et al., 2017). Human endometrial pieces were decellularized with Triton X-100 and sodium deoxycholate for 48 hours, decellularized fragments were recellularized with expanded endometrial cells and finally 28- day hormone protocol was used to mimic the human menstrual cycle. The three-dimensional model described here permits to study the physiology and patho-physiology of the human endometrium.

2.4.2 Whole uterus decellularization

The last and unique advantage of decellularized biological scaffold is the ability to decellularize entire organs by perfusion. By using the vascular system, decellularization agents are delivered to all layers of the organ, where they lyse the cells. Cellular debris is then removed, leaving an acellular vascularized three-dimensional bioscaffold. The scaffold can then be placed in a bioreactor, where (autologous) stem cells are introduced to recreate whole new organs (figure 10). This bioengineering approach could be an answer to the main problems currently plaguing transplantations, namely shortage of donor organs, organ rejection and immunosuppressant-related side effects (Sayegh and Carpenter, 2004).

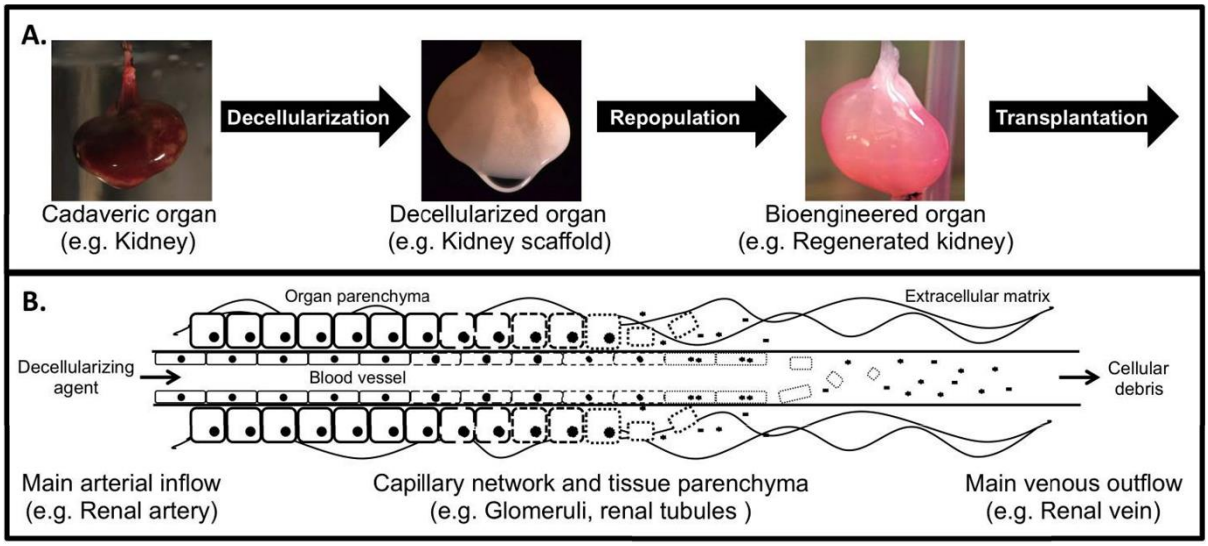

Figure 10. Decellularization of solid organs by perfusion. *Concept of whole-organ tissue engineering to obtain vascularized three-dimensional scaffolds as a platform to bioengineer functional organs. Organs from cadaveric donors are obtained and subjected to a specific DC protocol, preserving vasculature and specific extracellular ultra-architecture and composition. Reconstitution takes place in a biomimetic bioreactor using (stem)cells, the recreated (autologous) organ can then be transplanted (A). Visualization of the perfusion decellularization process. Decellularizing agents are pushed through the organ using peristaltic pumps, removing cells and cellular debris via the vascular system (B). Reprinted from* (Tapias and Ott, 2014) *with permission of Wolters Kluwer Health, Inc.*

While the first decellularization step is already relatively well established, the optimal protocol is yet to be determined for each individual organ. Furthermore, while the creation and extraction of (induced) pluripotent stem cells is making much progress, there is still much research to be done to effectively recellularize these scaffolds in pursuit of the creation of a fully functional solid organ.

The seminal work done by Ott *et al.* in 2008, where a decellularized mouse heart was repopulated with neonatal cardiocytes, represented a breakthrough in the field of TE (Ott et al., 2008). Eight days after cell seeding, the construct showed spontaneous contractions and was responsive to drugs; Even though the construct was not mature enough to become transplantable and it did not recapitulate heart functions perfectly *ex vivo,* it was a very important pioneering study showing the possibilities of whole organ tissue engineering.

The first study describing this in reproductive organs was published by Miyazaki and Maruyama in 2014 (Miyazaki and Maruyama, 2014). Firstly, they demonstrated the successful DC after aortic perfusion with anionic detergents (SDS), showing that the tissue architecture and microvasculature of the rat uterus was preserved in the acellular tridimensional scaffold. Moreover, *in vitro* recellularization (RC) was achieved after reseeding endometrial cells in the new structure; the *in vivo* approach suggested the promising use of this scaffold to regenerate the uterus.

In parallel, Hellström and collaborators compared three different protocols for whole rat uterus DC. These protocols were based on the perfusion of different ionic and detergent solutions with or without freeze-thaw steps; a comparison was made by proteomic analysis, protein and DNA quantification and mechanical tests, among others (Hellström et al., 2014). This study was done to further the development of organ-specific decellularization protocols for the uterus. In a follow-up study the recellularization efficiency and regenerative capability these scaffolds were investigated. Using these protocols, three patches were repopulated *in vitro* with uterine primary cells and GFP-MSCs (Green Fluorescent Protein-Mesenchymal Stem Cells) and transplanted in the uterine horn. The constructs were able to support pregnancy, and interestingly no labeled MSCs remained 8-9 weeks after transplantation. Concluding, whole uterus DC in rats provides an excellent tool for uterine tissue repair giving rise to bioengineered constructs/patches suitable for recellularization, transplantation and future pregnancies (Hellström et al., 2016).

In pursuit of a whole organ DC protocol usable for large reproductive organs, Campo and collaborators have recently described the application of these techniques towards this goal (Campo et al., 2017). They demonstrated the complete removal of cells and DNA

content, the preservation of ECM components, the maintenance of 3D ultra-architecture and vascular integrity. Furthermore, they showed that disc shaped endometrial fragments, when covered with endometrial Side Population (SP) stem cells formed organoid like structures, where selected cell functions and phenotypes were preserved.

Despite these efforts, whole organ recellularization and regaining some functionality *in vitro* as done in other organs has not been achieved (Garreta et al., 2017; Ott et al., 2008; Remuzzi et al., 2017). Bioengineering of the uterus is still very much in its infancy and further studies are required to be able to apply these techniques for human reproductive medicine. An interesting and versatile alternative for using these solid scaffolds are hydrogels, who have the potential to improve many current investigative models and even provide novel treatment options for patients.

3 Synthesis and applications of hydrogels in reproductive medicine

3.1 Hydrogels: form and function

Hydrogels are made of an insoluble network of crosslinked hydrophilic polymers, capable of absorbing thousands of times their dry weight in water or biological fluids through capillary, osmotic and hydration forces (Hoffman, 2012; Kopeček, 2007). Because of this, hydrogels swell instead of dissolve and have a soft, rubbery consistency mimicking that of biological tissue, thus minimizing the inflammatory reaction of the surrounding cells (Buwalda et al., 2014). This three-dimensional (3D) hydrated polymeric network is mechanically stable and porous, permitting the transport of nutrients, oxygen and metabolic waste products. Furthermore, depending on their method of crosslinking, cells can be incorporated uniformly in the 3D environment during gelation (Drury and Mooney, 2003; Uludag et al., 2000). Based on these different mechanisms we can distinguish chemical and physical hydrogels, these can be made of synthetic, natural polymers or both. Physical crosslink mechanisms are generally reversible and include entangled chains, hydrogen bonding, hydrophobic interaction and crystallite formation. Chemical hydrogels on the other hand are crosslinked covalently, are permanent and mechanically stronger, but its polymerization can have toxic effect on cells (Maitra and Shukla, 2014; Varaprasad et al., 2017).

In addition, hydrogels can be categorized based on the source of the polymers, the polymeric composition, network electrical charge and physical appearance (Figure 11)

(Ahmed, 2015). Using the latter, we can make a division between solid, semisolid and liquid hydrogels. For REPROTEN and regenerative medicine the most interesting type is liquid hydrogels, which have a liquid precursor solution that can be complemented with cells, drugs or other molecules of interest. When injected at the site of interest a gel is formed in the body, perfectly adapting to its surroundings (Yang et al., 2014).

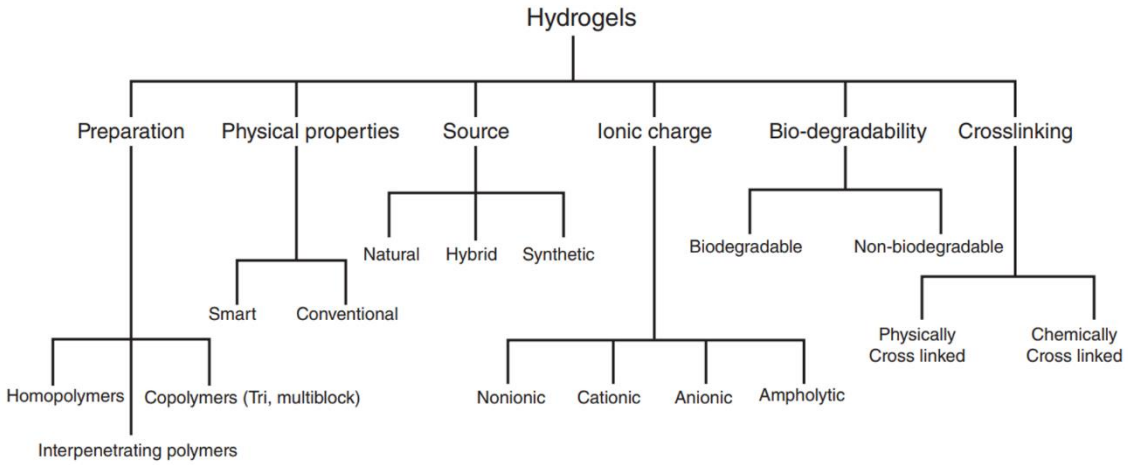

Figure 11. The different classifications of hydrogels. *This can be based on different features such as preparation, physical properties, source, ionic charge, bio-degradability and crosslinking we can classify the hydrogels. Reprinted from (Kumar and Erothu, 2016) with permission of John Wiley and Sons.*

Hydrogels could be an option to improve treatment via cell therapy, which solely relies on the administration of living cells. These cells are usually (induced) stem cells of different plasticity and can be autologous/homologous cells (from the same individual), heterologous/allogeneic cells (from the same species but different person/animal), and xenogeneic cells (different species) (Weinberg, 2013). For now, 2257 clinical trials using stem cells have been completed and about the same amount are still underway or starting up (data from www.clinicaltrials.gov). A preference is found for autologous cells, alleviating possible immune reaction concerns. Likewise, these cells can be administered in a non-invasive fashion simply by injection. Major limitations are high cell death and low engraftment efficiency, diminishing its effect and usability. Nevertheless it is a promising line of investigation for various fertility restricting pathologies (Herraiz et al., 2018; Santamaria et al., 2016). A tissue-engineering approach using hydrogels could mitigate most of these problems simultaneously maintaining advantages such as injectability and immunomodulatory characteristics.

Hydrogels are also compatible with a variety of fabrication techniques such as 3D printing, micropatterning and electrospinning, making them even more versatile. An important downside is that they have lower mechanical strength making it a more suited

scaffold for soft tissues, such as the endometrium, but less ideal for load-bearing applications.

A summary of the advantages and disadvantages of hydrogels for TE purposes was given by Hoffman *et al.* and can be found in table 5. As a tool for TE, they have been widely researched for *in vitro* and *in vivo* uses for all tissues, including the uterus (Cook et al., 2017; Hoffman, 2012; Lutolf and Hubbell, 2005; Yang et al., 2017). The distinction here will be primarily made based on the synthetic, natural or hybrid polymeric source.

Advantages	Disadvantages
• Aqueous environment can protect cells and fragile drugs (peptides, proteins, oligonucleotides, DNA) • Good transport of nutrient to cells and products from cells • May be easily modified with cell adhesion ligands • Can be injected *in vivo* as a liquid that gels at body temperature where they adapt to every irregular surface • Usually biocompatible	• Can be hard to handle • Usually mechanically weak • May be difficult to load drugs and cells and then crosslink *in vitro* as a prefabricated matrix • May be difficult to sterilize

Table 5. Advantages and disadvantages of hydrogels for regenerative medicine and in vitro models. *Adapted from (Hoffman, 2012) with permission of Elsevier.*

3.2 Hydrogel applications in reproductive medicine

Hydrogels provide an ideal substrate, encapsulating cells in an aqueous environment. Here, nutrients and oxygen can diffuse to the cells while metabolites and waste products migrate out of the scaffold. The major advantages and drawbacks of natural and synthetic hydrogels coincide mainly with those mentioned previously in section 2.3 "Solid biomaterials for reproductive medicine: synthetic and naturally derived polymers". To summarize, biomaterials derived from natural origins generally have excellent cell interaction, adhesion, growth and biocompatibility. They are also biodegradable and can be remodeled natively (Nair and Laurencin, 2007). Negative aspects are possible pathogen transmission, lesser mechanical strength and complex extraction and purification techniques that could affect price and reproducibility (Alaribe et al., 2016). The most relevant examples here are collagen I, gelatin, fibrin, Matrigel, hyaluronic acid and agarose hydrogels. Synthetic hydrogels on the other hand can control and adapt their physicochemical and biological properties in a very reproducible fashion. Furthermore, they are mechanically stronger and more durable (Garnica-Palafox and Sánchez-Arévalo, 2016). The most commonly used synthetic hydrogels are poly-(ethylene glycol) (PEG), poly-(vinyl

alcohol) (PVA), and poly-(2-hydroxyethyl methacrylate) (PHEMA). The last one being used for over five decades since the pioneering work in the field of hydrogels by Wichterle and Lim (Wichterle and Lím, 1960). An innovative and interesting approach using hydrogels derived from the decellularized reproductive organ could entail the next step from these studies (see section 3.3 "A new era in reproduction and regenerative medicine: extracellular matrix hydrogels and coatings").

The three most frequently used hydrogels for uterine bioengineering are the naturally derived Matrigel and collagen I, and the synthetic polymer PEG. These hydrogels are studied *in vivo* as a novel treatment for uterine pathologies or as *in vitro* 3D cell culture model with the goal of becoming platforms for drug testing, investigating cell-cell interactions, modelling implantation and studying pathophysiology. In the following sections we will discuss how and for which goals hydrogels in reproductive medicine are being used.

3.2.1 Three-dimensional organotypic culture models

Hybrid hydrogels made with functionalized PEG polymers were used to investigate 3D heterotypic cell cultures in two studies by the group of Linda G. Griffith (Cook et al., 2017; Valdez et al., 2017). Cook *et al.* created a modular synthetic ECM using vinyl sulfone activated PEG crosslinked with an MMP substrate for remodeling and with attachment ligands. For this hybrid gel, *PHSRN-K*-RGD, a mimic of the FN-III 9–10 domain binding site was selected as the optimal ligand for initial attachment of both epithelial and stromal cells (Cook et al., 2017). Using the same methodology Valdez *et al.* created a modular, synthetic and dissolvable ECM (MSD-ECM). For this, a substrate for exogenous sortase A (SrtA), a bacterial transpeptidase with very few known mammalian substrates was added to the previous model. The gel rapidly dissolves (5 minutes) and neither the construct nor SrtA negatively affected stromal-epithelial co-cultures. This model enables the measurement of cytokine and growth factors within the gel, instead of the supernatant, without using standard proteolytic methods that also deplete the proteins of interest. A rudimentary computational network model was presented as a proof-of- concept to possibly test disease models and discover potential therapeutic targets in the future (Valdez et al., 2017).

These models are a significant improvement over the first 3D endometrial culture system; these "organ culture explant systems" consisted of whole pieces of endometrium left in culture conditions (Glenister, 1961; Landgren et al., 1996). These culture systems cannot be maintained for long periods of time because of necrosis, are very complex to manage and have much variability between samples (Fasciani et al., 2003; Schafer et al., 2011). The first use of hydrogels as 3D models were published by Bentin-Ley *et al.*; in this study stromal cells

were embedded in a collagen matrix, covered by a Matrigel layer and covered with epithelial cells. This resulted in a polarized epithelium with collagen IV deposition at the basal side and microvilli/cilia at the apical side (Bentin-Ley et al., 1994). Comparable models were used to study stromal-epithelial cell interactions (Arnold et al., 2001, 2002; Schutte et al., 2015), decidual differentiation (Kim et al., 2005; Schutte and Taylor, 2012) and endometrial cancer invasion (Park et al., 2003). The specific role of the paracrine and endocrine signaling in their 3D conformation and/or between the endometrial stromal and epithelial cells (ESC and EEC respectively) was investigated using primary culture derived cells and/or immortalized cell lines.

The most advanced models mimicking the endometrial function *in vitro* used only the glandular structures in an organoid culture. Glands play an important role in many biological processes vital for reaching and maintaining pregnancy (Filant and Spencer, 2014). Blauer *et al.* was the first to incorporate endometrial glands in Matrigel. These epithelial organoids were co-cultured with stromal cells, stained positive for epithelial markers cytokeratin-18 and E-cadherin and reacted to sex steroids in a more phenotypical correct manner (Bläuer et al., 2005). Turco *et al*. established culture conditions for human non-pregnant endometrium, decidua and even endometrial cancer while Boretto *et al.* similarly did this for the mouse and human endometrium, representing the most accurate *in vitro* cultures of the endometrium to date (Boretto et al., 2017; Turco et al., 2017). In conclusion, progresses are being made to recapitulate endometrial physiology *in vitro*, expanding our molecular understanding of its processes and pathology.

3.2.2 Embryo culture for *in vitro* fertilization and investigation approaches

Artificial reproductive technologies comprise the advances made in fertility medication, fertilization and surrogacy designed to improve reproductive outcomes. Culturing embryos *in vitro* plays a central role in ART and is continually evolving together with our understanding of the preimplantation embryo and its environment. Initially, improving *in vitro* embryo culture techniques was mainly centered in optimizing its chemical soluble environment by changing the concentrations of metabolic substrates, amino acids, growth factors, salts and macromolecules and assessing the effect of adding or removing other supplements (Biggers et al., 2004; Lane and Gardner, 2007). These advances are complemented by further developments in static and dynamic culture platforms where the efficiency of auto/paracrine signaling and secreted factors is improved and the embryos are subjected to mechanical stimulation, similar to that in the female genital/reproductive tract (Hur et al., 2016; Smith et al., 2012; Swain and Smith, 2011).

The last improvement could be accomplished at the culture surface level, for now generally inert surfaces such as polystyrene, glass and polydimethylsiloxane (PDMS) are used. It goes without saying that this does not constitute a realistic substitute of the reproductive tract. For this reason many ECM derived polymers are used as coating or suspended in culture medium, such as Matrigel (Dawson et al., 1997; Lazzaroni et al., 1999) and hyaluronic acid (Palasz et al., 2016). Other 2D culture systems investigated used co-culture of embryos with different types of cells. While co-culture with for example Vero cells or cumulus cells is conceptually interesting, results vary in experimental setting and the impact could be limited, possibly due to optimization of culture medium (d'Estaing et al., 2001; Kattal et al., 2008). Furthermore, this would imply the introduction of another laborious, complicated and possibly less reproducible protocol in ART laboratories (Swain et al., 2016).

Pre-implantation embryos were grown on natural hydrogels such as Matrigel, agarose and collagen I. Han *et al.* co-incubated collagen hydrogels with porcine endometrial tissue treated with interleukin 1 beta for 24 hrs, secreting vascular endothelial growth factor (VEGF). Porcine embryos 48 hrs after fertilization were cultured on these enriched hydrogels for 120 hours. There were no improvements of hatching rates, but the quality did improve, demonstrated by the higher blastocyst cell numbers (Han et al., 2017). Morris *et al.* used glass bonded polyacrylamide hydrogels coated with collagen 1, after demonstrating that laminin and fibronectin coatings resulted in very low embryo attachment. Gene expression of the embryo *in vitro* was similar to that of *in vivo* and confocal time-lapse microscopy was used to analyze embryo development, showing that no invasion occurred and the embryos acquired a flattened aspect (Morris et al., 2012).

Several models are in use to study implantation *in vitro* (Weimar et al., 2013). Lopata et al. cultured marmoset blastocysts on a Matrigel hydrogel; within 24hrs they attached at the polar trophoblast. It was also reported that they started to invade the hydrogel and retained their form until day 6 (Lopata et al., 1995). For the study of embryo implantation, Chang et al encapsulated primate blastocyst stage embryos in Matrigel, providing a 3D structure, and were co-cultured with a feeder layer of buffalo rat liver (BRL) cells. Growth and differentiation were demonstrated by immunohistochemical staining and the observation of signs of implantation and invasion (embryo mass enlargement and proliferation of trophoblast outgrowths) (Chang et al., 2018).

Based on the model presented by Bentin-ley in 1994, further publications by the same group demonstrated the usefulness of 3D organotypic culture models. Here, fertility

regulating drugs used as emergency contraception were investigated for their effects of on blastocyst attachment and endometrial receptivity markers (Berger et al., 2015; Lalitkumar et al., 2007; Meng et al., 2009). Furthermore, the model allows for the investigation of possible future fertility regulating agents such as polyethylene glycated leukemia inhibitory factor (LIF) antagonist (PEGLA), which reduced embryo attachment rate and decreased blastocysts survival (Lalitkumar et al., 2013). Wang *et al.* studied the attachment of Jar spheroids in a 3D culture model using primary cultured endometrial cells and a human fibrin + agarose-based hydrogel. An improvement of attachment rate compared to various monolayer setups was observed. Moreover, this is one of the few studies reporting spontaneous gland formation in the stromal fraction, possibly through epithelial endometrial cell contamination (Wang et al., 2012). This group also reconstructed the myometrium, stromal and epithelial endometrium in the rabbit model. The construct showed a myometrial layer with α-actin–positive bundles, stromal cells with gland-like structures (when mixed with EEC) and polarized epithelial cells. When mouse one-cell embryos were cultivated on this model, 79.4% of reached the blastocyst stage (compared to 40.9% in the control group) (Lü et al., 2009). Interestingly, with endometrial cells that were expanded using sex steroids (E2 and P4), a lower amount of embryos reaching this stage was observed (22.45%)(Wang et al., 2010).

3.2.3 *In vivo* treatment of pathologies

For now, there have been only two hydrogel-based treatments studied, each using different types of hydrogels. Xu *et al.* used a natural collagen I-based hydrogel with human umbilical cord derived mesenchymal stem cells (UC-MSCs) to treat uterine scars (Xu et al., 2017). Scar tissue was induced by excising parts of the uterine wall and they were treated 30 days later with PBS, cells, scaffold or a combination of the last two. Tissue regeneration improved in the cells/collagen I group, possibly through the upregulation of MMP-9 and subsequent collagen degeneration. Furthermore, embryo implantation in the scarred areas significantly improved.

PEG is by far the most versatile and most popular synthetic polymer in uterine tissue engineering. It is an FDA approved, biocompatible but non-biodegradable material, which can be resolved by copolymerization with biodegradable polymers (Han and Hubbell, 1997). An example for this is poloxamers; their chemical structure is usually made of a hydrophobic block flanked by hydrophilic blocks. These amphiphilic polymers are soluble at low temperatures however, at higher temperatures a physical gelation mechanism occur (Gyles et al., 2017). Pluronics F-127 (also called poloxamer 407) consist out of a PEG-polypropylene

glycol-PEG triblock that has been used as drug delivery carrier and for bioprinting of cellularized thermosensitive hydrogels (Basak and Bandyopadhyay, 2013; Gioffredi et al., 2016). Nonetheless, encapsulation in pure PF-127 is associated with cell apoptosis and inhibition of growth. To improve BMDSCs viability, Yang *et al.* included vitamin C (Vit c) as a membrane-stabilizing agent and reactive oxygen species scavenger. The mixture was tested to improve endometrial generation in a rat intra-uterine adhesion (IUA) model. Treatment with BMDSC/PF-127/Vit c decreased fibrotic area in the stroma and resulted in a thicker endometrium with more glands compared to the other treatments (Yang et al., 2017).

3.3 A new era in reproduction and regenerative medicine: extracellular matrix hydrogels and coatings

As described in section 2.3 "Decellularization of tissues and organs", the decellularization of entire organs is of vital importance in the pursuit of engineering a transplantable organ. Not only do the important tissue specific biochemical and biophysical properties of the ECM remain, but also the hierarchical organization of the tissue including their native vasculature persists, allowing for the culture of cells in a much ticker scaffold than previously possible. However, a decellularized organs' usability is not only limited to this goal, given that the complex mixture of extracellular proteins can be processed in various ways to serve different purposes (figure 12) (Agmon and Christman, 2016). For instance, sections or blocks of decellularized tissues can de be made and seeded with primary culture cells, progenitor cells or SP stem cells to create three-dimensional cell culture systems (Campo et al., 2017; Vyas et al., 2017; Xiao et al., 2017).

Finally, these acellular scaffolds can be converted into ECM powders, solubilized and used as hydrogels or coatings. This concept was first introduced almost 20 years ago, where the *in vitro* effectiveness of both decellularized tissue and ECM hydrogels showed improvement over commercially available substrata (Voytik-Harbin et al., 1998).

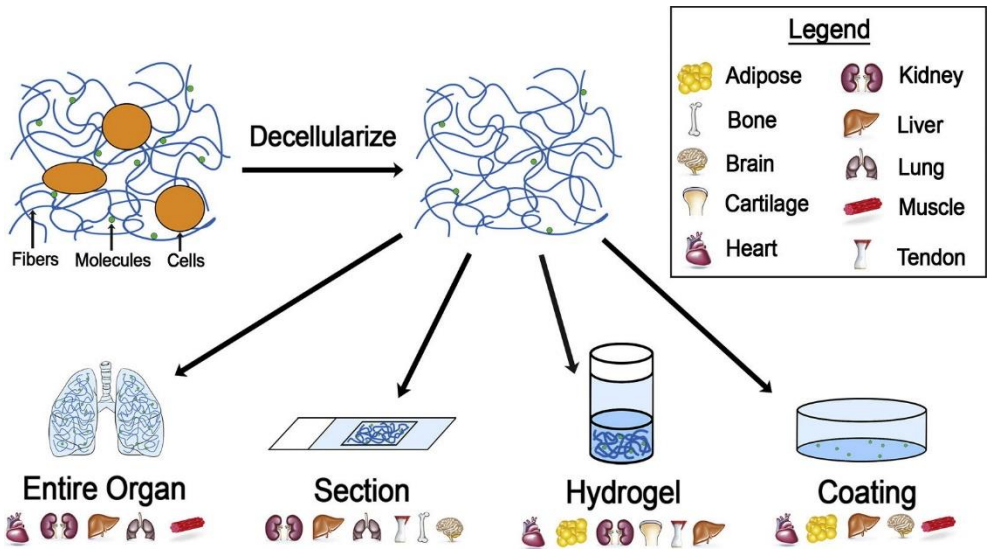

Figure 12. The various ways decellularized tissue materials can be processed. *Decellularization can be done with entire organs or sections; these can be processed further into tissue-specific hydrogels of coatings. Reprinted from (Agmon and Christman, 2016) with permission of Elsevier.*

Saldin *et al.* described the different methods to create hydrogel that were developed for different tissues. Here, ECM material has to be solubilized into its protein monomeric components, followed by a temperature- and/or pH-controlled neutralization to induce spontaneous reformation of the intramolecular bonds of the monomeric components into a homogeneous gel (Saldin et al., 2017). An urea buffer can be used for solubilization, but usually pepsin digestion in an acid solution (for 24 to 72 hrs) is performed in the laboratory setting (Freytes et al., 2008; Uriel et al., 2008; Voytik-Harbin et al., 1998). The bioactivity and gelation parameters of the gel is dependent on the solubilization methods, neutralization parameters (pH, temperature, ionic strength utilized) and digestion times (pepsin incubation times affect the profile of cryptic molecules) (Agrawal et al., 2011; Johnson et al., 2011; Kusuma et al., 2018). By converting the tissues into substrata such as hydrogels or coatings, the spatial organization of the ECM proteins is lost, but important specific biochemical elements remain intact. These biological cues are contained in a more flexible substrate expanding its *in vivo* and *in vitro* usability.

This is evident when looking at the multitude of *in vitro* studies performed, where the viability of cells on the surface has not been negatively affected for cell lines (Wolf et al., 2012), primary culture cells (Lee et al., 2014) and stem cells (DeQuach et al., 2010; Pouliot et al., 2016; Uriel et al., 2008; Zhang and Dong, 2015). It has been demonstrated in the liver that when stem cells (adipose-derived stem cells) were grown on ECM coatings hepatic differentiation, gene expression and hepatocyte related protein secretion improved compared to frequently used substrata such as collagen I or Matrigel (Lee et al., 2014; Zhang and Dong, 2015).

ECM hydrogels undergo a non-toxic, collagen-based self-assembly process into a nanofibrous hydrogel when incubated at 37°C or injected *in vivo*, which makes them an interesting option for regenerative medicine purposes. A good example of this is given in a study of Ungerleider *et al.*, where different injectable hydrogels were used in a rodent hindlimb ischemia model. The regenerative potential of decellularized porcine skeletal muscle (SKM) hydrogel was compared to a human umbilical cord-derived matrix (hUC) hydrogel, representing a younger age of the tissue source. It was shown that, compared to saline injection, perfusion increased thanks to increased arteriole diameter and higher density of larger arterioles. Pax-7, a transcription factor involved in early stage muscle lineage commitment was expressed higher in the SKM treated group, showing tissue-specific activity of the hydrogel. Furthermore, a pro-regenerative environment was reported using the SKM gel, further establishing that tissue-specificity of ECM hydrogels is retained in both *in vivo* and *in vitro* models.

The best example for the therapeutic potential of this type of hydrogels is a porcine-derived myocardial ECM hydrogel developed by the same group, the Christman laboratory, which is currently in clinical trials to treat patients after myocardial infarction (MI) (ClinicalTrials.gov Identifier: NCT02305602). Rat and porcine MI models showed an improvement of neovascularization, cardiac function and increase in cardiac muscle. It was also demonstrated that the porcine-based hydrogels performed similarly to human myocardial pre-gel solutions and even displayed more reliable gelation *in vivo* (Johnson et al., 2014).

The specific mechanisms by which the coatings and hydrogels modulate the cell behavior is yet to be fully understood; it is more than likely that it is the result of various factors, such as growth factor, cytokines and chemokines bound to the fibers. The degradation of the ECM also releases matricryptic molecules, which are involved in stem/progenitor cell recruitment, angiogenesis and other functions (Beattie et al., 2008; Davis et al., 2000). Furthermore, it has been reported that the enzymatic digestion of ECM bioscaffolds releases bioactive matrix-bound nanovesicles (Huleihel et al., 2016).

In other words, ECM hydrogels represent an interesting platform for *in vitro* and *in vivo* REPROTEN applications. These gels are not only compatible with cells, but they can also be improved or adapted with growth factors. For future applications in reproductive medicine it has also been shown that ECM hydrogels can be used as the basis for hybrid materials (Jakus et al., 2017) or bioinks for 3D tissue printing (Kuo et al., 2018). For now, there has been no reports of an ECM hydrogel made of endometrial tissue.

Chapter

II

HYPOTHESIS

II. HYPOTHESIS

The hypothesis of this study is that the decellularization of whole uteri, a novel tissue-engineering technique, from different species has not only the potential to, one day, create tissue-engineered, transplantable organs but that the decellularized endometrial fraction can also be processed further into thin sections, ECM hydrogels and coatings that can be used as a biocompatible tissue-specific substrate for cell and embryo culture. Moreover, we intend to corroborate that the differences in the cyclically and drastically changing endometrium are translated to these hydrogels and coatings, possibly affecting the development of embryo culture.

Chapter

III

OBJECTIVES

III. OBJECTIVES

The main objective of this thesis is to develop tissue-engineering approaches based on decellularized uterine tissues obtained from whole organs to improve several aspects within reproductive medicine. Different approaches will be investigated that can not only improve current investigative *in vitro* models but also has the potential to be used, in the future, as a novel treatment for female pathologies leading to reproductive dysfunction.

This global objective can be divided into several specific objectives:

- To establish a protocol for the perfusion-based decellularization of large reproductive organs, namely the porcine and rabbit uterus.
- To test the biocompatibility of the newly created bioscaffolds by first recellularizing acellular pig endometrial disks with human Side Population stem cells and creating organoid-like structures.
- To develop a microdissection-based protocol to separate the rabbit endometrium from whole decellularized organs and convert it into a tissue-specific ECM hydrogel and coating.
- To assess the usability of these ECM hydrogels and coatings for the *in vitro* culture of rabbit embryos.
- To investigate the effects of substrata from decellularized synchronous and non-synchronous endometrial tissues in the embryo culture model.

Chapter

IV

MATERIALS AND METHODS

IV. MATERIALS AND METHODS

For the purposes of this thesis, the animal models of the pig and rabbit uterus were used. This separation will be reflected in the structure of the material and methods, results and discussion chapters.

1 The pig model: whole uterus decellularization and recellularization of the acellular endometrium

1.1 Study design

The goal of this study was to develop a perfusion-based DC protocol usable for large reproductive organs, resulting in a biocompatible bioscaffold. The effect of a prior freeze/thaw step was also assessed. For this, three frozen-thawed and three fresh uteri were subjected to an DC protocol we optimized for the pig uterus. DC efficiency was tested by histology techniques (H&E, Masson's Trichrome, and Alcian blue) and by DNA and protein quantification. Vascular corrosion cast, immunofluorescence (Collagen I & IV, elastin, laminin and fibronectin), scanning and transmission electron microscopy (SEM, TEM) were performed to assess the effect on organ vasculature, ECM composition and its ultrastructure respectively, a workflow of this process is described in figure 13. Finally, to test the *in vitro* biocompatibility for possible subsequent recellularization, human endometrial Side Population stem cell lines (ICE6&7) were used to recellularize endometrial sections and organoid-like structures were created.

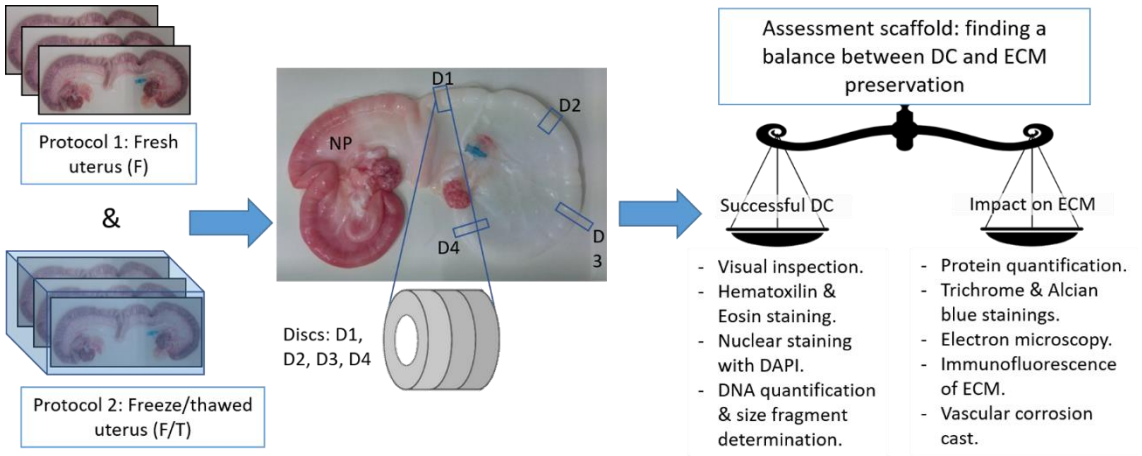

Figure 13. Workflow of the pig model. *Diagram describing the methodology followed for each sample, from initial manipulations and application of decellularization protocols until final sample extraction and characterization. Here, a balance was made between the successful decellularization and the impact of the protocol on the ECM (NP: non-perfused horn, D1-4: decellularized horn 1 to 4 different locations).*

1.2 Whole uterus decellularization

For this study, uteri were obtained from pigs weighing approximately 220 kg. All organs were donated for scientific research by the Mercavalencia slaughterhouse (complying with the ISO 9001 quality management system). They were sacrificed by exposure to increasing concentrations of CO_2, which led to metabolic acidosis and reduction of intracellular pH, resulting in gradual loss of consciousness and sensibility. Exsanguination was performed by transection of the jugular vein. The uteri were collected early in the morning from the local slaughterhouse (Mercavalencia, Spain) and preserved in ice during transport. The controls that are being used in all experiments correspond to these uteri before any treatment.

1.2.1 Uterus cannulation and decellularization

In total six uteri were selected, three for each protocol, based on their morphology and much attention was given to their vascular system. The uterine artery of a single horn was cannulated (decellularized horn), leaving the other one without perfusion. After cleaning the artery from surrounding tissue, 20-G cannulas (BD, Apósitos Navarro, S.L.) were inserted pushing PBS by syringe (Sigma-Aldrich; pH 7.4) to dilate the artery. The cannula was fixed into place using braided silk sutures after guaranteeing that the cannula was properly inserted, and that blood was exiting the uterine vein (Laboratorio Aragó, Barcelona, Spain).

The cannulated uterine horn was carefully attached to a peristaltic pump (Cole-Parmer instruments, Chicago, USA) using L/S 16 tubing (Masterflex, Fisher scientific) for DC. An initial perfusion of PBS for one hour was done to remove the remaining blood and cell debris. The perfusion speed for all protocols was set at a physiological flow rate of 15 mL/min (Geisler et al., 2012). Figure 14 shows a typical setup for perfusion-based DC.

Figure 14. Decellularization setup. *The selected perfusion media are pushed from the containers (a) through a peristaltic pump (b) into the organ with cannulated arteries. The organs are submerged in a deep tray, cells are lysed, and cellular material is removed through the perfusion with the DC medium, the exiting medium overflows from the tray into the sink (c).*

Two decellularization protocols, called freeze/thaw (F/T, *n* = 3) and fresh (F, *n* = 3) pig uteri using chemical and/or physical agents, were carried out along this experimental approach (see Table 6 for full protocol).

Protocol 1: Frozen/thawed samples (P1: F/T). The uterus (*n* = 3) was frozen after cannulation, thawed, and underwent two identical cycles after the initial perfusion with PBS. Each cycle took 24 hours and consisted of four perfusion steps: first for 18 hours (overnight) with a 0.1% SDS solution (Sigma-Aldrich), followed by 30 min of dH_2O, 30 min of 1% Triton X-100 (Sigma-Aldrich), and finally five hours of PBS.

Protocol 2: Fresh samples (P2: F). The second protocol also used the same cycles twice, consisting of perfusion steps with SDS, dH_2O, Triton X-100, and PBS, but in contrast to the first protocol, here no F/T step after cannulation was done (*n* = 3).

		Reagent	Concentration	Duration
Day 1	Cycle 1	PBS	1X	1 hour
		SDS	0,10%	18 hours
		H_2Od	-	30 min
		Triton-X100	1%	30 min
		PBS	1X	5 hours
Day 2	Cycle 2	SDS	0,10%	18 hours
		H_2Od	-	30 min
		Triton X-100	1%	30 min
		PBS	1X	5 hours

Table 6. Decellularization protocol of frozen/thawed and fresh samples. *The main protocol is the same apart from the use of a freeze/thawed or fresh organ. A perfusion speed of 15 mL/min was used throughout. Sample preparation for the different protocols were as follows: Freeze/thawed uterus (at –20°C, one week max) (F/T) or fresh uterus (F). Abbreviations: PBS: phosphate buffered saline; H2Od: distilled water; SDS: sodium dodecyl sulfate*

1.2.2 Histological analysis

To visualize the morphology of each sample of the perfused horn histological analysis was performed, four ring-shaped segments with a thickness of about 5 mm were taken from equidistant locations for each uterus subjected to the aforementioned protocols (described in section 1.1 “Study design” and figure 13). The decellularized and fresh control segments were fixed for 24 hours in 4% paraformaldehyde (PFA) at 4°C for histological staining and immunofluorescence. Subsequently, they were transferred to 70% ethanol overnight at 4°C and dehydrated in graded alcohol. This was followed by immersion in xylenes and embedding in paraffin wax. The embedded samples were serially sectioned (4 µm) on a microtome (HM 310, Microm) and mounted onto glass slides (Superfrost plus, Thermo Scientific). For each histological analysis, three slides of the serial cuts were selected. To assess the efficacy of the DC protocols and the integrity of the ECM, cuts were rehydrated and stained with H&E, Masson's Trichrome (MT), and Alcian blue using the manufacturer’s

instructions. These techniques were done so as to demonstrate the presence of cellular components, collagen, and sulphated GAGs, respectively. For the detection of nuclear DNA, mounting media containing 6-diamidino-2-phenylindole (DAPI, Thermo-fisher Scientific) was utilized. All images, for both bright-field and fluorescence microscopy, were taken with a Nikon eclipse 80i microscope.

1.2.3 Immunofluorescence analysis

Immunofluorescence of five highly constitutive proteins of the ECM was performed, these are fibronectin (FN), elastin (ELN), collagens type I (COL1) and IV (COL4) and laminin (LM). This was done with decellularized samples procured from both protocols and compared to an untreated, fresh uterus as control to evaluate the integrity of the ECM. From each uterus (a total of seven slides, three from each protocol plus control), one slide of the serial cuts was deparaffinized and rehydrated as described above. Mouse monoclonal primary antibodies for fibronectin and elastin (final concentration for both: 1/300) and rabbit polyclonal primary antibodies for collagens type I and IV and laminin (final concentration for all: 1/200) were used (Abcam antibodies: #ab6328, #ab9519, #ab82504, #ab6586, and #ab11575, respectively). Enzymatic antigen retrieval was performed for fibronectin and elastin: slides were incubated for 10 min at 37°C with a 12 units/mL proteinase K solution in a humid chamber, followed by 10 min at room temperature and rinsing with TE buffer (pH = 8, Tris and Ethylenediaminetetraacetic acid (EDTA) buffer). Antigen retrieval of the remaining proteins was performed by incubation in citric acid solution (10 mM sodium citrate, 0.05% Tween-20, pH 6.0) at 95°C for 20 min and a cooling step on ice for another 20 min, following rinsing with PBS (TE buffer in case of laminin). Blocking against nonspecific binding was done by using a solution consisting of 5% bovine serum albumin (BSA), 5% normal goat serum (NGS), and 0.4% Triton X-100 in PBS for one hour at room temperature for collagen IV and at 37°C for collagen I. A 5% BSA/5% NGS/0.4% Triton X-100 in TE buffer mixture was used for one hour at room temperature in the case of elastin and fibronectin, whereas for laminin this was performed at 37°C. Primary antibodies were diluted to the required concentrations in their respective blocking buffer at 1%. After rinsing, the slides were incubated with secondary antibodies with Alexa Fluor 488 green-fluorescent dye at 1/500 (Invitrogen) in PBS or TE buffer; for fibronectin and elastin, the antibody used was goat anti-mouse (A21121, Invitrogen). In the other cases, a goat anti-rabbit secondary antibody was used (A11034, Life Sciences). Slides were visualized under a fluorescence microscope and Olympus FV1000 confocal microscope. Three-dimensional stacks of the samples were also obtained.

1.2.4 DNA quantification and fragment-size determination

For DNA quantification, circular segments were dried on filter paper to remove the excess liquid and cut longitudinally in one side to lay it flat. From the obtained slab, cubic pieces weighing less than 25 mg were procured. These were further cut up by hand and DNA was extracted by using a commercial kit (DNeasy Blood & Tissue, Qiagen) following manufacturer's instructions. Measurements of DNA concentration were done on a Nanodrop (Thermo Scientific). The sample from the decellularized horn with the highest amount of DNA from each uterus (P1, n = 3; P2, n = 3) was loaded on a 2% agarose gel containing Gel Red nucleic acid stain (Biotium #41003) for a total runtime of 90 min at 100 V. 1000 ng of DNA from each sample were loaded and a 1 kb plus DNA ladder (Invitrogen) was used for comparison.

1.2.5 Protein extraction and quantification

As with DNA quantification, circular fragments were taken, dried on filter paper, weighed, and minced to examine the total amount of proteins. Protein extraction was done by using a modified Laemli buffer (0.125M Tris HCl, 4% SDS 10% β-mercaptoethanol) for 48 hours at 37°C under agitation. The Pierce BCA protein assay kit (Thermo-Fisher Scientific) was used for total protein quantification following the manufacturer's protocol and quantified using a spectramax 190 (Molecular Devices).

1.2.6 Scanning electron microscopy and transmission electron microscopy

Ultrastructure was investigated by SEM and TEM. The decellularized samples from each uterus were fixed in 4% PFA overnight and stored in 50% EtOH after another overnight step with 70% EtOH. The selected samples (only one location) were subjected to critical point drying, gold/palladium (Au/Pd) sputter coating (SC7640 Sputter Coater, Quorum technologies) and ultimately put under an FEG Hitachi S-4800 scanning electron microscope. For TEM, samples were postfixed in 1% osmium tetroxide in 100 mM phosphate buffer and embedded in resin. After ultrasectioning, a JEOL JEM1010 transmission electron microscope was used. Advanced microscopy techniques were carried out in the Servicio Central de Apoyo a la Investigación Experimental (SCSIE) facilities at the Universidad de Valencia.

1.2.7 Vascular corrosion cast

To assess the integrity of the vascular tree, Batson's No.17 plastic replica and corrosion kit (Polysciences, Inc., ImmunoStep SL) was used on the decellularized uteri and control uteri. The perfusion mixture was made as described by the protocol provided, two different

perfusion speeds (2.5 and 15 mL/min) were used for the corrosion cast of the control, F/T Protocol (P1) and F Protocol (P2). The 2.5 mL/min perfusion speed was selected as the lower speed after comparing perfusion speeds used in previous experiments with the liver (Debbaut *et al.*, 2011). After perfusion, all the veins and arteries of the uteri were clamped and left overnight at 4°C for polymerization. The tissue was macerated using a 10% NaOH mixture overnight; this step was repeated until the mixture remained clear, indicating that all the tissue was successfully removed. Circular cuts were made of the vascular mold and opened; these samples were photographed under a stereomicroscope and submitted to Au-Pd sputtering for SEM.

1.3 Recellularization of uterine extracellular matrix disks

1.3.1 Cell culture of human endometrial Side Population cell lines (ICE6/7)

To test the *in vitro* biocompatibility of the decellularized endometrium, Side Population (SP) derived cell lines were used. These endometrial stem cells are called ICE6 and ICE7 for the stem cell lines of epithelial and stromal origin respectively. These were isolated in 2010 by flow cytometry using the well-known efflux Hoechst method, and later characterized for stem cell features by, among others, the expression of mesenchymal markers CD73, CD90, and CD105 (Cervelló et al., 2011b). Cells were cultured and maintained until passage 11 under hypoxic conditions (2% O2) until confluence in clonal medium (DMEM, 10% fetal bovine serum, 2mM L-glutamine, 1/1000 Streptomycin/Penicillin/Amphotericin). Cells were trypsinized for 7 minutes at 37ºC, resuspended in clonal medium, mixed at physiological ratios and centrifuged to create the viscous pellet.

1.3.2 Recellularization of acellular endometrial disks

Figure 15 shows the workflow to recellularize endometrial disks. Biopsies obtained from P2 decellularized organs oriented with the endometrium facing up were embedded in Tissue-Tek O.C.T. compound (OCT, Sakura Finetek USA Inc., VWR). A maximum of four cuts at 100 µm were made with the cryotome to assure that only endometrial tissue is used. Punch biopsies with a diameter of 5 mm were made and put in a cooled chamber slide (µ-Slide 8 Well, Ibidi). Sterilization was performed by exposure to UV light for two hours, ensuring that the scaffolds did not dry out.

These circular scaffolds were seeded with a viscous pellet consisting of a mixture of stromal and epithelial SP stem cells (4/5 ICE6 and 1/5 ICE7, respectively, corresponding to their physiological ratio in the endometrium). Next, 0.5 million of ICE mixed stem cells from

the 11th passage was seeded and cultured on the scaffolds under hypoxic conditions. Endometrial culture medium was changed after 3, 6, and 9 days of culture.

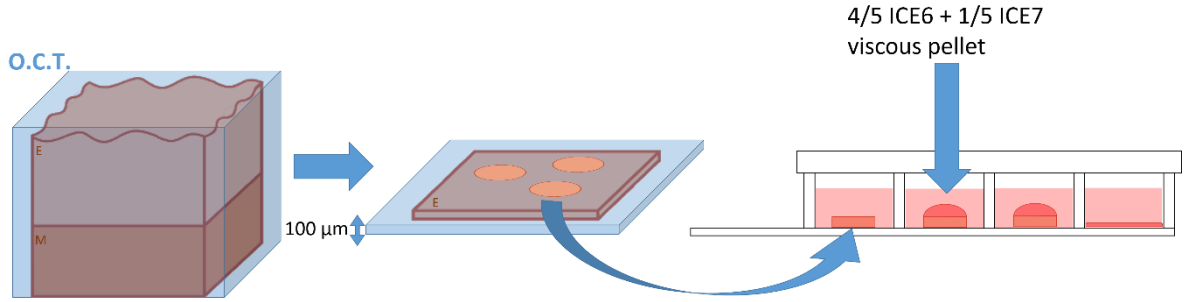

Figure 15. Testing biocompatibility of decellularized scaffold. *Diagram describing the workflow followed for the creation of endometrial organoid-like structures. Punch biopsies of decellularized endometrial sections were sterilized and covered with a viscous pellet of Side Population stem cells. These were cultured for 9-12 days under hypoxic conditions.*

1.3.3 Histological and immunofluorescence analysis

After this, the organoid-like structure was embedded in paraffin and serial cuts (4 µm) were made. Successful recellularization (RC) and correct cell differentiation were assessed by H&E staining and indirect immunofluorescence against human vimentin [1:200, antivimentin antibody (ab8069), Abcam] and human anticytokeratin [1:500, anticytokeratin 18 antibody (ab52948), Abcam]. Goat anti-mouse Alexa fluor 488 (A21121, Thermo-Fisher) and goat anti-rabbit Alexa fluor 555 (A21428, Thermo-Fisher) were used as secondary antibodies. Positive (human endometrium) and negative (mouse kidney) controls were used in this methodology (data not shown). Standard blocking solution and antigen retrieval were performed along with this protocol. Slides were examined under a Nikon Eclipse 80i fluorescence microscope.

1.4 Statistical data analysis

Statistical analysis was performed to identify any significant differences between the data obtained from the protocols and the fresh control at DNA and protein levels. This was done first by using ANOVA; if the means of the three populations were not considered as equal, this was followed up with a posthoc test (Bonferroni method). A *P*-value of ≤0.05 was considered statistically significant

2 The rabbit model: whole uterus decellularization, solubilization of acellular endometrium and embryo culture on tissue-engineered substratum

2.1 Study Design

The goal of this study was to create coatings and hydrogels from different decellularized endometrial tissues and compare *in vitro* embryo culture development between these substrata, but also with commercial coatings and standard culture conditions. A complete overview of the methodology is given in Figure 16. Four whole uteri were first decellularized, 2 of which were from rabbits that were not stimulated and two from rabbits 72 hours after ovarian stimulation. The latter type will be referred to as synchronous (S) from here on because of the synchronization between the embryo and tissue (both at day 3). After testing the decellularization efficiency, the acellular endometrium was separated via microdissection, lyophilized and milled. This powder enriched with complex ECM proteins was put into suspension by partial digestion, the pre-gel solution was aliquoted and stored at -80°C. Day 3 late stage morulae were cultivated for 48 hours in 8 different embryo culture conditions as depicted in figure 16: on top of different biological surface coatings (C) and hydrogels (H) made from non-synchronous (NSC and NSH), synchronous (SC and SH) acellular endometrium and Matrigel (MC and MH) and in two standard culture conditions using uncoated wells with culture medium supplemented with and without 10% Fetal Bovine Serum (FBS), C+FBS and C-FBS respectively. After that, hatching rates, morphometry and expression of three core pluripotency markers were analyzed and compared.

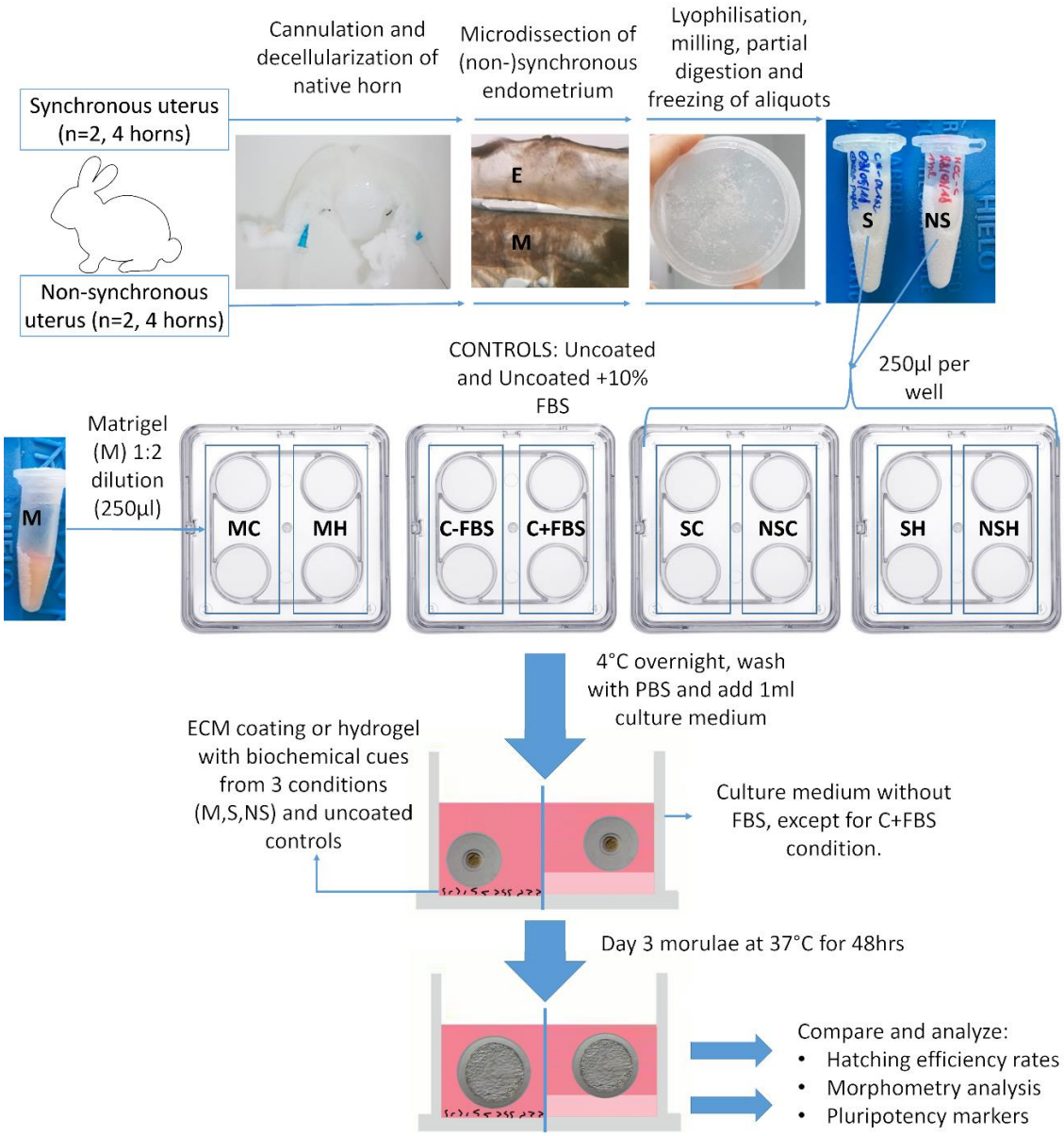

Figure 16. Workflow rabbit model. *Diagram describing the workflow followed from uterus extraction, decellularization, hydrogel creation until embryo culture. Abbreviations: FBS: fetal bovine serum; MC: Matrigel coating; MH: Matrigel hydrogel; NSC: non-synchronous coating; NSH: non-synchronous hydrogel; SC: synchronous coating; SH: synchronous hydrogel.*

2.2 Whole rabbit uterus decellularization

All experimental procedures used in this study were performed in accordance with Directive 2010/63/EU EEC for animal experiments and were reviewed and approved by the Ethical Committee for Experimentation with Animals of the Universidad Politecnica de Valencia, Spain (research code: 2018/VSC/PEA/0116). Animals were housed at the Universidad Politecnica de València experimental farm in flat deck indoor cages (75×50×30 cm), with free access to water and commercial pelleted diets. The photoperiod is set to

provide 16 h of light and 8 h of dark, and the room temperature is regulated to keep temperatures between 10°C and 28°C.

2.2.1 Uterus extraction and decellularization

Non-synchronous uterus (n=2) were obtained from nulliparous rabbits, where ovulation was not induced. For the synchronous uterus (n=2), ovulation was induced 72 hours before extracting the uterus using hormonal treatment with 1 µg of Buserelin acetate (Hoechst Marion Roussel S.A., Madrid, Spain). To cannulate both uterine arteries, rabbits were euthanized with an intravenous injection of 200 mg/kg of pentobarbital sodium and the uterus was exposed by a midline abdominal incision, followed by liberation and cannulation of both uterine arteries with 22G cannulae. The uterine horns were flushed with PBS, and EDTA (Sigma-Aldrich) was pushed to prevent clotting.

To decellularize both uterine rabbit horns the cannulated uterus was perfused by a peristaltic pump (Cole-Parmer instruments, Chicago, USA) using L/S 16 tubing (Masterflex, Fisher scientific) (figure 14). A protocol for the decellularization of pig uterus was slightly adapted for this study (Campo et al., 2017). Table 7 shows the complete two-day decellularization protocol for rabbit uterus. Any residual DNA was removed in the last cycle by perfusion with a 2µg/mL DNase I solution (D4513-1VL, Sigma-Aldrich), diluted in 1,3 mM $MgSO_4$ and 2 mM $CaCl_2$ (Sigma-Aldrich). The perfusion speed was set at 8 mL/min per horn.

		Reagent	Concentration	Duration
Day 1	Cycle 1	PBS	1X	1 hr
		SDS	0.10%	18 hrs
		H_2Od	-	30 min
		Triton-X100	1%	30 min
Day 2	Cycle 2	PBS	1X	5 hrs
		SDS	0.10%	18 hrs
		H_2Od	-	30 min
		Triton X-100	1%	1 hr
		PBS	1X	1 hr
		DNase I solution	2 µg/mL	1hr
		PBS	1X	3-4 hrs

Table 7. Decellularization protocol for whole rabbit uteri. *This two-day protocol was adapted from (Campo et al., 2017), using detergents like Triton X-100 and SDS. Throughout the experiment a perfusion speed of 8 mL/min was used. Abbreviations: PBS: phosphate buffered saline; H2Od: distilled water; SDS: sodium dodecyl sulfate.*

2.2.2 Histological analysis

Circular segments of about 5 mm thick were obtained from each decellularized horn and native tissue for histological analysis. These were fixed overnight with 4% paraformaldehyde (PFA, Sigma-Aldrich) at 4°C. Following this, they were dehydrated in graded alcohol/xylene baths and embedded in paraffin wax before being serially sectioned

on a microtome (4µm, HM 310, Microm) and mounted on glass slides (Superfrost plus, Thermo Scientific). To assess the DC efficiency and ECM architecture, sections were rehydrated and H&E and MT stainings were used to assess the morphology, presence of cellular components and collagens. To detect nuclear DNA, mounting media containing DAPI (Thermo-fisher Scientific) was used. All images were taken with a Nikon eclipse 80i microscope.

2.2.3 DNA and Protein quantification

Circular segments were taken from each horn as performed for the histological analysis. These were put on filter paper to remove excess liquid and DNA was extracted from cubic pieces weighing less than 25 mg using a commercial kit (DNeasy Blood & Tissue, Qiagen), following the manufacturer's protocol. DNA concentration was measured using the Qubit™ dsDNA HS Assay Kit (Thermo-fisher Scientific).

For protein quantification, pieces weighing around 0.1 g were minced and incubated with 100µl of a modified Laemli buffer (0.125M TrisHCl, 4% SDS, 10% β-mercaptoethanol, (Sigma-Aldrich)) for 48 hours at 37°C under agitation. After this, the mixture was spin down for 15min at 12.000 rpm and 4°C. The resulting supernatant was stored at -20°C and the protein concentration was determined using the Qubit Protein Assay Kit (Thermo-fisher Scientific).

2.3 Preparation of non-synchronous and synchronous hydrogels

2.3.1 Separation of acellular endometrial matrix for gelation and coating

Large segments (approximately 5 cm long) of decellularized and fresh horns were frozen, sliced into 1 mm thick circular cuts by hand and washed 3 times in ice-cold PBS. When put under a stereomicroscope (SMZ800, Nikon) a transparent ribbon is apparent due to the orientation of the muscle fibers of the innermost myometrial layer. Pure endometrial tissue was removed by cutting at the luminal side. Again, endometrial and myometrial fractions were washed 3 times in ice-cold PBS to remove all residual SDS and stored at -80°C. To pulverize the tissue, the endometrial fraction was lyophilized (Lyoquest-85, Telstar) overnight at 20 Pa and –80°C and milled with dry ice in an ultra-centrifugal mill (ZM 200, Retch). The resulting powder was frozen one last time in liquid nitrogen, grinded by mortar,pestle and stored at –20°C.

The decellularized endometrial powder was solubilized using an adapted protocol from Freytes (Freytes et al., 2008). Here, 1% (w/v) powder was suspended in 0.01 M HCl (Sigma-

Aldrich) with 0.1% (w/v) of pepsin (Sigma-Aldrich), and left to digest for 48 hours under constant agitation using a sterilized magnetic stirrer. Afterwards, the solution was left on ice and neutralized with 10% (v/v) 0.1 M NaOH (Sigma-Aldrich), and 11.11% (v/v) 10X PBS. pH test strips were used to test if the pH measured around 7.4 (P3536-100EA, Sigma-Aldrich). The resulting solution was aliquoted, flash frozen in liquid nitrogen and stored at -80°C.

To coat the 4-well Nunc plate (Thermo-fisher Scientific) with acellular endometrial derived ECM, 250 µl of each solution (non-synchronous/NSC, synchronous/SC and 1:2 diluted Matrigel/MC) was added and left overnight at 4°C to let the proteins adhere nonspecifically. The coating solution was aspirated, and wells were rinsed once with PBS before adding the culture medium. In addition, the NSH, SH and MH were made by incubating 250 µl of each hydrogel solution for 1 hour at 37°C before adding the culture medium.

2.3.2 Properties of hydrogels: fiber size, gelling kinetics and sterility

To analyze the fiber density and thickness, scanning electron microscopy (SEM) was used; hydrogels were fixed in 2.5% glutaraldehyde in PBS (Sigma Aldrich, Grade II, 25%) overnight at 4°C, followed by 2 washes with PBS and dehydration in a graded series of alcohol (30%-100%). Samples were then slowly critical point dried, coated with Au-Pd for 2 minutes using a SC7640 Sputter Coater (Quorum technologies) and imaged with a SEM FEG Hitachi S-4800. Advanced microscopy techniques were carried out in the SCSIE facilities at the Universidad de Valencia. Fiber diameter was measured using ImageJ software.

The gelation kinetics were evaluated by turbimetry, 100µl of each solution was added in triplicate in 96-well plates and measured spectrophotometrically in a plate reader. Absorbance was measured at 405 nm every 2 min, values were normalized by the following formula taken from (Wolf et al., 2012): $NA = \frac{A-A_0}{A_{max}-A_0}$ (NA: normalized absorbance, A: measurement at given time, A0: absorbance at t=0m, A_{max}: maximum absorbance). Two gelation kinetic parameters were calculated: the time to half gelation ($t_{1/2}$) was defined as the time necessary to reach 50% of the maximal absorbance, and the lag time (t_{lag}) was defined as the moment that the gelation curve increases from 0% normalized absorbance.

In addition, hydrogels (NSH, SH and MH) were formed by incubation at 37°C for one hour. To test structural stability and sterility they were left in DMEM/F12 medium containing 10% FBS and 0.1% antibiotics for 7 days.

2.4 Biological characteristics and applications of hydrogels

To assess the biological activity of the resulting hydrogels from uterine decellularized matrix, an *in vitro* embryo culture experiment was done, evaluating its hatching/hatched rate, degree of expansion and the expression of the three core pluripotency factors.

2.4.1 Embryo collection

Twelve New Zealand White rabbits were used as embryo donors. Briefly, to collect the embryos females were artificially inseminated with a heterospermic pool of semen from male animals of the same line to randomize male effect. Immediately, ovulation was induced as mentioned previously. After 72 hours, females were euthanized with an intravenous injection of 200 mg/kg of pentobarbital sodium, and the embryos were collected at room temperature by flushing the oviducts and the uterine horns with 10 mL of embryo recovery media (Dulbecco PBS with 0.2% (w/v) FBS and antibiotics (100 IU/mL Penicillin and 0.01 mg/mL streptomycin)). The experiment was performed in three sessions, obtaining finally 602 embryos catalogued as good quality embryos (synchronic developmental stage, presenting homogenous cellular mass, mucin coat and spherical zona pellucida).

2.4.2 *In vitro* development on different substrata

Next, embryos were cultured for 48 hours in Tissue Culture Medium 199 (TCM199 (Sigma-Aldrich) with antibiotics) at 38.5°C, 5% CO2 and saturated humidity. Table 8 shows the total number of embryos used over 3 experiments for each condition.

Substrata	NSC	NSH	SC	SH	MC	MSH	C-FBS	C+FBS
Number of embryos used	91	70	92	69	86	65	77	59

Table 8. Total number of embryos used for biological characterization of substrata. *Abbreviations: C±FBS: uncoated control with or without serum in culture medium; MC: Matrigel coating; MH: Matrigel hydrogel; NSC: non-synchronous coating; NSH: non-synchronous hydrogel; SC: synchronous coating; SH: synchronous hydrogel.*

The *in vitro* development ability of embryos was assessed based on the hatching/hatched rate (proportion of hatching and hatched blastocyst at 48h of culture from total cultured embryos). The hatched state was achieved when more than 50% of the embryonic mass cell was extruded of zona pellucida.

2.4.3 Morphometric analysis of hatched embryos

Following this, a morphometric analysis of the hatched embryos was performed. This and further analysis were only done with the control and coating embryo culture batches, after comparing the hatching rates it was clear that all hydrogel groups (MSH, NSH and SH)

had a vastly inferior development. Briefly, digital images of fully hatched blastocysts were taken using a Nikon optical microscope from 43, 43, 22, 41 and 48 embryos cultured in C-FBS, C+FBS, MC, NSC and SC experimental groups, respectively. For each embryo, 2 diameters were measured in the maximal cross-sectional image, and the mean diameter value was calculated as mean = (D1+D2)/2. D1 and D2 are referred to the maximum and minimum distance of an adjusted oval section drawn around the embryo (figure 17). Pictures were analyzed using the ImageJ program after calibration with a graduated ruler.

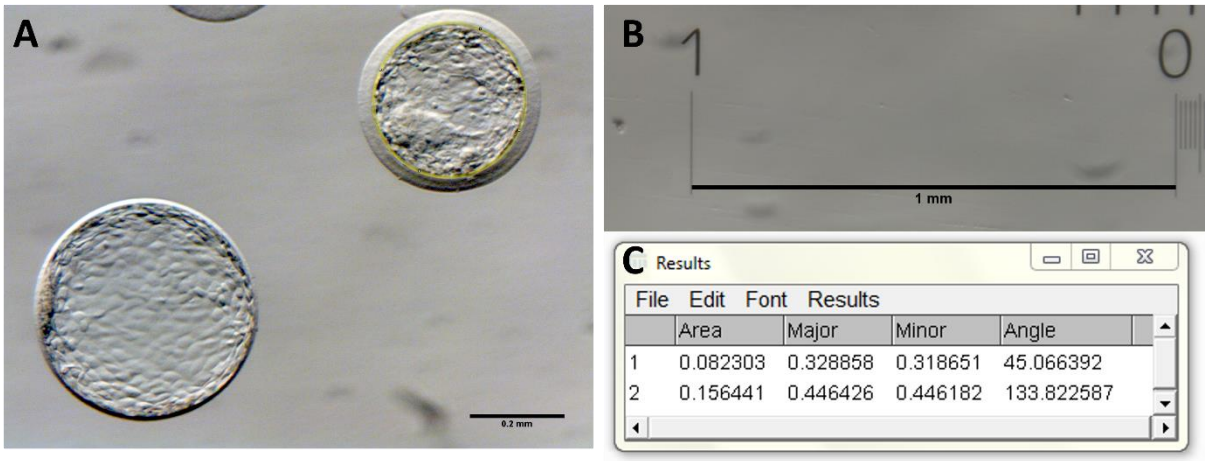

Figure 17. Morphometric analysis of embryos. *Representative image of day 5 blastocysts after 48 hours of in vitro culture and methodology of measurement (A). Calibration with a graduated 1mm ruler (B). Results panel of ImageJ software with area, minor and maximal diameter of an adjusted oval section drawn around the embryo (C).*

2.4.4 mRNA expression of core pluripotency factors

Finally, the gene expression profile of three core pluripotency factors (*OCT4*, *NANOG* and *SOX2*) was assessed after the 48 hours of *in vitro* culture in the C-FBS, C+FBS, MC, NSC and SC experimental groups. All embryos were used to mRNA expression determination. One pool of embryos per experimental group and per session were analyzed. Total RNA was extracted using the Dynabeads kit (Life Technologies, Carlsbad, CA, USA), following the manufacturer's instructions. Then, reverse transcription was carried out using qScript^{TM}cDNA Synthesis kit (Quanta Biosciences, Beverly, MA, USA) following the manufacturer's instructions. Real time PCR reactions were performed in an Applied Biosystems 7500 system (Applied Biosystems). Every PCR was performed from 5 µL diluted 1:10 complementary DNA (cDNA) template, 250-nM of forward and reverse specific primers (Table 9), and 15 µL of Power SYBR Green PCR Master Mix (Fermentas Gmbh, Madrid, Spain) in a final volume of 20 µL. The PCR protocol included an initial step of 50 °C (2 minutes), followed by 95 °C (10 minutes), and 42 cycles of 95 °C (15 seconds) and 60 °C (30 seconds). After quantitative PCR, a melting curve analysis was performed by slowly

increasing the temperature from 65 °C to 95 °C, with continuous recording of changes in fluorescent emission intensity. The specificity was confirmed by melting curve analysis. Relative gene expression was calculated via ΔΔCt method adjusted for PCR efficiency, applying the geometric average of the glyceraldehyde-3-phosphate dehydrogenase (*GAPDH*) and the H2A histone family member Z (*H2AFZ*) housekeeping genes as normalization factor (Llobat *et al*., 2012). The expression of a cDNA pool from various samples was used as a calibrator to normalize all samples within one PCR run or between several runs.

Gene symbol	Forward primer	Reverse primer	Fragment (bp)
OCT4	CGAGTGAGAGGCAACTTGG	CGGTTACAGAACCACACACG	125
NANOG	CCAGGTGCCTCTTACAGACA	TCACTACTCTGGGACTGGGA	104
SOX2	AGCATGATGCAGGAGCAG	GGAGTGGGAGGAAGAGGT	270
H2AFZ	AGAGCCGGCTGCCAGTTCC	CAGTCGCGCCCACACGTCC	85
GAPDH	GCCGCTTCTTCTCGTGCAG	ATGGATCATTGATGGCGACAACAT	144

Table 9. List of primers used for quantitative real-time polymerase chain reaction. *Abbreviations: OCT4: transcription factor octamer-binding 4; NANOG: NANOG homeobox; SOX2: sex-determining region Y-box 2; H2AFZ: H2A histone family member Z; GAPDH: glyceraldehyde-3-phosphate dehydrogenase.*

2.5 Statistical data analysis

To identify any significant differences of DNA and protein levels before and after DC ANOVA was first used. If the means of the three populations were not considered as equal, the Bonferroni method posthoc test was used. A P-value obtained in a two-tailed test ≤0.05 was considered statistically significant.

A general linear model was fitted for the analysis *in vitro* development rate, including as fixed effect the experimental groups with five levels (NSC, SC, MC, C-FBS, C+FBS). Development rate were computed as the difference in their least squares means ± standard error of means.

Differences in the morphometric and gene expression between the experimental groups (NSC, SC, MC, C-FBS, C+FBS) were estimated using Bayesian inference. Bounded flat priors were used for all unknowns and the marginal posterior distributions were estimated by Gibbs sampling. Both descriptive statistics and phenotypic differences were computed with the program Rabbit developed by the Institute for Animal Science and Technology (Valencia, Spain). After some exploratory analyses, results were based on Markov chain Monte Carlo chains consisting of 60.000 iterations, with a burn-in period of 10.000, and saving only 1 of every 10 samples for inferences. Summary statistics from the marginal

posterior distributions were calculated directly from the samples saved. In all analyses, convergence was tested using the Z criterion of Geweke. The parameters obtained from the marginal posterior distributions of the differences between experimental groups were the mean of the difference between the experimental groups, the highest posterior density region at 95% of probability ($HPD_{95\%}$) and the probability (P) of the difference being greater than 0 when $D_{CP\text{-}VP} > 0$ or lower than 0 when $D_{CP\text{-}VP} < 0$. Differences were considered relevant if $P \geq 0.8$ (80%). A more detailed description of these features can be found in (Blasco, 2005).

Chapter

V

RESULTS

V. RESULTS

1 The pig model: whole uterus decellularization and recellularization of the acellular endometrium

1.1 Visual, histological, and quantitative assessment of successful decellularization

Upon visual inspection of the uterine horn, a color change from pink to opaque white was observed, indicating successful DC after 49 hours for both protocols (Figure 18). No difference in opacity or color was seen between protocols (P1 and P2).

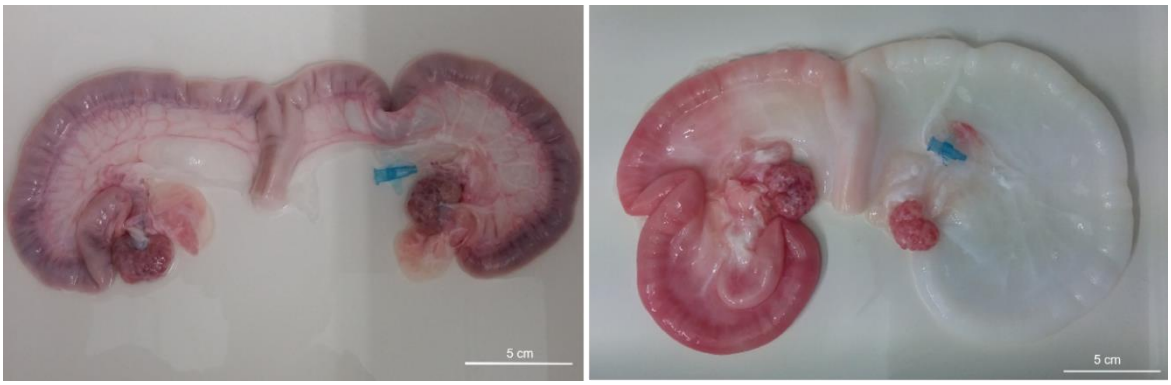

Figure 18. Visual assessment of decellularization. *Macroscopic inspection of uterine horns before (left) and after DC protocols (right). Adapted from (Campo et al., 2017) with permission of Oxford University Press.*

H&E and DAPI staining demonstrated the absence of nuclei and, as such, indicated the efficient removal of DNA while preserving tissue structure (Figure 19 A & B). Further, there was no noticeable difference between the replications (n=3) nor along the four sample locations, demonstrating the reproducibility of the protocols. Hence, in further figures only one representative replicate is shown. Histology showed that the ECM structure appeared slightly more uniform after the fresh protocol.

The successful removal of cellular material was further confirmed by the quantification of residual DNA; a significant reduction from the normal DNA content of a fresh uterus (1571.41 ± 427.17 ng DNA per mg wet tissue) was observed. The remaining DNA for F/T and F protocol was measured as 139.604 ± 89.561 and 40.792 ± 16.462 ng DNA per mg wet tissue, respectively, which corresponds to a decrease to 9.06% and 2.65% compared to the unprocessed uterus (Figure 19 C). Gel electrophoresis did not show any visible bands or signal. The Bonferroni method showed no significant difference between the two protocols with a p-value <0.05. The quantification of the total ECM protein fraction displayed a similar

trend: a statistically significant drop from 8.35 ± 1.8 µg protein/mg wet tissue for the control to 3.26 ± 1.98 and 2.5 ± 1.64 µg protein/mg wet tissue for both protocols respectively was observed (Figure 19 D).

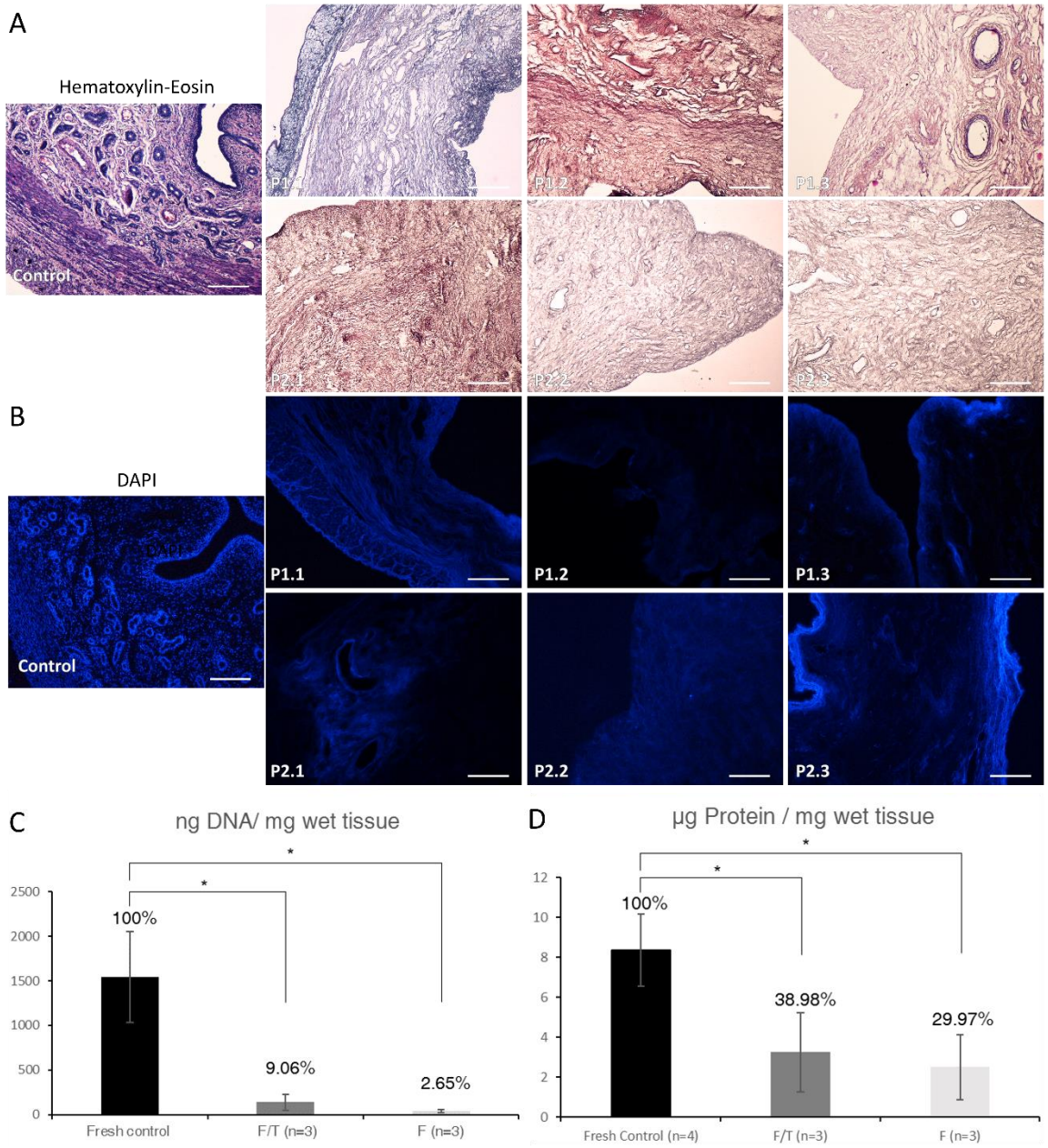

Figure 19. Histological and quantitative assessment of decellularization. *Pictures showing the hematoxylin and eosin (A) and DAPI (B) staining of n=3 repeats for both protocols (Freeze/thaw (PI): F/T and Fresh (P2): F). Quantification of residual DNA showing a drop to 9.06% and 2.65% for the F/T and F protocol, respectively (C). Quantification of remaining protein fraction showing a drop to 38.98% and 29.97% (D). Scale bars: 100 µm. Significance levels = *p < 0.05. Adapted from (Campo et al., 2017) with permission of Oxford University Press.*

1.2 Histological composition of the novel uterine bioscaffold

To investigate the effects of DC on the composition of the ECM, two types of histological staining were used; Masson's trichrome is a three-color staining protocol that dyes collagen

fibers blue, nuclei black and the cytoplasm and muscle cells red. Alcian blue, on the other hand, stains acidic polysaccharides such as GAGs.

MT staining was able to demonstrate both the complete removal of cellular material and the preservation of the most important structural ECM proteins following DC, namely the collagens. The red staining of the cytoplasm was completely removed after both protocols, while the blue stained collagen fibers remained (figure 20 A). The qualitative analysis of sulphated GAGs by Alcian blue staining showed a widespread distribution with a higher signal at the epithelial layer of the endometrium and secretory glands. After DC, only this widespread distribution remained in both protocols with a noticeably lower signal at the epithelium (figure 20 B). The diminished staining of Alcian blue is comparable to results reported in other publications (Gilpin *et al.*, 2014; Oliveira *et al.*, 2013).

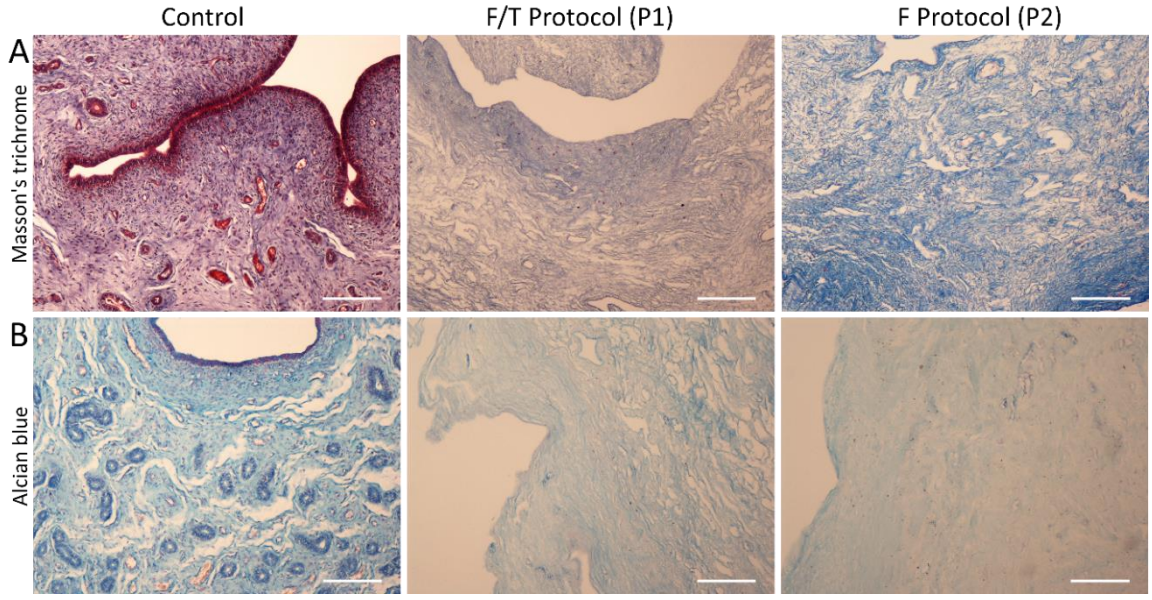

Figure 20. Histological analysis of ECM components. *Masson's trichrome (A) and Alcian blue (B) staining to assess decellularization and the detection of collagen and sulphated GAGs, respectively. In both cases, the positive control corresponds to the pig uterus before DC. Scale bars: 100 µm. Adapted from (Campo et al., 2017) with permission of Oxford University Press.*

1.3 Immunofluorescence of the main extracellular matrix proteins

To further assess the effect of both protocols on the ECM, the presence of major ECM components before and after DC were investigated using immunofluorescence (Figure 21 and 22). These are the structural ECM proteins collagen type I and elastin, fibronectin (important for cell interactions), and basement membrane components collagen type IV and laminin.

Collagen type I, the most abundant component in collagen fibers, gives structural support to resident cell and remained, as expected, evenly dispersed in ECM before and after

DC (figure 21 A). Elastin, another major structural constituent of the ECM is important for the elasticity of the scaffold and is of special interest for uterine scaffolds that need to expand and contract with the uterus during pregnancy. A signal was found mainly in the myometrium, basal endometrium, and around arteries (figure 21 B). After DC there was a noticeably weaker signal in the interstitial endometrium, while myometrium and arteries remained unaffected.

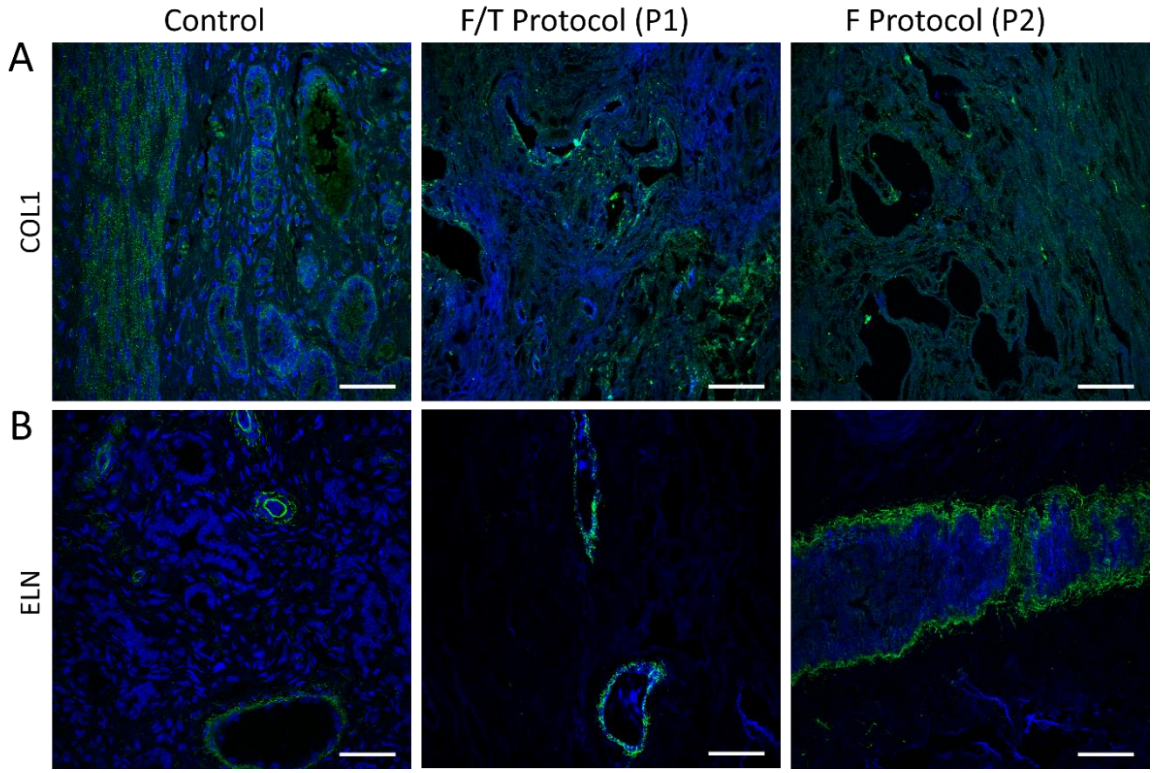

Figure 21. Immunofluorescence staining of the major structural ECM proteins. *Images showing blue signal for nucleus (DAPI) and green signal for collagen I (COL1, A) and elastin (ELN, B) proteins. Pig uterus before DC was used as positive control. Intensity projection over Z-axis. (40x magnification, scale bars: 50 µm. Adapted from (Campo et al., 2017) with permission of Oxford University Press.*

Fibronectin, sometimes referred to as the "master organizer" for the biogenesis of the extracellular matrix (Sabatier *et al.*, 2009), was unaffected and evenly dispersed in ECM, before and after both protocols (figure 22 A). Two of the prominent components of the basement membrane, collagen IV and laminin (important in cellular processes like cell differentiation, migration, and adhesion) were detected before and after DC in endothelial layers around blood vessels and glandular structures in both layers. Collagen IV was also observed in the myometrium (figure 22 B&C).

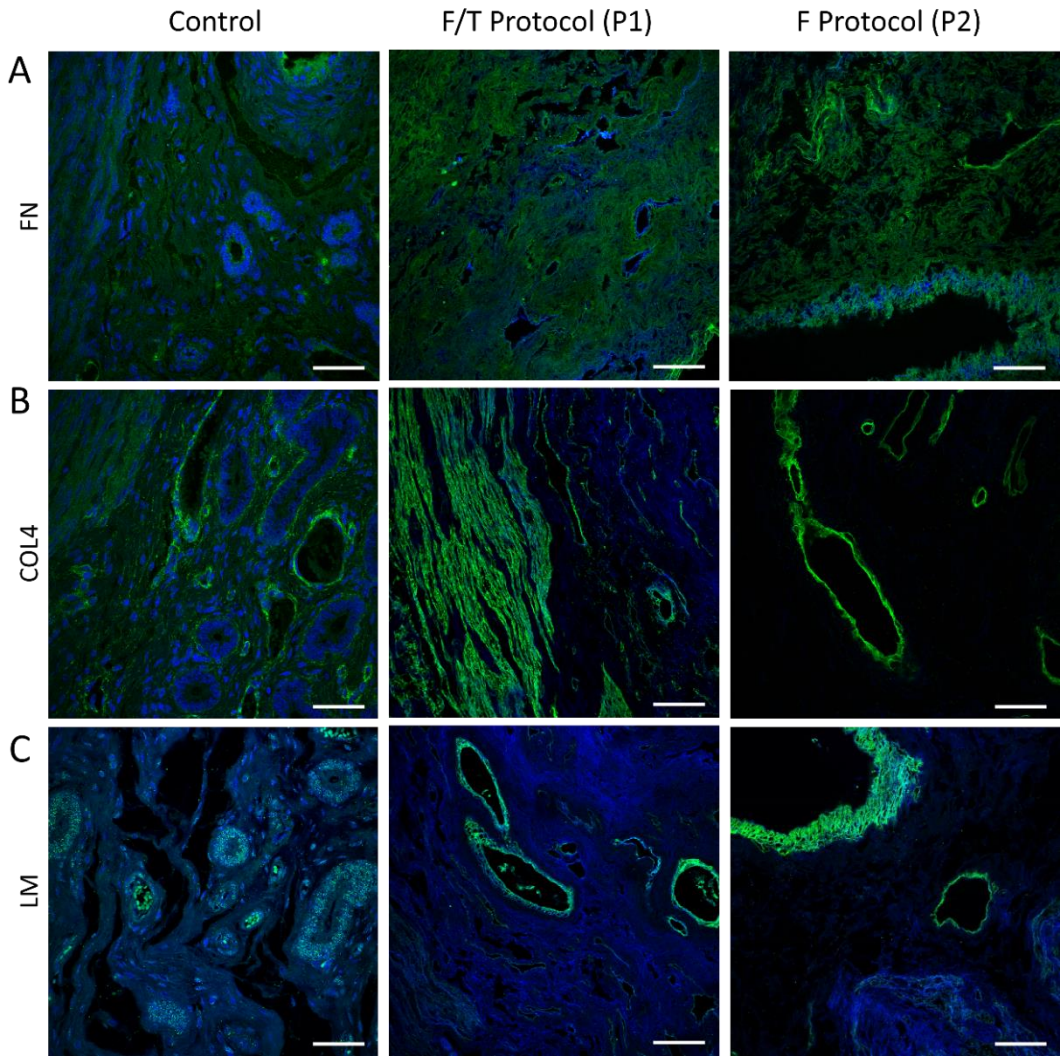

Figure 22. Immunofluorescence staining of main cell-interacting ECM proteins. *Images showing blue signal for nucleus (DAPI) and green signal for fibronectin (FN, A), collagen IV (COL4, B), and laminin (LM, C) proteins. Positive control used in all the cases corresponds to the pig uterus before DC. Intensity projection over Z-axis. (40x magnification, scale bars: 50 μm. Adapted from (Campo et al., 2017) with permission of Oxford University Press.*

1.4 Ultrastructure of the decellularized uterus

Scanning electron micrographs at low magnification allowed for the investigation of the surface topography, the epithelial/stromal interface and the upper part of the stromal fraction of the endometrium.

All elements of the endometrial lumen, the epithelial surface and glandular structures, remained intact and there were no significant differences observed between all conditions, both before and after DC (Figure 23 A). Figure 23 B shows the epithelial layer in tissue from the fresh protocol appeared to be more damaged, but this was due to manipulation of the sample. Furthermore, the preservation of the complex hierarchical organization and fibrous aspect of the stromal interstitial ECM before and after treatments can be appreciated. At both higher and lower magnifications, structures corresponding to the specialized ECM of

the basement membrane can be identified (Figure 23 B and C, black arrows). At higher magnification it was clear that the fibers and topography retained their appearance in both protocols and vascular conduits kept their conformation (Figure 23 C). Transmission electron micrographs showed collagen fibrils, which maintained their striated patterns and were abundant in all orientations throughout the tissue (Figure 23 B). No noticeable differences at ultrastructural level between the protocols were observed.

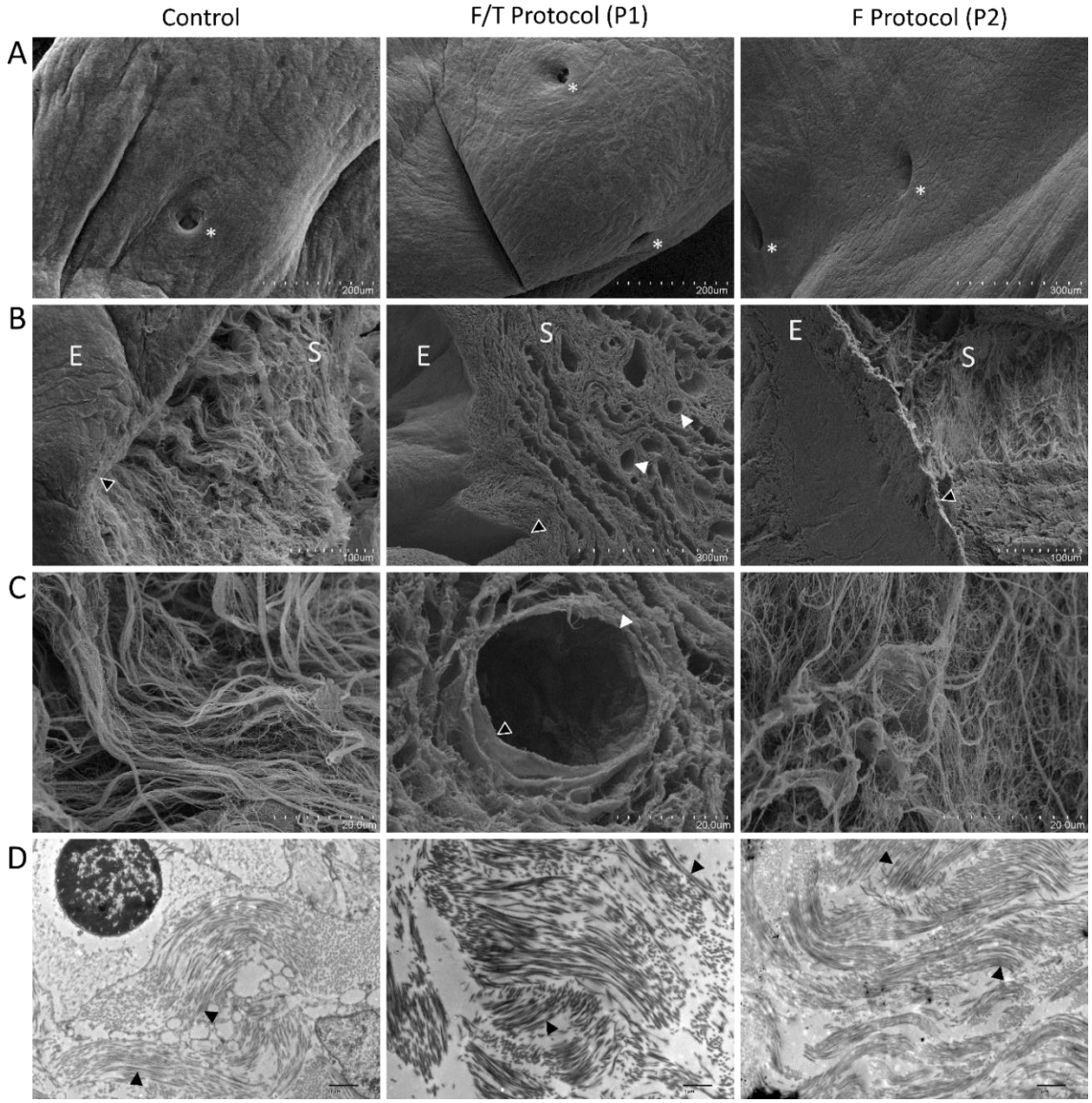

Figure 23. (Ultra-) structural and histological comparison after decellularization protocol with both P1 and P2 conditions. *Scanning electron micrographs at lower magnification (300x magnification) showing the lumen of the endometrium with glandular structures, as indicated by the white asterisks (A). Micrographs of epithelial (E) and stromal (S) fractions at the E-S interface of the luminal epithelium (B). Higher magnification images of the fibrous stroma demonstrate the aspect of the fibers at the interstitium and basement membrane after P1 and P2 (800x magnification, C); white and black arrowheads indicating blood vessels and basement membrane structures respectively. Transmission electron micrographs showing collagens and elastin fiber bundles (black arrowheads), (3000x magnification, scale bars: 1 µm, D). The positive control corresponds to the pig uterus before DC. Adapted from (Campo et al., 2017) with permission of Oxford University Press.*

1.5 Vascular tree network cast of the decellularized organ

Four uteri were successfully perfused at two different perfusion speeds with the monomer solution to make a vascular corrosion cast (Figure 24).

Macroscopic analysis showed a lack of rigidity at the uterine horn after both DC protocols. At many locations, the tubular uterine horn did not form a closed circle, in contrast to the control. Both controls were extensively perfused with PBS for one hour to remove all possible clots and blood, but this was not done for the acellular horns. The vascular deformation was observed more clearly when sections were placed under a stereomicroscope. The control also displayed a noticeable white region corresponding to saponified tissue that was not completely removed at the subepithelial capillary plexus region of the endometrium, which was also present to a lesser extent in the decellularized samples. Interestingly, when this white zone was investigated at higher magnification, it appeared to be in fact the relatively intact subepithelial capillary plexus, with capillaries at the correct range of thickness with averages of 11.84±4.99, 9.68±2.34, 10.94±1.56 μm for control, P1 and P2 decellularized uteri respectively. The diameter of these capillaries were not significantly different and are similar to those found in the rat uterus (with averages of 7.5 ± 0.4 and up to 18.5 ± 2.5 microns closest to the site of embryo implantation) (Tawia and Rogers, 1992).

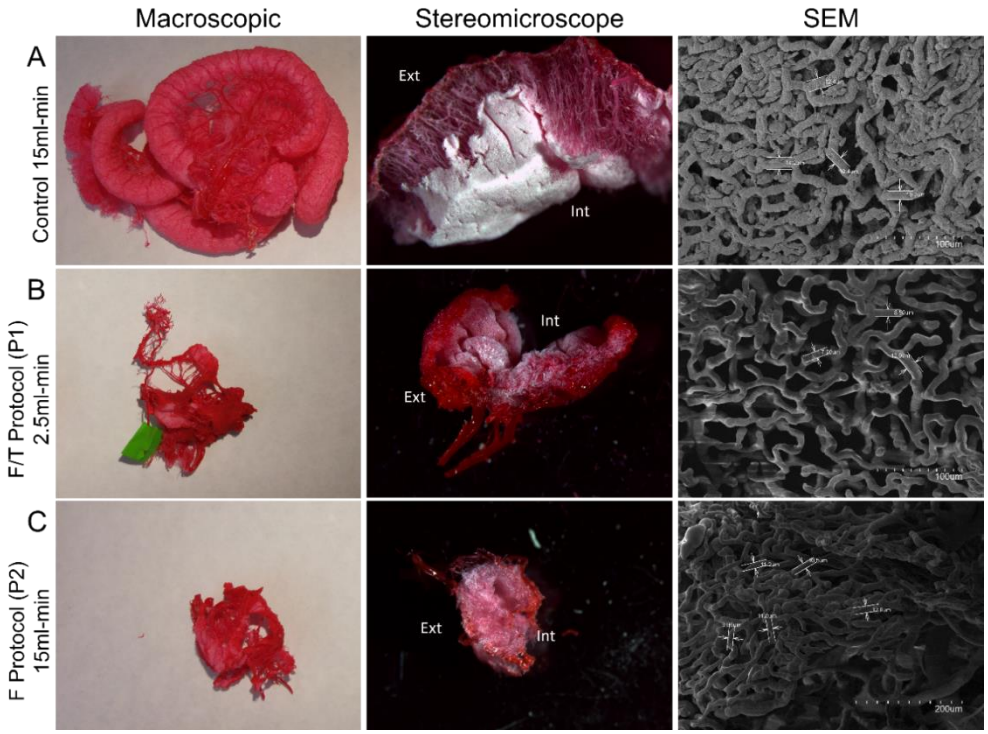

Figure 24. Corrosion cast of vascular network of the uterine horn. *After maceration of tissue the integrity of vasculature was assessed macroscopically (left column). Sections of the cast were used for stereoscopic close-up (middle column, ext and int referring to external border of perimetrium and inner lumen of the porcine horn) and consequently for scanning electron micrograph of capillaries at the epithelial layer (right column). Pictures from the uterus control (A), F/T DC protocol (B), and F DC protocol (C) representing macroscopic, stereomicroscopic, and SEM, respectively. Reprinted from (Campo et al., 2017) with permission of Oxford University Press.*

1.6 Recellularization of uterine three-dimensional scaffolds

ECM discs from the acellular endometrium were recellularized with human Side Population (SP) cells (ICE 6/7) to demonstrate the feasibility of whole organ recellularization and to assess the bio-inductive capacity of the bioscaffold.

For this, tissue from the P2 protocol were used as it provided the most uniform ECM. After seeding human SP cells, the coated scaffolds rolled up and contracted, forming an organoid-like structure (Figure 25 A). H&E staining showed that the cells were encapsulated within the decellularized scaffold, demonstrating that cells were attaching and interacting closely with the endometrial ECM (Figure 25 C).

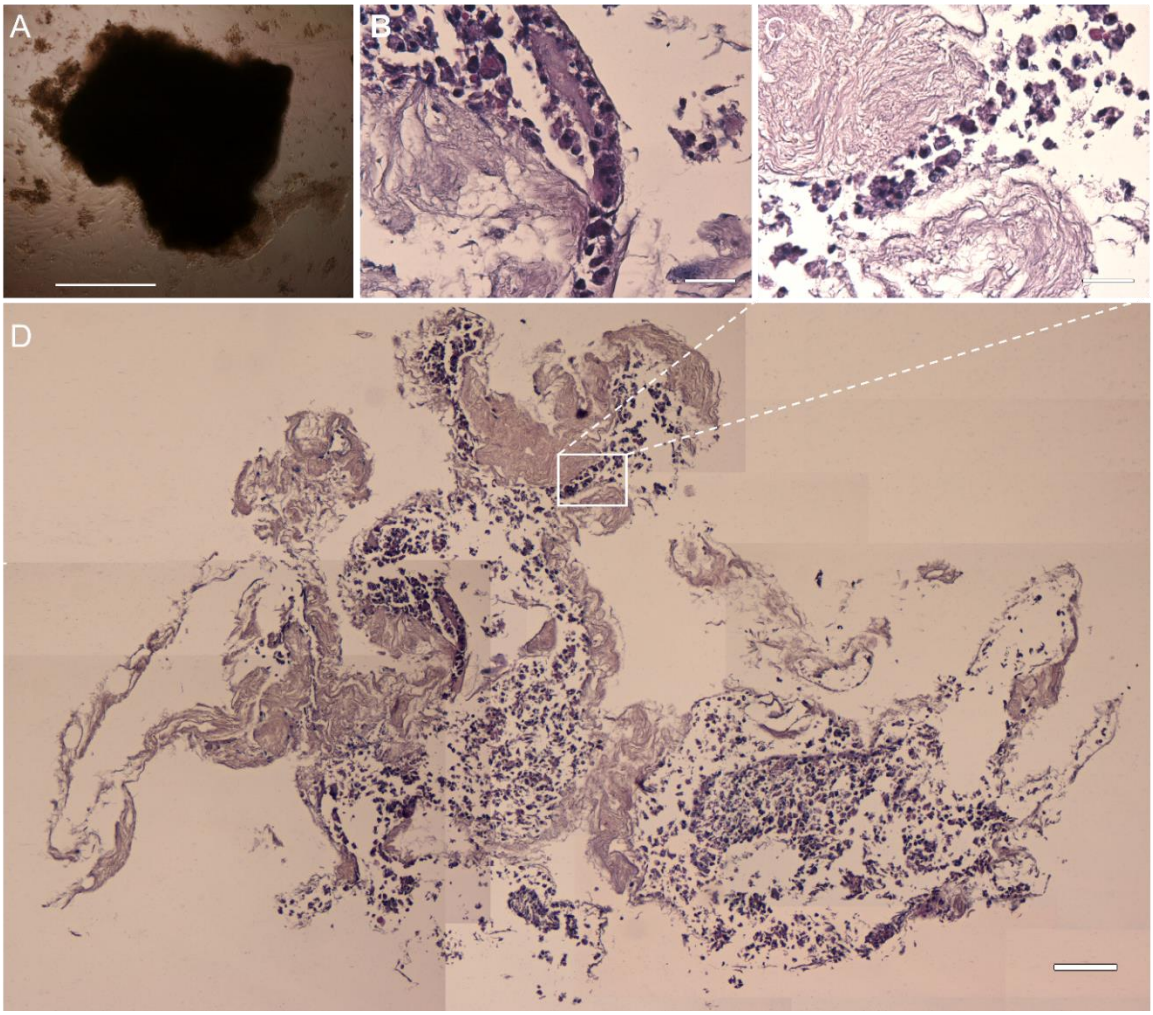

Figure 25. Organoid-like structure formation and histology. *Endometrial decellularized discs obtained from whole organs formed an organoid-like structure after 3-4 days under hypoxic culture conditions (scale bar = 50 µm) (A). H&E staining showing the organization of the structure, with human SP cell lines interacting closely with the ECM after cell seeding and 9-12 days of culture on scaffold (B&C, scale bar = 20 µm). A merged photo of the showing the transection of the organoid-like structure (D, scale bar = 100 µm). Adapted from (Campo et al., 2017) with permission of Oxford University Press.*

To demonstrate the tissue-specific phenotypical behavior of the SP stem cells, immunofluorescent staining of typical endometrial markers was performed (Figure 26). Cells with a positive signal for vimentin, an intermediate filament protein expressed in mesenchymal cells, were observed throughout the entire structure. Cells expressing cytokeratin, a marker for epithelial cells, were also present in the organoid-like structure (Figure 26 B).

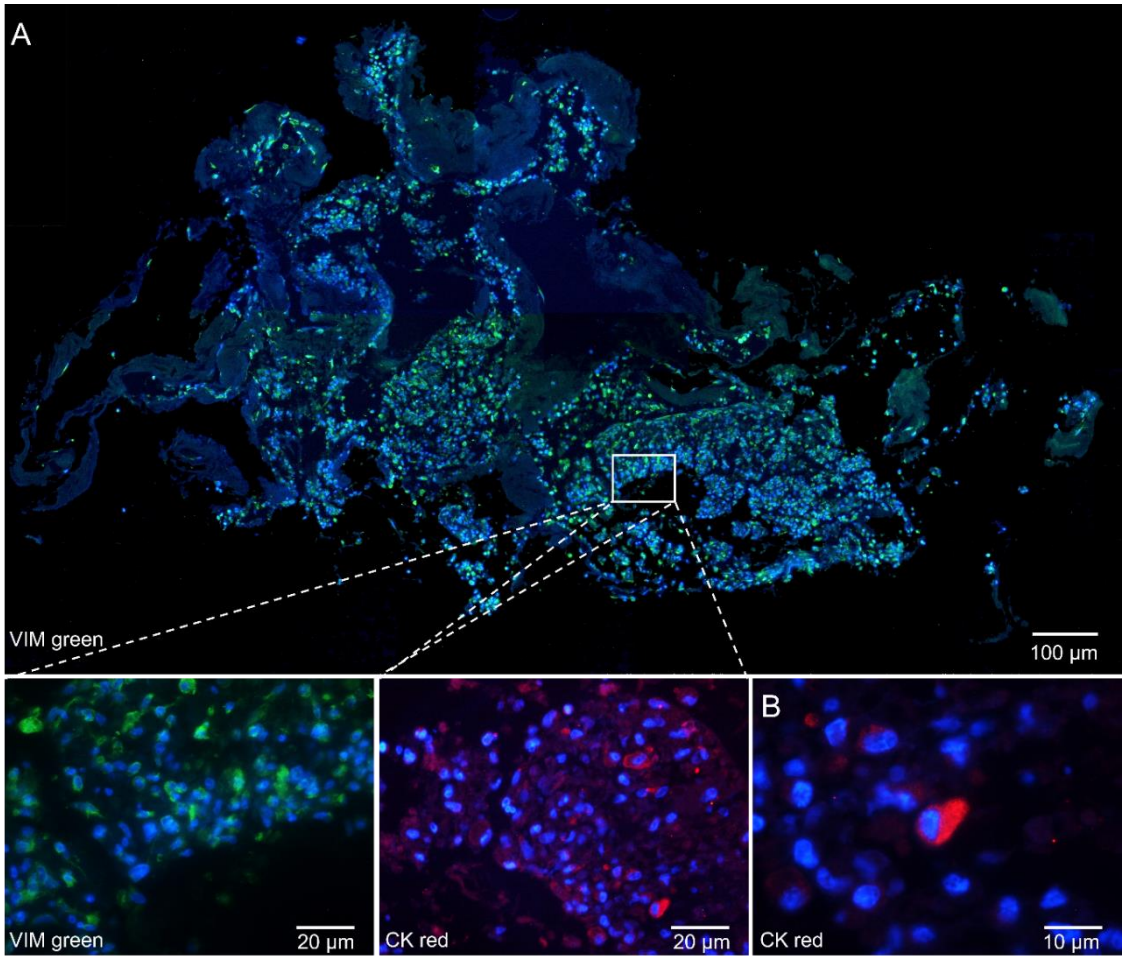

Figure 26. Immunofluorescence analysis of organoid-like structure. *Immunofluorescence staining of vimentin (green) and cytokeratin (red) after cell seeding of human SP cell lines for 9-12 days on scaffold, nuclear staining appears blue (DAPI) (A). Detail of cytokeratin-positive cell (B). Adapted from (Campo et al., 2017) with permission of Oxford University Press*

2 The rabbit model: whole uterus decellularization, solubilization of acellular endometrium and embryo culture on tissue-engineered substratum

2.1 Macroscopical, histological and quantitative analysis of decellularization

Visually, both horns of the uterus (n=4) turned white/opaque after the DC protocol, with no meaningful differences observed between non-synchronous and synchronous uteri,

nor within the replications (Figure 27 A&B). Rabbit uteri described as non-synchronous and synchronous correspond to hormonally untreated and treated animals respectively, as described in the materials and methods section.

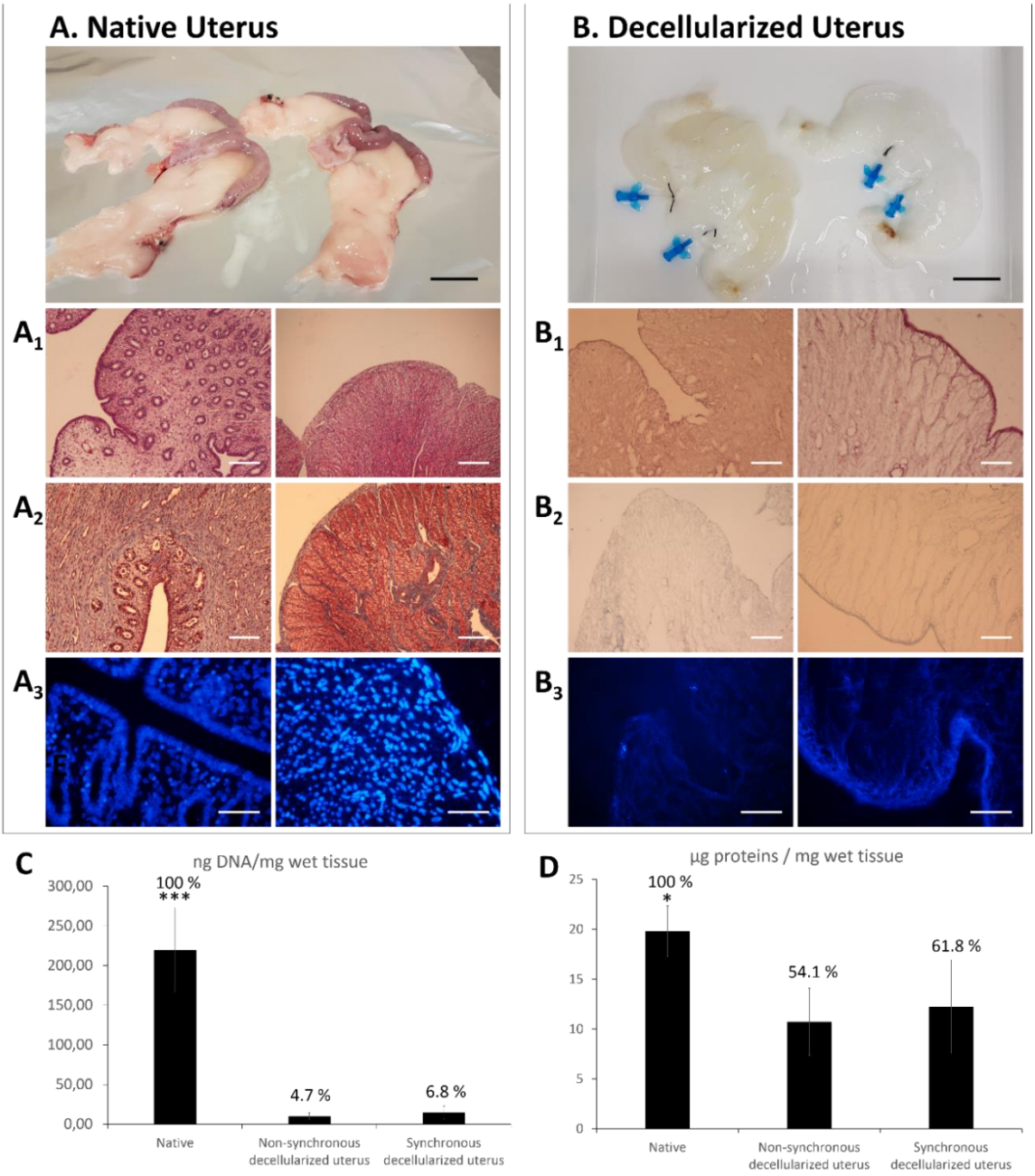

Figure 27. Decellularization of rabbit uterus. *Macroscopic aspect of rabbit uteri before (A) and after (B) decellularization (n=3), blood and cellular material was lysed and removed via perfusion resulting in an opaque/white organ. Representative histological images of native and decellularized endometrium (left) and myo-perimetrium (right) demonstrating full DC throughout the uterus. H&E (A1 & B1) and Masson's trichrome stain (A2 & B2) demonstrate removal of cellular material and an intact ECM rich in collagens. Scale bars are 150 µm. (A3 & B3) DAPI stain showing complete destruction of nuclei though all layers. Scale bars are 50 µm. (C) DNA quantification with Qubit™ dsDNA HS Assay confirmed a 95.3% and 93.2% reduction in double stranded DNA for the non-synchronous and synchronous decellularized uterus respectively. (D) Qubit Protein Assay Kit showed a 45.9% and 38.2% decrease in protein concentration in both tissues. *** and * denote significance from all other data points as indicated by an ANOVA with Bonferroni correction (*** p<0.001 and *p<0.05)*

DC was first verified by histological methods: H&E and MT staining showed the complete removal of cellular material and nuclei in all layers while preserving the ECM architecture consisting predominantly out of collagens (Figure 27 A1-2 & B1-2). Representative images of the histology were used. Furthermore, DAPI staining confirmed the complete destruction of the nuclei in all uterine layers (Figure 27 A3 & B3).

This was corroborated by the quantification of the residual DNA, a significant reduction ($P < 0.001$) compared to the native uterus was measured for both non- synchronous and synchronous uterus (219.46 ± 53.25 vs 10.31 ± 4.26 and 14.93 ± 7.89 ng DNA per mg wet tissue respectively, Figure 27 C). Similarly, protein content significantly ($P < 0.05$) dropped from 19.8 ± 2.56 to 10.72 ± 3.36 and 12.24 ± 4.70 µg proteins per mg wet tissue respectively (Figure 27 D). No difference in histology (not shown) or quantification ($P < 0.05$) was observed between both types of uterus.

2.2 Microdissection of decellularized endometrial tissue

When the thin circular cuts (of approximately 1mm thick) were placed under a stereomicroscope, a transparent layer became apparent in the native tissue; moreover, the elongated fibrous ECM of the myometrium is also apparent in the decellularized tissue (Figure 28 A and C).

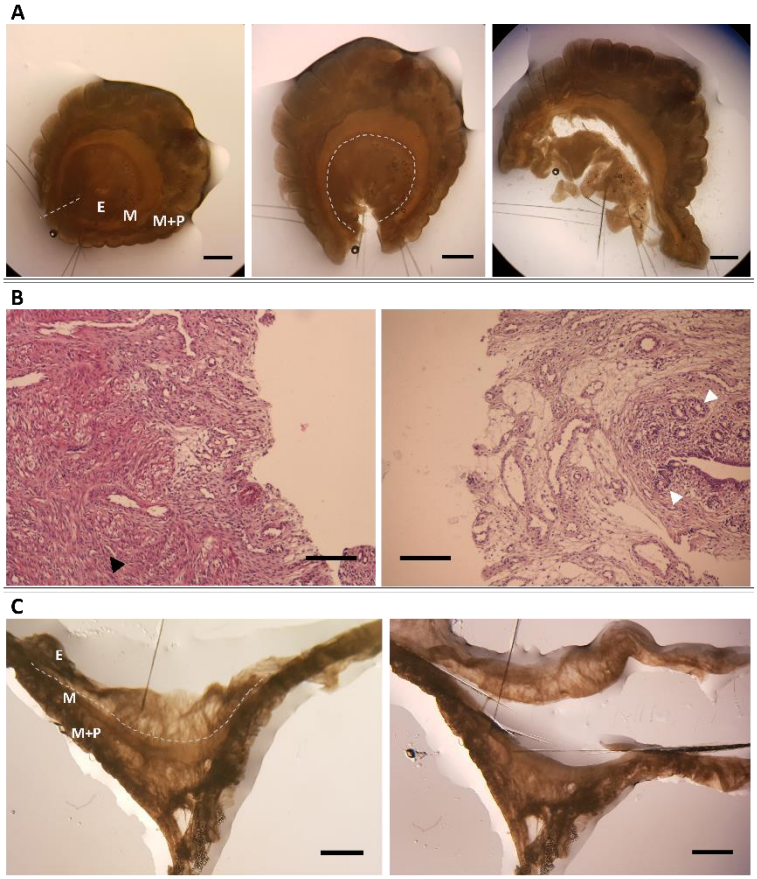

Figure 28. Microdissection of uterine tissues. *separation of endometrium in native tissue as proof-of-concept, the 3 prominent layers are apparent (E: endometrium, M: inner myometrium, M+P: outer myometrium + perimetrium), in total 2 cuts are being made as shown by the dotted line, one to open the uterine horn (left) and the other one where cuts are being made at the luminal side of the myometrial layer (middle). scale bars are 0.2 cm (A). Representative images of H&E stain of separated native myometrium (left) and endometrium (right), black arrow head showing the inner circular smooth muscle layer, white arrow heads showing gland of non-synchronous endometrium (B). Scale bars are 150 µm. separation of decellularized tissue, the aligned ECM from the*

myometrial cells is distinguishable (M) and cuts were made following the dotted line (C). Scale bars are 0.2 cm.

This ribbon appears because the rabbit myometrium consists of an inner circular and outer longitudinal smooth muscle layer, and by making circular cuts we aligned the correct muscle fibers and could use it as separation guide. After opening the uterine horn, the endometrium was cut at the luminal side of the myometrium (Figure 28 A & C). To verify the endometrial purity, a collection of separated endo- and myometrium of the native tissue were included in PFA, cut and stained by H&E (Figure 28 B). Here it is apparent that the incisions are being made above the muscle layer, in the endometrium, resulting a pure tissue (showing typical stromal and epithelial glandular structures) for both native and decellularized tissue.

2.3 Tissue-specific powder appearance, pre-gel creation and evaluation of sterility

The lyophilized non-synchronous (NS, n=3) and synchronous (S, n=3) acellular endometrium were milled with dry ice in an ultracentrifugal mill to reach grain size smaller than 0.0625mm^2. This powder was digested in pepsin until no more tissue was visible (Figure 29 A-C).

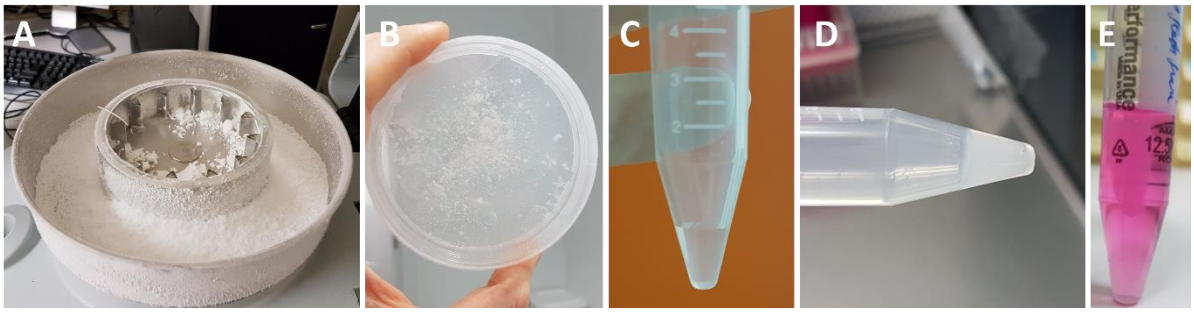

Figure 29. Creation of pre-gel solution, gelation and sterility of endometrial hydrogel. *Milling of the lyophilized endometrial tissue by ultracentrifugal mill and dry ice (A) resulted in a fine powder with fragments smaller than 0.0625mm2 after the sublimation of the dry ice (B). A transparent and viscous pre-gel solution was obtained after partial digestion (C) that gelled after 1 hour at 37°C (D). (E) Hydrogel after 7 days incubation at 37°C in cell culture medium, demonstrating structural long-term stability and sterility.*

The resulting viscous pre-gel solutions formed stable hydrogels that required gentle handling when left at 37°C for one hour (Figure 29 D). Long-term structural stability and sterility of this ECM-derived gel was demonstrated by incubating them at 37°C in standard cell culture medium for 7 days (Figure 29 E). The hydrogel remained intact during this period and no bacterial growth was observed.

2.4 Gelation kinetics of ECM hydrogels

Both hydrogels were subjected to turbimetric analysis, for which gelation kinetics were measured spectrophotometrically and important parameters were calculated (t_{lag} and $t_{1/2}$). Both gelation kinetics followed a sigmoidal curve, but significant differences were observed in the $t_{1/2}$ parameters (Figure 30 A). Gelation of the S hydrogel started earlier tended to have a lower lag time than the NS hydrogel (t_{lag} =2.98 ± 0.86 min vs 4.9 ± 0.33 min). The time to reach 50% of the maximal gelation did show significant differences, where the S gel needed about 5 minutes less than the NS hydrogel ($t_{1/2}$ = 10.43 ± 0.74 min and 15.46 ± 0.29 min respectively, Figure 30 B).

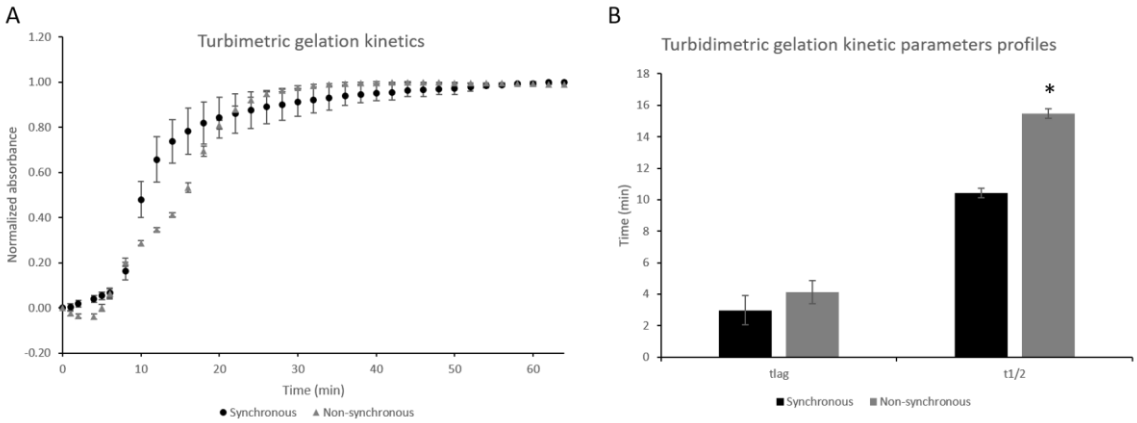

Figure 30. Turbidimetric gelation kinetics and kinetic parameters of ECM hydrogels. *Pre-gel solutions were thawed on ice and pipetted in the wells of a 96-well plate; gelation was induced at 37 °C and absorbance was measured and every minute at 405nm. Results were normalized between 0 (initial absorbance) and 1 (maximum absorbance) and from the kinetic profiles (A) the lag time (t_{lag}, time until gelation starts) and half maximum absorbance time ($t_{1/2}$, time to 50% maximum absorbance) were calculated (B). * denotes significance between both hydrogels as determined by a two-sided student-t test with equal variance (*p<0.05).*

2.5 Ultrastructure of endometrial ECM hydrogels

Even though the hydrogels lost their original hierarchical organization, scanning electron microscopy of the gel surface showed that both NS and S gels have a homogenous, randomly interlocking fibrillar structure of similar density (Figure 31 F-G).

Fiber diameter of the NS and S hydrogels was analyzed from images taken at 60.000X resolution (>30 measurements per gel). The diameter of the re-assembled nanofibers from both gels range between 50 and 149 nm, measuring on average 70.04 ± 9.15 vs 102.90 ± 22.66 for the non-synchronous and synchronous hydrogel respectively (Figure 31 F). A significant difference between both fiber diameters was found. It is possible that the collagen fibrils, having a thickness of 50 nm on average remained more bundled in the S hydrogel, or that components interacting with the fibers persisted. It is also apparent that

the majority of fibers of the NS and S hydrogels show the D-periodicity typical for collagen fibrils, in contrast to the Matrigel hydrogel (Figure 31 C-E).

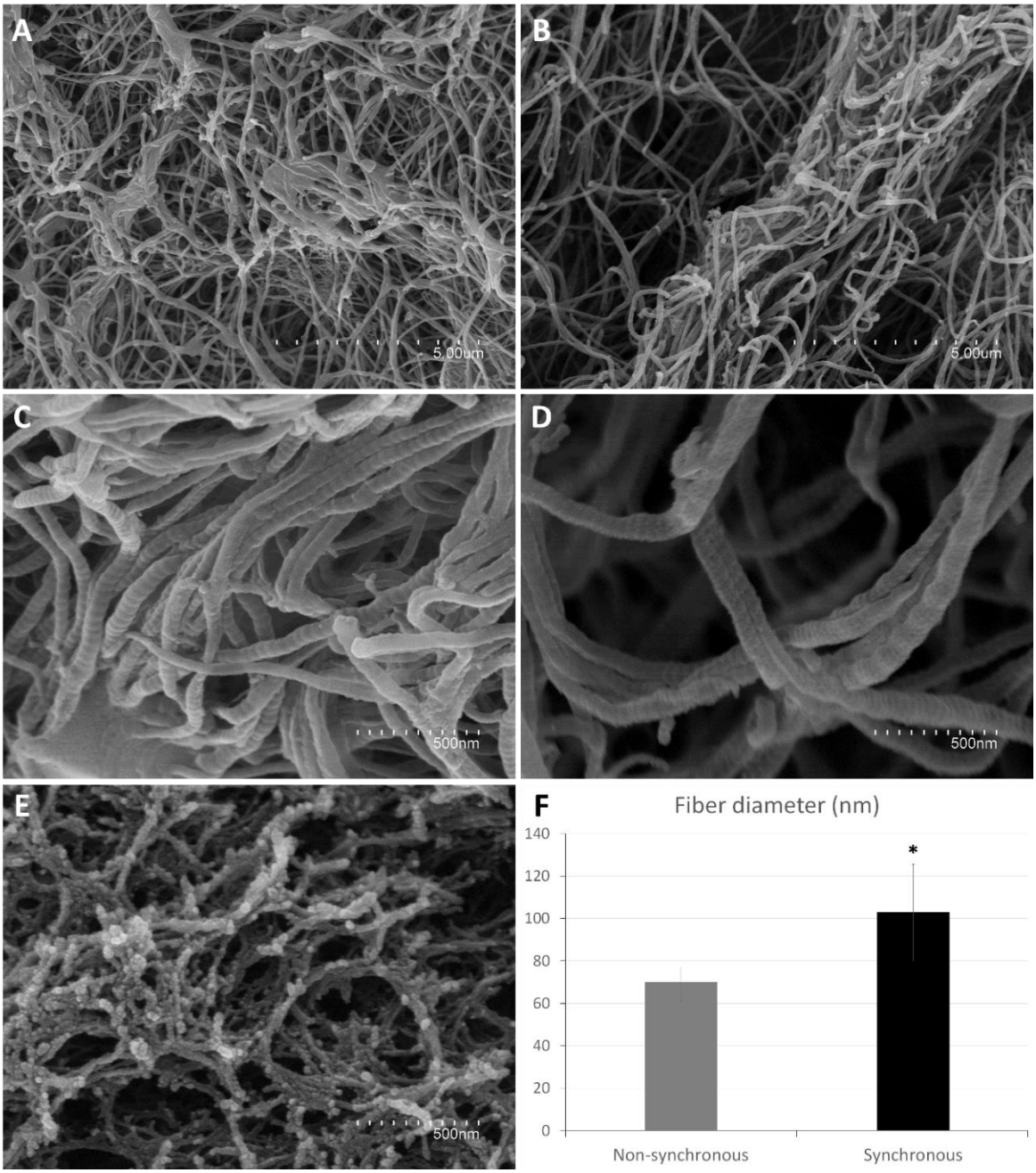

Figure 31. Ultrastructure of endometrial ECM hydrogels. *Representative scanning electron micrographs at 10.000x magnification of ultrastructure of non-synchronous (A) and synchronous (B) gel with nanofibers ranging between approximately 50-150 nm thick and showing similar density. Scale bars are 5µm. Fibers were evaluated and measured using micrographs at 60.000x magnification of non-synchronous (C), synchronous (D) hydrogel and Matrigel (E), showing their characteristic morphologies such as D-periodicity for the ECM hydrogels. These and similar images were used to measure the diameter with ImageJ software. Scale bars are 500 nm. The average diameter of both ECM hydrogels shows a significant difference (F). The differences of fiber diameter between NS and S gels were calculated with a significance level = *p < 0.05.*

2.6 Effect of endometrial hydrogels on *in vitro* development and mRNA expression at blastocyst stage

Figure 32 shows the expected *in vitro* development of day 3 embryos after 24 (Figure 32 B) and 48 hours (Figure 32 C), which was found for both control and coated conditions. *In vitro* development was not significantly affected by culture conditions on the NSC/SC/MC coatings, the mean value of hatching/hatched rates here was 89.4±3.13% which is very similar to the control conditions.

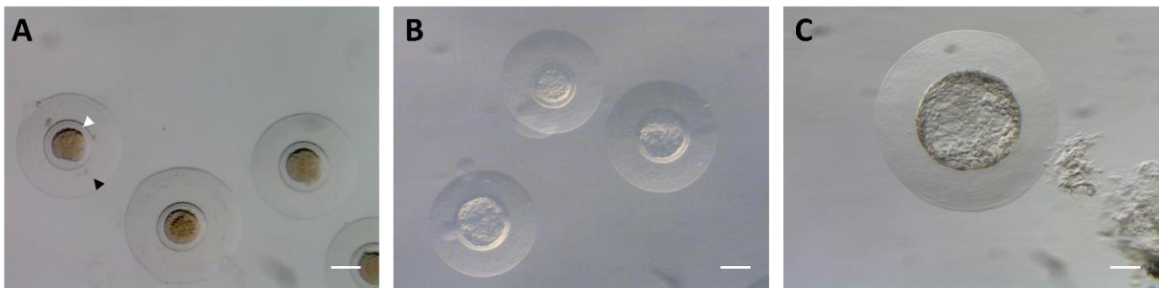

Figure 32. Correct embryo development on substrata. *Representative morphology of in vitro developing embryo 72hrs after insemination on SC. Late stage morulae/early stage blastocyst after collection showing homogenous cellular mass, spherical zona pellucida (white arrowhead) and mucin coat (black arrowhead) (A). Hatching blastocysts after 24hrs of in vitro culture (B). Fully hatched blastocyst after 48hrs of in vitro culture (C). Scale bars are 0.1mm.*

However, this was not the case for the when they were cultured on hydrogels, the detrimental effect of this condition (NSH, SH and MH) on the development was very noticeable, with hatching/hatched rates averaging around 27.64±26.38%. An interesting observation was that not only that the development was impaired in the Matrigel hydrogel (MH) conditions (Figure 33 A) but also that some embryos showed an aberrant morphology in the corresponding coating (MC) condition (Figure 33 B).

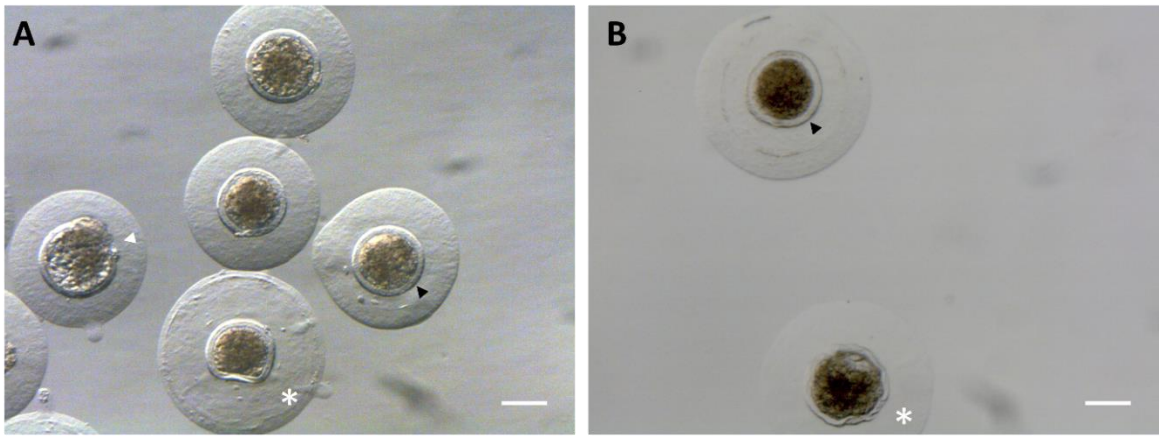

Figure 33. Impaired embryo development on Matrigel hydrogel and coating. *Morphology of in vitro developing embryos after 48hrs of in vitro culture on MH (A) and MC (B). The embryos shown here have hatching (white arrowhead) and stalled (Black arrowhead) morphology, note the aberrant morphology of some of embryos with the undulations in the zona pellucida (white asterisk). Scale bars are 0.1mm.*

The mean diameter of the embryos of SC and C+FBS groups with 0.2656 and 0.2727 mm respectively was significantly higher than the diameter of the NSC, C-FBS and MC groups after 48 hours of *in vitro* culture, with a mean diameter of 0.2562, 0.2483 and 0.2271 mm respectively (Figure 34).

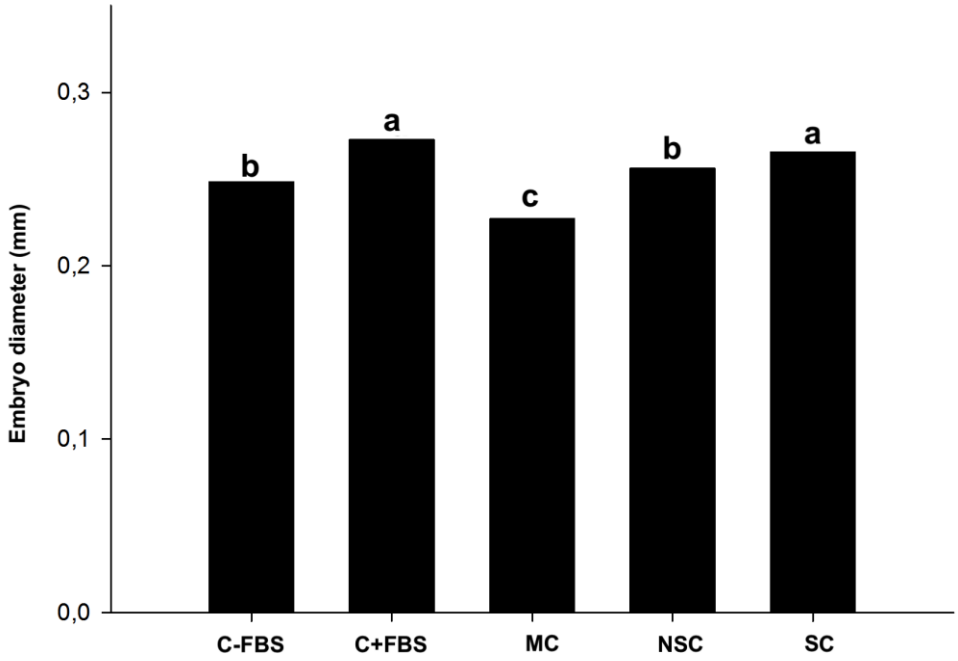

Figure 34. Morphokinetic analysis of day 5 embryos. *Effect of different biological surface coatings made from non-synchronous acellular endometrium (NSC), synchronous acellular endometrium (SC) and Matrigel (MC) and two standard culture conditions using uncoated wells with culture medium supplemented with and without 10% Fetal Bovine Serum (C+FBS and C-FBS, respectively) on embryo diameter after 48 h of in vitro culture. Identical letters represent similar results.*

In addition, the pattern of mRNA expression of NANOG was not significantly affected by culture conditions. Nevertheless, blastocysts developed in the NSC group showed higher levels of *OCT4* transcript abundance than C-FBS group, while SOX2 transcript abundance was higher in the blastocysts developed in SC, NSC and C+FBS groups compared to the MC and C-FBS groups (Figure 35). As with the morphometric analysis (Figure 34) SC and C+FBS groups showed similar trends in the expression of *OCT4* and *SOX2* (a,b).

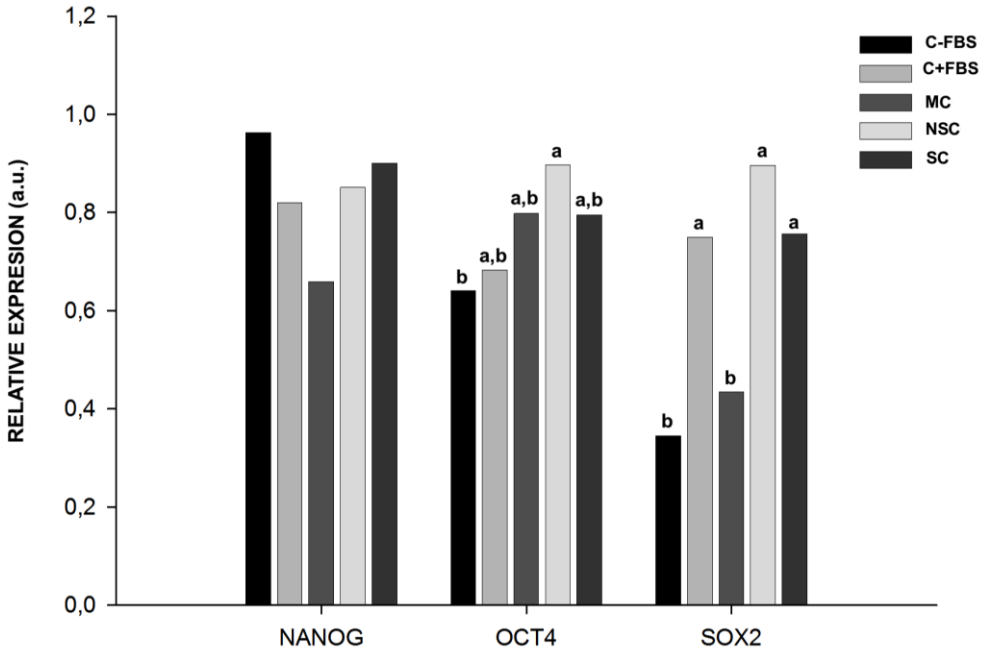

Figure 35. mRNA expression of three core pluripotency factors. *Analysis of mRNA transcription levels for NANOG, OCT4 and SOX2 in blastocysts/hatched blastocysts after in vitro culture for 48 h in different biological surface coatings made from non-synchronous acellular endometrium (NSC), synchronous acellular endometrium (SC) and Matrigel (MC) coatings and two standard culture conditions using uncoated wells with culture medium supplemented with and without 10% Fetal Bovine Serum (C+FBS and C-FBS, respectively). Values from real-time PCR were normalized to geometric average of H2AFZ and GAPDH. Identical letters represent similar results.*

Chapter

VI

DISCUSSION

VI. DISCUSSION

With more than 70 million couples affected, infertility is considered a worldwide public health issue, affecting both males and females, many of which come from developed countries (Ombelet et al., 2008). In the United States alone, 12% of 15-44 years old women (7.3 million) have impaired fecundity (data from 2002)(Chandra et al., 2005). These issues resulted in the birth of medically assisted reproduction, and great advances in treating pathologies leading to reproductive dysfunction have been made ever since. However, as discussed in section 1.4 "Uterine pathologies affecting the human reproductive outcome" of the introduction chapter, some of the diseases resulting in female infertility are still poorly treatable and can profit greatly from advances made by reproductive bioengineering.

One of the main afflictions in reproductive medicine that was untreatable until recently is Absolute Uterine Factor Infertility (AUFI). Until recently, gestational surrogacy is the only alternative to conceive genetically related offspring, however, it is an expensive solution with many legal and ethical challenges/problems (Ber, 2000; Shenfield et al., 2005). The only definitive treatment for AUFI is allogeneic transplantation. Uterine transplantation is a very complicated procedure and attempts were unsuccessful until very recently (Fageeh et al., 2002; Ozkan et al., 2013). The Brännström group provided the first proof-of-concept of this treatment with the first live birth after uterus transplantation (Brännström et al., 2015). Although being a milestone in reproductive medicine, it suffers from the same problems associated with all organ transplantations, which is also used to cure end-stage organ failure. Apart from the inherent risk of surgery, there are long waiting periods caused by the lack of compatible donor organs and the need for long-term immunosuppression after the transplantation. The former is a less pressing issue in this situation seeing that the uterus is a non-vital organ. The latter, however, is associated with severe side effects lowering the quality of life of the patients. Examples of this are nephrotoxicity, increased susceptibility to infections, diabetes and accelerated arteriosclerosis (Azimzadeh et al., 2011).

Many techniques and technologies are being developed to resolve these issues. One line of investigation, the de- and recellularization of whole organs, has shown promising results to possibly someday engineer transplantable organs (Ott et al., 2008). Here, organs could be regenerated by incubating vascularized complex scaffolds with cells in a bioreactor to create, in theory, an endless supply of allogeneic donor organs that do not trigger an immune response (O'Brien, 2011). This type of scaffold is created by perfusion with

decellularizing agents, removing cells and (xeno- or allogeneic) antigens responsible for the foreign body response (Crapo et al., 2011). Furthermore, constituents of the extracellular matrix (ECM) are highly conserved between species, opening the possibility of using xenogeneic donors. Immune rejection in the recipient can be avoided if the antigens are successfully removed without compromising the ECM morphology (Wong et al., 2016).

In other words, the main objective of DC is to create 3D biological acellular matrices that are re-implantable in future recipients and can be recellularized with several types of cells (autologous and/or allogeneic stem cells, etc.) (Peloso et al., 2015). The DC procedure's success depends on tissue density, thickness, and cellularity. Hence, protocols must be adapted to the organ of interest; one technique does not always translate from one organ to the other or even between the same organs of different species, and optimization and comparison of protocols is necessary (Hellström et al., 2014; Santoso et al., 2014). Because of this, many specialized DC protocols are established in a multitude of organs (Baptista et al., 2013; Crapo et al., 2011; Gilpin et al., 2014; Hellström et al., 2014; Ott et al., 2008; Sullivan et al., 2012).

While intact decellularized whole organs can be used to engineer organs for transplantation, they can also be processed further into other categories of materials, such as thin sections, hydrogels or coatings (Agmon and Christman, 2016). The main objective of this thesis was to study these categories related to reproductive medicine, from whole decellularized uteri to endometrial coatings, and to develop tissue-engineering approaches that can not only improve current investigative *in vitro* models, but also have the potential to be used, in the future, as a novel treatment for certain female pathologies leading to reproductive dysfunction. For this, a DC protocol was first established for large porcine uteri, and the effects on the ECM, ultrastructure and vasculature was evaluated extensively to evaluate the protocol for possible whole organ bioengineering. Then, the biocompatibility was tested by recellularizing thin sheets of the endometrium with human endometrial SP stem cells. Additionally, this perfusion protocol was adapted for the rabbit uterus that is synchronous or nonsynchronous with an embryo at day 3 of development, the endometrium was separated and converted into a solution to form hydrogel and coat substrates. These substrata were then used for embryo culture.

The pig model: whole uterus decellularization and recellularization of the acellular endometrium

The pig model is very popular in tissue engineering approaches since phylogenetically, it is closely related to humans and has similar sized organs. In addition, porcine tissues like heart valves have been used in the past in regenerative medicine with high success (Yap et al., 2013). Furthermore, many of the commercial decellularized biologic scaffolds used in tissue engineering and regenerative medicine originate from porcine small intestinal submucosa (SurgiSIS®), bladders (ACell, Inc), heart valves (Synergraft®) and livers (MIRODERM Fenestrated®). The pig uterus is a bicornuate organ comprised of two horns fused into a uterine body and irrigated by two uterine arteries; its size ranges from 30-35 centimeters (for pigs weighing approximately 220 kg). Apart from the morphological differences with humans, the horns comprise the typical histological elements of the uterus: endometrium (epithelial, stromal, and vascular cells), myometrium, and perimetrium. The effect of a freeze-thaw (F/T) cycle before a DC protocol developed for large reproductive organs was compared along our study, followed by the recellularization using human endometrial stem cells. Different DC protocols were tested by perfusing uterine horns at a physiological flow rate of 15 mL/min in an experimental setup allowing for reproducible results (Geisler et al., 2012). A comparison was made between F/T versus fresh organs, using a protocol consisting of SDS and Triton X-100 cycles. After two identical 24-hr cycles a macroscopically acellular matrix was produced, having a semi-transparent and white appearance. SDS is an ionic detergent that is widely used for DC (Crapo et al., 2011a), when used in low concentrations it can effectively remove cell residues with minimal damage to the ECM (Shupe et al., 2010). Furthermore, the F/T step, a physical decellularization method, induced cellular lysis and did not noticeably affected the ECM architecture in our experience. Moreover, studies reported that a single F/T cycle can reduce adverse immune responses in vascular ECM scaffolds (Lehr et al., 2011), suggesting that this initial step could be an interesting and very convenient option for both preserving, transporting and decellularizing donor organs. Using the perfusion setup, we were able to further investigate the effects of DC in standardized conditions (n=3 for each protocol).

This was done first by demonstrating a significant reduction of DNA and proteins content after DC, corroborating the results of the histology that showed the removal of the cellular fraction in the tissue. The absence of these vital cellular constituents shows that a sufficient amount of native cell material (and thus, its epitopes) was removed to consider the organ as a 'decellularized scaffold'. Additionally, the physical and possible mechanical

properties of ECM were demonstrated by the presence of native collagen fibers visualized with Masson's trichrome and Alcian blue staining (Wang et al., 2013; Youngstrom et al., 2013).

For possible recellularization it was important to demonstrate the preservation of the native structure of the ECM, including the vasculature. The major components of the ECM, such as collagens I and IV, elastin, laminin and fibronectin, were preserved with our methodology as shown by immunofluorescence. These results and those of electron microscopy imply that the interstitial ECM proteins and basement membrane remained intact under both DC conditions. This is an important observation because these key components act in the microenvironment to provoke changes like cell migration, proliferation, and differentiation (Halper and Kjaer, 2014). The maintenance of the protein composition in recellularization processes contributes to support cell homing, cell attachment, tissue integration, development, and normal cellular phenotypic functions (Hynes, 2009; Watt and Huck, 2013). Altogether, it is apparent that the destructive structural changes to the ECM are reduced to a minimum, offering a usable complex bioscaffold for future recellularization experiments.

Preservation of the vascular network is also critical, first for the efficient perfusion of detergents while avoiding degeneration of veins, arteries, and capillaries; and second for the future use of the circulatory system to repopulate the organ (Sánchez et al., 2015). By making a vascular corrosion cast and analyzing it with electron microscopy, perfusable vascular conduits up to the capillary level were detected, showing proper structural and functional features. It is important to mention that when arteries and veins are not distended by an initial perfusion with PBS, the subsequent perfusion with the monomer solution is impaired. This is possibly the cause for the affected macroscopic aspect of the DC casts. Nonetheless, this technique demonstrated that protocols only slightly compromised the vascular integrity, which opens up the possibility to recellularize the whole organ by adding cells via perfusion or injection, and creating a system capable of nutrient and gas exchange in the neo-organ/new generated organ (Baptista et al., 2011). The generated scaffolds can then be used to build an organized tissue that mimics the original organ using the native vascular tree.

The final step was to verify the biocompatibility and assess the bio-inductive properties of the generated xenogeneic scaffolds *in vitro*. This was done by performing preliminary experiments where a punch biopsy of decellularized endometrial tissue was seeded with human endometrial Side Population (SP) stem cells cell lines generated in our laboratory

(Cervelló et al., 2011b). After 3 to 4 days of cell culture in hypoxic conditions the seeded scaffolds contracted and rolled up, after 9-12 days 3D structures similar to the structure of an organoid were observed. This structure was further investigated to determine if the human cells were able to recapitulate the *in vivo* tissue architecture. The self-organizing aspect of this structure was apparent macroscopically when the flat discs formed a 3D structure on their own and histology showed a tight interaction between the cells and the scaffold. Furthermore, endometrial cells of both epithelial and stromal fractions were identified in the structure. This was done by immunofluorescence, demonstrating the presence of vimentin and cytokeratin (CK) positive cells in the 12 day old structure (Fatehullah et al., 2016).

While these results are encouraging, we are aware of the limitations of this study. The pig uterus is morphologically distinct from a human uterus and it remains to be seen if the DC protocol is applicable for both. Furthermore, more optimization and investigation have to be done to be able to confirm if formed structures are functional organoids. Interesting future steps includes increasing incubation times, adapting the ratio of ICE 6 and ICE 7 to increase the amount of CK positive cells in the construct to increase the likelihood of glandular formation and subject the organoids to functional studies. If successful, this would imply a significant improvement over currently the most advanced organoid cultures which uses only endometrial glands (Turco et al., 2017). Lastly, one of the major challenges lays in the recellularization efficiency of the whole organ and the optimization of the entire process for applicability in humans.

The rabbit model: whole uterus decellularization, solubilization of acellular endometrium and embryo culture on tissue-engineered substratum

Ever since the publication over 20 years ago (Voytik-Harbin et al., 1998), the decellularization and solubilization of tissues has been rising in popularity and has been applied to all important organ systems (Saldin et al., 2017). To the best of our knowledge, this has never been done before for reproductive tissues. In this context, a dual hypothesis was formulated. First, that a biologically native ECM derived from endometrial decellularized tissues renders a more physiologically suitable microenvironment for cell and embryo culture techniques. Secondly, that the drastic cyclical changes within the endometrium are translated to these substrata, and that this is noticeable during *in vitro* embryo culture.

Based on earlier results in the pig model, the protocol using SDS and Triton X-100 was slightly adapted for the rabbit uterus (Campo et al., 2017). Histology showed that the general morphology of the non-synchronous (NS) and synchronous (S) uteri after DC was very similar and that tissue organization was preserved with little cellular material left, this was further corroborated by DNA quantification, where a sufficient reduction of around 95% in wet DNA content was observed. It is possible that the total DNA per dry weight exceeds that of previously established criteria (Crapo et al., 2011a), but the significance of this is still up for debate. For example, aortic root scaffolds with much higher DNA contents have shown no tissue rejection after transplantation (Friedrich et al., 2014), making it unlikely for this bioscaffold to elicit such response, especially after converting it into a less dense pre-gel solution.

Several studies using *in vitro* culture have demonstrated the inductive capacities and the beneficial effects of decellularized tissues to guide the differentiation of stem cells (Lorvellec et al., 2017) and to preserve the phenotype of primary culture (Lang et al., 2011). These advantages have also been described for ECM hydrogel coatings, where the substrata are biocomparable with their *in vivo* counterparts, improving the current culture systems (DeQuach et al., 2010; French et al., 2012). This is probably due to the preservation of the tissue-specificity of these coatings (Zhang and Dong, 2015; Zhang et al., 2009). The biochemical and biomechanical differences after DC are not only retained between different tissues, but have also been shown to be the case within tissues, for example when suffering from certain pathologies such as fibrosis (Miyauchi et al., 2017), amyloidosis (Mangione et al., 2017; Mazza et al., 2016) or cancer (Piccoli et al., 2018; Pinto et al., 2017). The acellular tumor ECM maintains the proteins that are differentially expressed during angiogenesis, giving insight into pancreatic cancer progression (Naba et al., 2017) and even has a role in the increasing resistance to chemotherapy (Hoshiba and Tanaka, 2016). Apart for these intrusive pathologies, slight differences in the composition of the ECM from one type of tissues to another could affect the interactions with cells in a specific manner (McClelland et al., 2008). Even the age of the donor tissue has been shown to affect the *in vitro* culture of a 3D bioengineered model of cortical brain tissue (Sood et al., 2016).

In the reproductive field, the endometrium suffers, under the influence of the female sex steroids, cycles of drastic growth and reorganization in order to accept the embryo (Evans et al., 2011; Jabbour et al., 2006). For the rabbit, these changes already start from the first days post coitum (Denker, 1982). The ECM of the endometrial tissue follows this cycle with differential expression of both interstitial and basement membrane proteins, many of

which remain after DC (Harrington et al., 1999; Jones-Paris et al., 2017; Yamanaka et al., 1996). Furthermore, growth factors can be immobilized *in vivo* through sulfated glycosaminoglycans linked to ECM proteins (Patel and Mikos, 2004). In other words, the endometrial cells produce different secretory compounds and growth factors during the different phases of the reproductive/menstrual/endometrial cycle that could be sequestered by the native ECM and retained after DC (Parmar et al., 2008). Here we theorized that the complex mixture of ECM proteins and sequestered biochemical signals between a NS and S endometrium are distinct enough, even after DC and solubilization treatment. Furthermore, that this specificity allows us to see differences between in the most sensitive *in vitro* model, namely the embryo development.

The separation of tissues from whole decellularized structures has been published recently by other groups (Simões et al., 2017), and comparable techniques were used to separate the acellular NS and S endometrium from myometrium and perimetrium along this study. It was considered to perform the embryo culture on circular tissue sections of the ECM, but primary testing showed that it was poorly transparent and that much manipulation of the embryo was necessary to be able perform the embryo quality assessment and morphokinetic analysis. To be able to create a more manageable platform that is more easily comparable and compatible with existing culture/ *in vitro* methods, thin ECM hydrogels and coatings were investigated. It is possible that the effect on the pluripotency factors expression is augmented when cultured with decellularized ECM sections, which paves the way for an interesting future experiment. The separated endometrial tissues were prepared to be converted into a pre-gel solution by washing in ice-cold PBS to remove all SDS. SDS is difficult to remove after DC, has been associated foreign body responses, and has a negative effect on *in vitro* culture (Friedrich et al., 2018). After incubation with the hydrogel for 3 days at 37 °C, no SDS was measured in PBS. While only slight differences were observed between the tissues, this was not the case when comparing the ultrastructures of the NS and S hydrogel. Here, significantly thicker fibers are observed. However, the development of embryos that were cultured on these NS, S or Matrigel (M) hydrogels was severely impaired, in contrast to their coating counterparts. One possible explanation could be that the hydrogel density and rigidity play a role in the development, or that some inhibitory factor remains within the hydrogel as a result from the tissue processing. Given that the embryos do grow well on the coatings, an interesting future experiment could use coated polyacrylamide gels with various degrees of stiffness to

elucidate its effect; in fact, similar experiments have been performed to recreate the biomechanical cues of the cell niche (Young et al., 2013).

It has been shown that cells start remodeling the absorbed ECM surface after the first interaction and that the cellular proteolytic activity increases and even induces apoptosis when interfacing with a strongly bound ECM substratum when no serum in the culture medium is present (González-García et al., 2018). Rabbit blastocyst use a fusion type of implantation and does not invade the endometrium, nonetheless, it has been reported that it also produces proteases (Denker, 1982). It is possible that these proteases produced by the blastomeres of hatching embryos release more proteins from the substratum, positively influencing embryo development. When the coating was made from the synchronous endometrium, the similar blastocyst hatching rates and size resembles those grown in standard positive conditions (using FBS), effectively compensating for the absence of adhesion proteins and growth factors of the serum in the culture medium. Our results showed a similar pattern in the expression of pluripotency markers *OCT4* and *SOX2* for the synchronous endometrium and supplemented serum group. The Sox2-Oct4-Nanog regulatory complex controls expression of pluripotency genes through feed-forward loops (Chickarmane et al., 2006), including these three genes, in an autoregulatory circuit (Okumura-Nakanishi et al., 2005). Perhaps, an inadequate mRNA expression might trigger failures in the development and implantation of the embryos. The important role of Sox2 in the preimplantation mouse embryo highlights this premise (Keramari et al., 2010). Recently, it has been described that Sox2 maternal transcripts and proteins are likely to play an important role in the earliest function of Sox2 (Keramari et al., 2010). Thus, these results seem to demonstrate for the first time in the reproductive field that synchronous acellular endometrium coating would retain and release compounds that permit in part mimic the endometrial environment under *in vitro* conditions. This observation was clearly demonstrated when comparing to the nonspecific Matrigel coating. Matrigel is a solubilized basement membrane solution extracted from Engelbreth-Holm-Swarm mouse sarcoma and is unlikely to have any use in a clinical setting. The use of matrigel and ECM component like hyaluronic acid as supplement of culture medium and coating for embryo culture were investigated in the past but conflicting results were reported (Dawson et al., 1997; Lazzaroni et al., 1999; Palasz et al., 2016). Here we clearly demonstrate that a tissue-specific coating is necessary to even approach or improve on serum free culture conditions and that the M coating has a distinct negative effect on the embryo. More investigation is still needed to fully demonstrate the possible uses of these hydrogels and coatings in applied human

research and reproductive medicine. Endometrial ECM hydrogels and coatings have the potential to become a platform used in the culture of stem/progenitor cells and primary culture cells to better maintain their tissue-specific phenotype, improving *in vitro* models while also having possible *in vivo* applications.

Altogether, in this study we present that endometrial tissue-specific ECM derived coatings obtained from whole decellularized organs create a biomimetic environment allowing for the growth of pre-implantation embryos. Furthermore, this sensitive *in vitro* technique demonstrates that the specific mixture of biochemical signals derived from the native microenvironment is retained after biochemical and mechanical treatments. We demonstrated the appropriate preservation of the ECM, providing for the first time the initial step to mimic the endometrial environment *in vitro*. When the coating is from the endometrium synchronized with the developing blastocyst, the expression and development of the embryo is improved compared to NS and M coatings and is the only condition investigated here that is comparable with the current golden standard of embryo culture in FBS enriched medium.

Future perspectives and applications of bioengineered uterine tissues in investigation and regenerative medicine

From the background and results presented, it has become apparent that the DC of whole organs provides an interesting platform for investigative models as well as novel treatments of uterus-related pathologies. However, when whole decellularized organs are implanted without recellularization, massive thrombosis upon implantation takes place (Ko et al., 2014). Even when thrombosis can be avoided, the scaffolds are broken down and reabsorbed (Remuzzi et al., 2017). Because of this, the recellularization and revascularization of whole organs is vital for the creation of transplantable engineered organs (Pellegata et al., 2018). To attempt this for large organs such as the pig uterus, an enormous amount of cells would be needed, considering that whole organ recellularization in small animal models uses between 40-80 million cells (Baptista et al., 2016; Caralt et al., 2015; Miyazaki and Maruyama, 2014; Ott et al., 2008). The creation of organoids from this tissue on the other hand, is an interesting approach because per experiment a large amount of homogenous scaffold material is created, and relatively little cells are used (approx. 0.5 million in our case). When these organoids behave similarly to *in vivo* tissues, they could be subjected to various functional studies. This could give insight in the reaction to hormones and drugs, improving on previously published 3D models (Meng et al., 2009; Olalekan et

al., 2017; Turco et al., 2017) or even giving insight into the organogenesis and pathological development (Vyas et al., 2017).

The recellularization of these sections is more efficient than that of whole organs, but another category of the investigated biomaterials, ECM hydrogels, can do this even more efficient, because of its unique properties previously discussed in section 3.1 "Hydrogels: form and function" of the introduction. Larger quantities can be made from the same amount of tissue and they retain cells more easily. By using the flexibility of these ECM hydrogels and coatings, many possible applications and investigations are promising in the future. Coating synthetic implants *in vivo* modulates the host immune response, improving biocompatibility and subsequent recovery (Faulk et al., 2014; Kumosa et al., 2018).

The most interesting aspects of these gels is that they are injectable and can be used as acellular scaffolds (Seif-Naraghi et al., 2013) or can be doped with stem cells (Gothard et al., 2015) or growth factors (Gothard et al., 2015; Seif-Naraghi et al., 2012). These gels hold promise to be used as possible non-invasive treatment for endometrial pathologies such as endometrial atrophy and Asherman's syndrome (AS), showing considerable improvements on previous investigations using cell therapy (Santamaria et al., 2016). This would entail a new class of potential therapies for AS, where materials such as microporous synthetic materials, SIS, and collagen hydrogels were previously used (Jonkman et al., 1986; Li et al., 2011; Taveau et al., 2004). A putative limitation concerning the clinical translation could be the animal origin of the ECM due to the potential for disease transmission and immunological reaction. However, the FDA has approved many decellularized tissue-specific ECM for human uses as porcine dermis, SIS and heart valves (Badylak et al., 2009) suggesting them as a viable option for *in vitro* techniques. Furthermore, an ECM hydrogel therapy for myocardial infarction is already in a Phase 1 clinical trial (clinicaltrials.gov Identifier: NCT02305602).

In conclusion, tissue engineering is a promising and burgeoning multidisciplinary field of investigation, poised to transform translational medicine and investigation. Even though it is only in its infancy for reproductive medicine, techniques such as the de- and recellularization of tissues and 3D *in vitro* approaches based on tissue-specific hydrogels have shown promise to treat even the most intrusive female pathologies that lead to infertility.

Chapter

VII

CONCLUSIONS

VII. CONCLUSIONS

The following conclusions can be drawn from this thesis:

1. A decellularization perfusion protocol using cycles of the ionic and non-ionic detergents SDS and Triton X-100 can efficiently remove all cellular material in large reproductive organs in the porcine model without compromising the morphology of the extracellular matrix.

2. Vital proteins of the extracellular matrix such as elastin, laminin, fibronectin, collagen type I and IV are retained after decellularization with the aforementioned protocol and a freeze-thaw cycle has little to no negative effects of on the composition or ultrastructure.

3. The resulting whole organ bioscaffold is biocompatible can be converted into different categories of endometrial biomaterials, such as thin sections. When human endometrial Side population stem cells are seeded on thin endometrial disks, organoid-like structures are formed, expressing typical endometrial epithelial and stromal cell markers.

4. Only slight modifications have to be made to apply this protocol to uteri of different species (rabbit), making it a good possible candidate for the future decellularization of the human uterus.

5. Decellularized endometrial tissue at different stages of the cycle can be separated through microdissection and converted into tissue-specific hydrogels and coatings.

6. When day-3 blastocysts are grown on synchronous, endometrial extracellular matrix-coatings, their development is similar to that obtained during standard embryo culture conditions. Furthermore, an improvement is shown compared to non-synchronous and Matrigel coatings.

BIBLIOGRAPHY

Agmon, G., and Christman, K.L. (2016). Controlling stem cell behavior with decellularized extracellular matrix scaffolds. Curr. Opin. Solid State Mater. Sci. *20*, 193–201.

Agrawal, V., Tottey, S., Johnson, S.A., Freund, J.M., Siu, B.F., and Badylak, S.F. (2011). Recruitment of progenitor cells by an extracellular matrix cryptic peptide in a mouse model of digit amputation. Tissue Eng. Part A *17*, 2435–2443.

Ahmed, E.M. (2015). Hydrogel: Preparation, characterization, and applications: A review. J. Adv. Res. *6*, 105–121.

Alaribe, F.N., Manoto, S.L., and Motaung, S.C.K.M. (2016). Scaffolds from biomaterials: advantages and limitations in bone and tissue engineering. Biologia (Bratisl.).

Amorim, C.A. (2017). Special Issue Devoted to a New Field of Regenerative Medicine: Reproductive Tissue Engineering. Ann. Biomed. Eng. *45*, 1589–1591.

Aplin, J.D., Charlton, A.K., and Ayad, S. (1988). An immunohistochemical study of human endometrial extracellular matrix during the menstrual cycle and first trimester of pregnancy. Cell Tissue Res. *253*, 231–240.

Aplin, J.D., Glasser, S.R., and Fazleabas, A.T. (2008). The endometrium: molecular, cellular and clinical perspectives (Informa).

Arnold, J.T., Kaufman, D.G., Seppälä, M., and Lessey, B.A. (2001). Endometrial stromal cells regulate epithelial cell growth in vitro: a new co-culture model. Hum. Reprod. Oxf. Engl. *16*, 836–845.

Arnold, J.T., Lessey, B.A., Seppälä, M., and Kaufman, D.G. (2002). Effect of normal endometrial stroma on growth and differentiation in Ishikawa endometrial adenocarcinoma cells. Cancer Res. *62*, 79–88.

Asherman, J. (1948). Amenorrhoea traumatica (atretica). J Obstet Gynaecol Br Emp *55*, 23–30.

Azimzadeh, A.M., Lees, J.R., Ding, Y., and Bromberg, J.S. (2011). Immunobiology of Transplantation: Impact on Targets for Large and Small Molecules. Clin. Pharmacol. Ther. *90*, 229–242.

Badylak, S.F. (2004). Xenogeneic extracellular matrix as a scaffold for tissue reconstruction. Transpl. Immunol. *12*, 367–377.

Badylak, S.F. (2007). The extracellular matrix as a biologic scaffold material. Biomaterials *28*, 3587–3593.

Badylak, S.F., Lantz, G.C., Coffey, A., and Geddes, L.A. (1989). Small intestinal submucosa as a large diameter vascular graft in the dog. J. Surg. Res. *47*, 74–80.

Badylak, S.F., Tullius, R., Kokini, K., Shelbourne, K.D., Klootwyk, T., Voytik, S.L., Kraine, M.R., and Simmons, C. (2004). The use of xenogeneic small intestinal submucosa as a biomaterial for Achille's tendon repair in a dog model. J. Biomed. Mater. Res. *29*, 977–985.

Baert, Y., Stukenborg, J.-B., Landreh, M., De Kock, J., Jörnvall, H., Söder, O., and Goossens, E. (2015). Derivation and characterization of a cytocompatible scaffold from human testis. Hum. Reprod. Oxf. Engl. *30*, 256–267.

Baptista, P.M., Siddiqui, M.M., Lozier, G., Rodriguez, S.R., Atala, A., and Soker, S. (2011). The use of whole organ decellularization for the generation of a vascularized liver organoid. Hepatology *53*, 604–617.

Baptista, P.M., Vyas, D., Moran, E., Wang, Z., and Soker, S. (2013). Human liver bioengineering using a whole liver decellularized bioscaffold. Methods Mol. Biol. Clifton NJ *1001*, 289–298.

Baptista, P.M., Moran, E.C., Vyas, D., Ribeiro, M.H., Atala, A., Sparks, J.L., and Soker, S. (2016). Fluid Flow Regulation of Revascularization and Cellular Organization in a Bioengineered Liver Platform. Tissue Eng. Part C Methods *22*, 199–207.

Basak, R., and Bandyopadhyay, R. (2013). Encapsulation of Hydrophobic Drugs in Pluronic F127 Micelles: Effects of Drug Hydrophobicity, Solution Temperature, and pH. Langmuir *29*, 4350–4356.

Beattie, A.J., Gilbert, T.W., Guyot, J.P., Yates, A.J., and Badylak, S.F. (2008). Chemoattraction of Progenitor Cells by Remodeling Extracellular Matrix Scaffolds. Tissue Eng. Part A *15*, 1119–1125.

Bentin-Ley, U., Pedersen, B., Lindenberg, S., Larsen, J.F., Hamberger, L., and Horn, T. (1994). Isolation and culture of human endometrial cells in a three-dimensional culture system. J. Reprod. Fertil. *101*, 327–332.

Ber, R. (2000). Ethical issues in gestational surrogacy. Theor. Med. Bioeth. *21*, 153–169.

Berger, C., Boggavarapu, N.R., Menezes, J., Lalitkumar, P.G.L., and Gemzell-Danielsson, K. (2015). Effects of ulipristal acetate on human embryo attachment and endometrial cell gene expression in an in vitro co-culture system. Hum. Reprod. *30*, 800–811.

Biggers, J.D., McGinnis, L.K., and Summers, M.C. (2004). Discrepancies between the effects of glutamine in cultures of preimplantation mouse embryos. Reprod. Biomed. Online *9*, 70–73.

Blasco, A. (2005). The use of Bayesian statistics in meat quality analyses: a review. Meat Sci. *69*, 115–122.

Bläuer, M., Heinonen, P.K., Martikainen, P.M., Tomás, E., and Ylikomi, T. (2005). A novel organotypic culture model for normal human endometrium: regulation of epithelial cell proliferation by estradiol and medroxyprogesterone acetate. Hum. Reprod. *20*, 864–871.

Bombard, D.S., and Shaker, M.A. (2014). Mayer–Rokitansky–Kuster–Hauser syndrome: complications, diagnosis and possible treatment options: a review. Gynecol. Endocrinol. *30*, 618–623.

Boretto, M., Cox, B., Noben, M., Hendriks, N., Fassbender, A., Roose, H., Amant, F., Timmerman, D., Tomassetti, C., Vanhie, A., et al. (2017). Development of organoids from mouse and human endometrium showing endometrial epithelium physiology and long-term expandability. Development *144*, 1775–1786.

Bornstein, P., Duksin, D., Balian, G., Davidson, J.M., and Crouch, E. (1978). Organization of Extracellular Proteins on the Connective Tissue Cell Surface: Relevance to Cell-Matrix Interactions in Vitro and in Vivo*. Ann. N. Y. Acad. Sci. *312*, 93–105.

Brännström, M., Johannesson, L., Bokström, H., Kvarnström, N., Mölne, J., Dahm-Kähler, P., Enskog, A., Milenkovic, M., Ekberg, J., Diaz-Garcia, C., et al. (2015). Livebirth after uterus transplantation. Lancet Lond. Engl. *385*, 607–616.

Buwalda, S.J., Boere, K.W.M., Dijkstra, P.J., Feijen, J., Vermonden, T., and Hennink, W.E. (2014). Hydrogels in a historical perspective: from simple networks to smart materials. J. Control. Release Off. J. Control. Release Soc. *190*, 254–273.

Campbell, G.R., Turnbull, G., Xiang, L., Haines, M., Armstrong, S., Rolfe, B.E., and Campbell, J.H. (2008). The peritoneal cavity as a bioreactor for tissue engineering visceral organs: bladder, uterus and vas deferens. J. Tissue Eng. Regen. Med. *2*, 50–60.

Campo, H., Baptista, P.M., López-Pérez, N., Faus, A., Cervelló, I., and Simón, C. (2017). De- and recellularization of the pig uterus: a bioengineering pilot study. Biol. Reprod. *96*, 34–45.

Caralt, M., Uzarski, J.S., Iacob, S., Obergfell, K.P., Berg, N., Bijonowski, B.M., Kiefer, K.M., Ward, H.H., Wandinger-Ness, A., Miller, W.M., et al. (2015). Optimization and critical evaluation of decellularization strategies to develop renal extracellular matrix scaffolds as biological templates for organ engineering and transplantation. Am. J. Transplant. Off. J. Am. Soc. Transplant. Am. Soc. Transpl. Surg. *15*, 64–75.

Cervelló, I., Gil-Sanchis, C., Mas, A., Delgado-Rosas, F., Martínez-Conejero, J.A., Galán, A., Martínez-Romero, A., Martínez, S., Navarro, I., Ferro, J., et al. (2010). Human endometrial side population cells exhibit genotypic, phenotypic and functional features of somatic stem cells. PloS One *5*, e10964.

Cervelló, I., Mirantes, C., Santamaria, X., Dolcet, X., Matias-Guiu, X., and Simón, C. (2011a). Stem cells in human endometrium and endometrial carcinoma. Int. J. Gynecol. Pathol. *30*, 317–327.

Cervelló, I., Mas, A., Gil-Sanchis, C., Peris, L., Faus, A., Saunders, P.T.K., Critchley, H.O.D., and Simón, C. (2011b). Reconstruction of endometrium from human endometrial side population cell lines. PloS One *6*, e21221.

Cervelló, I., Gil-Sanchis, C., Santamaría, X., Faus, A., Vallvé-Juanico, J., Díaz-Gimeno, P., Genolet, O., Pellicer, A., and Simón, C. (2017). Leucine-rich repeat-containing G-protein-coupled receptor 5-positive cells in the endometrial stem cell niche. Fertil. Steril. *107*, 510-519.e3.

Chan, B.P., and Leong, K.W. (2008). Scaffolding in tissue engineering: general approaches and tissue-specific considerations. Eur. Spine J. Off. Publ. Eur. Spine Soc. Eur. Spinal Deform. Soc. Eur. Sect. Cerv. Spine Res. Soc. *17 Suppl 4*, 467–479.

Chandra, A., Martinez, G.M., Mosher, W.D., Abma, J.C., and Jones, J. (2005). Fertility, family planning, and reproductive health of U.S. women: data from the 2002 National Survey of Family Growth. Vital Health Stat. 23. 1–160.

Chang, T.A., Bondarenko, G.I., Gerami-Naini, B., Drenzek, J.G., Durning, M., Garthwaite, M.A., Schmidt, J.K., and Golos, T.G. (2018). Trophoblast differentiation, invasion and hormone secretion in a three-dimensional in vitro implantation model with rhesus monkey embryos. Reprod. Biol. Endocrinol. *16*.

Chickarmane, V., Troein, C., Nuber, U.A., Sauro, H.M., and Peterson, C. (2006). Transcriptional Dynamics of the Embryonic Stem Cell Switch. PLOS Comput. Biol. *2*, e123.

Conforti, A., Alviggi, C., Mollo, A., De Placido, G., and Magos, A. (2013). The management of Asherman syndrome: a review of literature. Reprod. Biol. Endocrinol. RBE *11*, 118.

Cook, C.D., Hill, A.S., Guo, M., Stockdale, L., Papps, J.P., Isaacson, K.B., Lauffenburger, D.A., and Griffith, L.G. (2017). Local Remodeling of Synthetic Extracellular Matrix Microenvironments by Co-cultured Endometrial Epithelial and Stromal Cells Enables Long-term Dynamic Physiological Function. Integr. Biol. Quant. Biosci. Nano Macro *9*, 271–289.

Crapo, P.M., Gilbert, T.W., and Badylak, S.F. (2011). An overview of tissue and whole organ decellularization processes. Biomaterials *32*, 3233–3243.

Daley, W.P., Peters, S.B., and Larsen, M. (2008). Extracellular matrix dynamics in development and regenerative medicine. J. Cell Sci. *121*, 255–264.

Dallenbach-Hellweg, G. (1971). The Normal Histology of the Endometrium. In Histopathology of the Endometrium, (Springer, Berlin, Heidelberg), pp. 20–76.

Davis, G.E., Bayless, K.J., Davis, M.J., and Meininger, G.A. (2000). Regulation of tissue injury responses by the exposure of matricryptic sites within extracellular matrix molecules. Am. J. Pathol. *156*, 1489–1498.

Dawson, K.M., Baltz, J.M., and Claman, P. (1997). Culture with Matrigel Inhibits Development of Mouse Zygotes. J. Assist. Reprod. Genet. *14*, 543–548.

Debbaut, C., Monbaliu, D., Casteleyn, C., Cornillie, P., Van Loo, D., Masschaele, B., Pirenne, J., Simoens, P., Van Hoorebeke, L., and Segers, P. (2011). From vascular corrosion cast to electrical analog model for the study of human liver hemodynamics and perfusion. IEEE Trans. Biomed. Eng. *58*, 25–35.

Denker, H.-W. (1982). Proteases of the Blastocyst and of the Uterus. In Proteins and Steroids in Early Pregnancy, H.M. Beier, and P. Karlson, eds. (Springer Berlin Heidelberg), pp. 183–208.

DeQuach, J.A., Mezzano, V., Miglani, A., Lange, S., Keller, G.M., Sheikh, F., and Christman, K.L. (2010). Simple and High Yielding Method for Preparing Tissue Specific Extracellular Matrix Coatings for Cell Culture. PLOS ONE *5*, e13039.

Ding, L., Li, X., Sun, H., Su, J., Lin, N., Péault, B., Song, T., Yang, J., Dai, J., and Hu, Y. (2014). Transplantation of bone marrow mesenchymal stem cells on collagen scaffolds for the functional regeneration of injured rat uterus. Biomaterials *35*, 4888–4900.

Domínguez, F., Remohí, J., Pellicer, A., and Simón, C. (2003). Human endometrial receptivity: a genomic approach. Reprod. Biomed. Online *6*, 332–338.

Drury, J.L., and Mooney, D.J. (2003). Hydrogels for tissue engineering: scaffold design variables and applications. Biomaterials *24*, 4337–4351.

Eftekhar, M., Tabibnejad, N., and Tabatabaie, A.A. (2018). The thin endometrium in assisted reproductive technology: An ongoing challenge. Middle East Fertil. Soc. J. *23*, 1–7.

d'Estaing, S.G., Lornage, J., Hadj, S., Boulieu, D., Salle, B., and Guérin, J.-F. (2001). Comparison of two blastocyst culture systems: coculture on Vero cells and sequential media. Fertil. Steril. *76*, 1032–1035.

Evans, J., Kaitu'u-Lino, T., and Salamonsen, L.A. (2011). Extracellular matrix dynamics in scar-free endometrial repair: perspectives from mouse in vivo and human in vitro studies. Biol. Reprod. *85*, 511–523.

Fageeh, W., Raffa, H., Jabbad, H., and Marzouki, A. (2002). Transplantation of the human uterus. Int. J. Gynaecol. Obstet. Off. Organ Int. Fed. Gynaecol. Obstet. *76*, 245–251.

Fasciani, A., Bocci, G., Xu, J., Bielecki, R., Greenblatt, E., Leyland, N., and Casper, R.F. (2003). Three-dimensional in vitro culture of endometrial explants mimics the early stages of endometriosis. Fertil. Steril. *80*, 1137–1143.

Fatehullah, A., Tan, S.H., and Barker, N. (2016). Organoids as an in vitro model of human development and disease. Nat. Cell Biol. *18*, 246–254.

Faulk, D.M., Londono, R., Wolf, M.T., Ranallo, C.A., Carruthers, C.A., Wildemann, J.D., Dearth, C.L., and Badylak, S.F. (2014). ECM hydrogel coating mitigates the chronic inflammatory response to polypropylene mesh. Biomaterials *35*, 8585–8595.

Filant, J., and Spencer, T.E. (2014). Uterine glands: biological roles in conceptus implantation, uterine receptivity and decidualization. Int. J. Dev. Biol. *58*, 107–116.

Frantz, C., Stewart, K.M., and Weaver, V.M. (2010). The extracellular matrix at a glance. J. Cell Sci. *123*, 4195–4200.

French, K.M., Boopathy, A.V., DeQuach, J.A., Chingozha, L., Lu, H., Christman, K.L., and Davis, M.E. (2012). A naturally derived cardiac extracellular matrix enhances cardiac progenitor cell behavior in vitro. Acta Biomater. *8*, 4357–4364.

Freytes, D.O., Martin, J., Velankar, S.S., Lee, A.S., and Badylak, S.F. (2008). Preparation and rheological characterization of a gel form of the porcine urinary bladder matrix. Biomaterials *29*, 1630–1637.

Friedrich, E.E., Lanier, S.T., Niknam-Bienia, S., Arenas, G.A., Rajendran, D., Wertheim, J.A., and Galiano, R.D. (2018). Residual sodium dodecyl sulfate in decellularized muscle matrices leads to fibroblast activation in vitro and foreign body response in vivo. J. Tissue Eng. Regen. Med. *12*, e1704–e1715.

Friedrich, L.H., Jungebluth, P., Sjöqvist, S., Lundin, V., Haag, J.C., Lemon, G., Gustafsson, Y., Ajalloueian, F., Sotnichenko, A., Kielstein, H., et al. (2014). Preservation of aortic root architecture and properties using a detergent-enzymatic perfusion protocol. Biomaterials *35*, 1907–1913.

Gargett, C.E., and Masuda, H. (2010). Adult stem cells in the endometrium. Mol. Hum. Reprod. *16*, 818–834.

Garnica-Palafox, I.M., and Sánchez-Arévalo, F.M. (2016). Influence of natural and synthetic crosslinking reagents on the structural and mechanical properties of chitosan-based hybrid hydrogels. Carbohydr. Polym. *151*, 1073–1081.

Garreta, E., Oria, R., Tarantino, C., Pla-Roca, M., Prado, P., Fernández-Avilés, F., Campistol, J.M., Samitier, J., and Montserrat, N. (2017). Tissue engineering by decellularization and 3D bioprinting. Mater. Today *20*, 166–178.

Geisler, K., Künzel, J., Grundtner, P., Müller, A., Beckmann, M.W., and Dittrich, R. (2012). The perfused swine uterus model: long-term perfusion. Reprod. Biol. Endocrinol. *10*, 110.

Gilbert, T.W., Sellaro, T.L., and Badylak, S.F. (2006). Decellularization of tissues and organs. Biomaterials *27*, 3675–3683.

Gilpin, S.E., Guyette, J.P., Gonzalez, G., Ren, X., Asara, J.M., Mathisen, D.J., Vacanti, J.P., and Ott, H.C. (2014). Perfusion decellularization of human and porcine lungs: Bringing the matrix to clinical scale. J. Heart Lung Transplant. *33*, 298–308.

Gioffredi, E., Boffito, M., Calzone, S., Giannitelli, S.M., Rainer, A., Trombetta, M., Mozetic, P., and Chiono, V. (2016). Pluronic F127 Hydrogel Characterization and Biofabrication in Cellularized Constructs for Tissue Engineering Applications. Procedia CIRP *49*, 125–132.

Glasser, S.R., Lampelo, S., Munir, M.I., and Julian, J. (1987). Expression of desmin, laminin and fibronectin during in situ differentiation (decidualization) of rat uterine stromal cells. Differentiation *35*, 132–142.

Glenister, T.W. (1961). Organ Culture as a New Method for Studying the Implantation of Mammalian Blastocysts. Proc. R. Soc. B Biol. Sci. *154*, 428–431.

González-García, C., Cantini, M., Ballester-Beltrán, J., Altankov, G., and Salmerón-Sánchez, M. (2018). The strength of the protein-material interaction determines cell fate. Acta Biomater. *77*, 74–84.

Gothard, D., Smith, E.L., Kanczler, J.M., Black, C.R., Wells, J.A., Roberts, C.A., White, L.J., Qutachi, O., Peto, H., Rashidi, H., et al. (2015). In Vivo Assessment of Bone Regeneration in Alginate/Bone ECM Hydrogels with Incorporated Skeletal Stem Cells and Single Growth Factors. PLOS ONE *10*, e0145080.

Guillomot, M. (1999). Changes in Extracellular Matrix Components and Cytokeratins in the Endometrium during Goat Implantation. Placenta *20*, 339–345.

Gyles, D.A., Castro, L.D., Silva, J.O.C., and Ribeiro-Costa, R.M. (2017). A review of the designs and prominent biomedical advances of natural and synthetic hydrogel formulations. Eur. Polym. J. *88*, 373–392.

Halper, J., and Kjaer, M. (2014). Basic Components of Connective Tissues and Extracellular Matrix: Elastin, Fibrillin, Fibulins, Fibrinogen, Fibronectin, Laminin, Tenascins and Thrombospondins. In Progress in Heritable Soft Connective Tissue Diseases, J. Halper, ed. (Dordrecht: Springer Netherlands), pp. 31–47.

Han, D.K., and Hubbell, J.A. (1997). Synthesis of Polymer Network Scaffolds from l-Lactide and Poly(ethylene glycol) and Their Interaction with Cells. Macromolecules *30*, 6077–6083.

Han, H.-I., Lee, S.-H., and Park, C.-K. (2017). Development of In Vitro Embryo Production System Using Collagen Matrix Gel Attached with Vascular Endothelial Growth Factor Derived from Interleukin-1 Beta-Treated Porcine Endometrial Tissue. Tissue Eng. Part C Methods *23*, 396–403.

Harrington, D.J., Lessey, B.A., Rai, V., Bergqvist, A., Kennedy, S., Manek, S., Barlow, D.H., and Mardon, H.J. (1999). Tenascin is differentially expressed in endometrium and endometriosis. J. Pathol. *187*, 242–248.

Hashimoto, Y., Funamoto, S., Sasaki, S., Honda, T., Hattori, S., Nam, K., Kimura, T., Mochizuki, M., Fujisato, T., Kobayashi, H., et al. (2010). Preparation and characterization of decellularized cornea using high-hydrostatic pressurization for corneal tissue engineering. Biomaterials *31*, 3941–3948.

Hawkins, S.M., and Matzuk, M.M. (2008). Menstrual Cycle: Basic Biology. Ann. N. Y. Acad. Sci. *1135*, 10–18.

Hellström, M., El-Akouri, R.R., Sihlbom, C., Olsson, B.M., Lengqvist, J., Bäckdahl, H., Johansson, B.R., Olausson, M., Sumitran-Holgersson, S., and Brännström, M. (2014). Towards the development of a bioengineered uterus: comparison of different protocols for rat uterus decellularization. Acta Biomater. *10*, 5034–5042.

Hellström, M., Moreno-Moya, J.M., Bandstein, S., Bom, E., Akouri, R.R., Miyazaki, K., Maruyama, T., and Brännström, M. (2016). Bioengineered uterine tissue supports pregnancy in a rat model. Fertil. Steril. *106*, 487-496.e1.

Hellström, M., Bandstein, S., and Brännström, M. (2017). Uterine Tissue Engineering and the Future of Uterus Transplantation. Ann. Biomed. Eng. *45*, 1718–1730.

Herraiz, S., Buigues, A., Díaz-García, C., Romeu, M., Martínez, S., Gómez-Seguí, I., Simón, C., Hsueh, A.J., and Pellicer, A. (2018). Fertility rescue and ovarian follicle growth promotion by bone marrow stem cell infusion. Fertil. Steril. *109*, 908-918.e2.

Hiraoka, T., Hirota, Y., Saito-Fujita, T., Matsuo, M., Egashira, M., Matsumoto, L., Haraguchi, H., Dey, S.K., Furukawa, K.S., Fujii, T., et al. (2016). STAT3 accelerates uterine epithelial regeneration in a mouse model of decellularized uterine matrix transplantation. JCI Insight *1*.

Hoffman, A.S. (2012). Hydrogels for biomedical applications. Adv. Drug Deliv. Rev. *64*, 18–23.

Hooker, A.B., Lemmers, M., Thurkow, A.L., Heymans, M.W., Opmeer, B.C., Brölmann, H.A.M., Mol, B.W., and Huirne, J.A.F. (2014). Systematic review and meta-analysis of intrauterine adhesions after miscarriage: prevalence, risk factors and long-term reproductive outcome. Hum. Reprod. Update *20*, 262–278.

Hortensius, R.A., and Harley, B.A. (2016). Naturally derived biomaterials for addressing inflammation in tissue regeneration. Exp. Biol. Med. *241*, 1015–1024.

Hoshiba, T., and Tanaka, M. (2016). Decellularized matrices as in vitro models of extracellular matrix in tumor tissues at different malignant levels: Mechanism of 5-fluorouracil resistance in colorectal tumor cells. Biochim. Biophys. Acta *1863*, 2749–2757.

Hudson, T.W., Liu, S.Y., and Schmidt, C.E. (2004). Engineering an improved acellular nerve graft via optimized chemical processing. Tissue Eng. *10*, 1346–1358.

Huleihel, L., Hussey, G.S., Naranjo, J.D., Zhang, L., Dziki, J.L., Turner, N.J., Stolz, D.B., and Badylak, S.F. (2016). Matrix-bound nanovesicles within ECM bioscaffolds. Sci. Adv. *2*.

Hundepool, C.A., Nijhuis, T.H.J., Kotsougiani, D., Friedrich, P.F., Bishop, A.T., and Shin, A.Y. (2017). Optimizing decellularization techniques to create a new nerve allograft: an in vitro study using rodent nerve segments. Neurosurg. Focus *42*, E4.

Hur, Y.S., Ryu, E.K., Yoon, S.H., Lim, K.S., Lee, W.D., and Lim, J.H. (2016). Comparison of static culture, micro-vibration culture, and micro-vibration culture with co-culture in poor ovarian responders. Clin. Exp. Reprod. Med. *43*, 146–151.

Hynes, R.O. (2009). Extracellular matrix: not just pretty fibrils. Science *326*, 1216–1219.

Hynes, R.O., and Naba, A. (2012). Overview of the Matrisome--An Inventory of Extracellular Matrix Constituents and Functions. Cold Spring Harb. Perspect. Biol. *4*, a004903–a004903.

Ige, O.O., Umoru, L.E., and Aribo, S. (2012). Natural Products: A Minefield of Biomaterials.

Iwahashi, M., Muragaki, Y., Ooshima, A., Yamoto, M., and Nakano, R. (1996). Alterations in distribution and composition of the extracellular matrix during decidualization of the human endometrium. J. Reprod. Fertil. *108*, 147–155.

Jabbour, H.N., Kelly, R.W., Fraser, H.M., and Critchley, H.O.D. (2006). Endocrine regulation of menstruation. Endocr. Rev. *27*, 17–46.

Jakus, A.E., Laronda, M.M., Rashedi, A.S., Robinson, C.M., Lee, C., Jordan, S.W., Orwig, K.E., Woodruff, T.K., and Shah, R.N. (2017). "Tissue Papers" from Organ-Specific Decellularized Extracellular Matrices. Adv. Funct. Mater. *27*, 1700992.

Järveläinen, H., Sainio, A., Koulu, M., Wight, T.N., and Penttinen, R. (2009). Extracellular matrix molecules: potential targets in pharmacotherapy. Pharmacol. Rev. *61*, 198–223.

Johnson, T.D., Lin, S.Y., and Christman, K.L. (2011). Tailoring material properties of a nanofibrous extracellular matrix derived hydrogel. Nanotechnology *22*, 494015.

Johnson, T.D., DeQuach, J.A., Gaetani, R., Ungerleider, J., Elhag, D., Nigam, V., Behfar, A., and Christman, K.L. (2014). Human versus porcine tissue sourcing for an injectable myocardial matrix hydrogel. Biomater. Sci. *2014*, 60283D.

Jones-Paris, C.R., Paria, S., Berg, T., Saus, J., Bhave, G., Paria, B.C., and Hudson, B.G. (2017). Embryo implantation triggers dynamic spatiotemporal expression of the basement membrane toolkit during uterine reprogramming. Matrix Biol. *57–58*, 347–365.

Jonkman, M.F., Kauer, F.M., Nieuwenhuis, P., and Molenaar, I. (1986). Segmental uterine horn replacement in the rat using a biodegradable microporous synthetic tube. Artif. Organs *10*, 475–480.

Kabagambe, S.K., Lee, C.J., Goodman, L.F., Chen, Y.J., Vanover, M.A., and Farmer, D.L. (2018). Lessons from the Barn to the Operating Suite: A Comprehensive Review of Animal Models for Fetal Surgery. Annu. Rev. Anim. Biosci. *6*, 99–119.

Kakabadze, Z., Kakabadze, A., Chakhunashvili, D., Karalashvili, L., Berishvili, E., Sharma, Y., and Gupta, S. (2018). Decellularized human placenta supports hepatic tissue and allows rescue in acute liver failure. Hepatol. Baltim. Md *67*, 1956–1969.

Kämmerer, U., von Wolff, M., and Markert, U.R. (2004). Immunology of human endometrium. Immunobiology *209*, 569–574.

Kattal, N., Cohen, J., and Barmat, L.I. (2008). Role of coculture in human in vitro fertilization: a meta-analysis. Fertil. Steril. *90*, 1069–1076.

Keane, T.J., Swinehart, I.T., and Badylak, S.F. (2015). Methods of tissue decellularization used for preparation of biologic scaffolds and in vivo relevance. Methods *84*, 25–34.

Keramari, M., Razavi, J., Ingman, K.A., Patsch, C., Edenhofer, F., Ward, C.M., and Kimber, S.J. (2010). Sox2 Is Essential for Formation of Trophectoderm in the Preimplantation Embryo. PLOS ONE *5*, e13952.

Kim, M.R., Park, D.W., Lee, J.H., Choi, D.S., Hwang, K.J., Ryu, H.S., and Min, C.K. (2005). Progesterone-dependent release of transforming growth factor-beta1 from epithelial cells enhances the endometrial decidualization by turning on the Smad signalling in stromal cells. MHR Basic Sci. Reprod. Med. *11*, 801–808.

Ko, I.K., Abolbashari, M., Huling, J., Kim, C., Mirmalek-Sani, S.-H., Moradi, M., Orlando, G., Jackson, J.D., Aboushwareb, T., Soker, S., et al. (2014). Enhanced re-endothelialization of acellular kidney scaffolds for whole organ engineering via antibody conjugation of vasculatures. TECHNOLOGY *02*, 243–253.

Kopeček, J. (2007). Hydrogel Biomaterials: A Smart Future? Biomaterials *28*, 5185–5192.

Kumar, A.C., and Erothu, H. (2016). Synthetic Polymer Hydrogels. In Biomedical Applications of Polymeric Materials and Composites, (Wiley-Blackwell), pp. 141–162.

Kumosa, L.S., Zetterberg, V., and Schouenborg, J. (2018). Gelatin promotes rapid restoration of the blood brain barrier after acute brain injury. Acta Biomater. *65*, 137–149.

Kuo, C.-Y., Guo, T., Cabrera-Luque, J., Arumugasaamy, N., Bracaglia, L., Garcia-Vivas, A., Santoro, M., Baker, H., Fisher, J., and Kim, P. (2018). Placental basement membrane proteins are required for effective cytotrophoblast invasion in a three-dimensional bioprinted placenta model. J. Biomed. Mater. Res. A *106*, 1476–1487.

Kusuma, G.D., Yang, M.C., Brennecke, S.P., O'Connor, A.J., Kalionis, B., and Heath, D.E. (2018). Transferable Matrixes Produced from Decellularized Extracellular Matrix Promote Proliferation and Osteogenic Differentiation of Mesenchymal Stem Cells and Facilitate Scale-Up. ACS Biomater. Sci. Eng. *4*, 1760–1769.

Lalitkumar, P.G.L., Lalitkumar, S., Meng, C.X., Stavreus-Evers, A., Hambiliki, F., Bentin-Ley, U., and Gemzell-Danielsson, K. (2007). Mifepristone, but not levonorgestrel, inhibits human blastocyst attachment to an in vitro endometrial three-dimensional cell culture model. Hum. Reprod. *22*, 3031–3037.

Lalitkumar, S., Boggavarapu, N.R., Menezes, J., Dimitriadis, E., Zhang, J.-G., Nicola, N.A., Gemzell-Danielsson, K., and Lalitkumar, L.P.G. (2013). Polyethylene glycated leukemia inhibitory factor antagonist inhibits human blastocyst implantation and triggers apoptosis by down-regulating embryonic AKT. Fertil. Steril. *100*, 1160-1169.e2.

Landgren, B.-M., Johannisson, E., Stavreus-Evers, A., Hamberger, L., and Eriksson, H. (1996). A new method to study the process of implantation of a human blastocyst in vitro. Fertil. Steril. *65*, 1067–1070.

Lane, M., and Gardner, D.K. (2007). Embryo culture medium: which is the best? Best Pract. Res. Clin. Obstet. Gynaecol. *21*, 83–100.

Lang, R., Stern, M.M., Smith, L., Liu, Y., Bharadwaj, S., Liu, G., Baptista, P.M., Bergman, C.R., Soker, S., Yoo, J.J., et al. (2011). Three-dimensional culture of hepatocytes on porcine liver tissue-derived extracellular matrix. Biomaterials *32*, 7042–7052.

Langer, R., and Vacanti, J.P. (1993). Tissue engineering. Science *260*, 920–926.

Laronda, M.M., Jakus, A.E., Whelan, K.A., Wertheim, J.A., Shah, R.N., and Woodruff, T.K. (2015). Initiation of puberty in mice following decellularized ovary transplant. Biomaterials *50*, 20–29.

Law, J.X., Liau, L.L., Saim, A., Yang, Y., and Idrus, R. (2017). Electrospun Collagen Nanofibers and Their Applications in Skin Tissue Engineering. Tissue Eng. Regen. Med. *14*, 699–718.

Lazzaroni, L., Fusi, F.M., Doldi, N., and Ferrari, A. (1999). The use of Matrigel∗ at low concentration enhances in vitro blastocyst formation and hatching in a mouse embryo model ∗. Fertil. Steril. *71*, 1133–1137.

Le, S.J., Gongora, M., Zhang, B., Grimmond, S., Campbell, G.R., Campbell, J.H., and Rolfe, B.E. (2010). Gene expression profile of the fibrotic response in the peritoneal cavity. Differentiation *79*, 232–243.

Lee, J.S., Shin, J., Park, H.-M., Kim, Y.-G., Kim, B.-G., Oh, J.-W., and Cho, S.-W. (2014). Liver extracellular matrix providing dual functions of two-dimensional substrate coating and three-dimensional injectable hydrogel platform for liver tissue engineering. Biomacromolecules *15*, 206–218.

Lehr, E.J., Rayat, G.R., Chiu, B., Churchill, T., McGann, L.E., Coe, J.Y., and Ross, D.B. (2011). Decellularization reduces immunogenicity of sheep pulmonary artery vascular patches. J. Thorac. Cardiovasc. Surg. *141*, 1056–1062.

Li, X., Sun, H., Lin, N., Hou, X., Wang, J., Zhou, B., Xu, P., Xiao, Z., Chen, B., Dai, J., et al. (2011). Regeneration of uterine horns in rats by collagen scaffolds loaded with collagen-binding human basic fibroblast growth factor. Biomaterials *32*, 8172–8181.

Llobat, L., Marco-Jiménez, F., Peñaranda, D.S., Saenz-de-Juano, M.D., and Vicente, J.S. (2012). effect of embryonic genotype on reference gene selection for RT-qPCR normalization. Reprod. Domest. Anim. Zuchthyg. *47*, 629–634.

Lopata, A., Kohlman, D.J., Bowes, L.G., and Watkins, W.B. (1995). Culture of marmoset blastocysts on matrigel: A model of differentiation during the implantation period. Anat. Rec. *241*, 469–486.

López-Pérez, N., Gil-Sanchis, C., Ferrero, H., Faus, A., Díaz, A., Pellicer, A., Cervelló, I., and Simón, C. (2018). Human Endometrial Reconstitution From Somatic Stem Cells: The Importance of Niche-Like Cells. Reprod. Sci. Thousand Oaks Calif 1933719118766251.

Lorvellec, M., Scottoni, F., Crowley, C., Fiadeiro, R., Maghsoudlou, P., Pellegata, A.F., Mazzacuva, F., Gjinovci, A., Lyne, A.-M., Zulini, J., et al. (2017). Mouse decellularised liver scaffold improves human embryonic and induced pluripotent stem cells differentiation into hepatocyte-like cells. PLOS ONE *12*, e0189586.

Lü, S.-H., Wang, H.-B., Liu, H., Wang, H.-P., Lin, Q.-X., Li, D.-X., Song, Y.-X., Duan, C.-M., Feng, L.-X., and Wang, C.-Y. (2009). Reconstruction of Engineered Uterine Tissues Containing Smooth Muscle Layer in Collagen/Matrigel Scaffold *In Vitro*. Tissue Eng. Part A *15*, 1611–1618.

Lutolf, M.P., and Hubbell, J.A. (2005). Synthetic biomaterials as instructive extracellular microenvironments for morphogenesis in tissue engineering. Nat. Biotechnol. *23*, 47–55.

Lv, H., Wang, H., Zhang, Z., Yang, W., Liu, W., Li, Y., and Li, L. (2017). Biomaterial stiffness determines stem cell fate. Life Sci. *178*, 42–48.

MacKintosh, S.B., Serino, L.P., Iddon, P.D., Brown, R., Conlan, R.S., Wright, C.J., Maffeis, T.G.G., Raxworthy, M.J., and Sheldon, I.M. (2015). A three-dimensional model of primary bovine endometrium using an electrospun scaffold. Biofabrication *7*, 025010.

Mahajan, N., and Sharma, S. (2016). The endometrium in assisted reproductive technology: How thin is thin? J. Hum. Reprod. Sci. *9*, 3–8.

Maitra, J., and Shukla, V.K. (2014). Cross-linking in Hydrogels - A Review. Am. J. Polym. Sci. *4*, 25–31.

Mangione, P.P., Mazza, G., Gilbertson, J.A., Rendell, N.B., Canetti, D., Giorgetti, S., Frenguelli, L., Curti, M., Rezk, T., Raimondi, S., et al. (2017). Increasing the accuracy of proteomic typing by decellularisation of amyloid tissue biopsies. J. Proteomics *165*, 113–118.

March, C.M., Israel, R., and March, A.D. (1978). Hysteroscopic management of intrauterine adhesions. Am. J. Obstet. Gynecol. *130*, 653–657.

Mascarenhas, M.N., Flaxman, S.R., Boerma, T., Vanderpoel, S., and Stevens, G.A. (2012). National, Regional, and Global Trends in Infertility Prevalence Since 1990: A Systematic Analysis of 277 Health Surveys. PLOS Med. *9*, e1001356.

Maybin, J.A., and Critchley, H.O.D. (2015). Menstrual physiology: implications for endometrial pathology and beyond. Hum. Reprod. Update *21*, 748–761.

Mazza, G., Simons, J.P., Al-Shawi, R., Ellmerich, S., Urbani, L., Giorgetti, S., Taylor, G.W., Gilbertson, J.A., Hall, A.R., Al-Akkad, W., et al. (2016). Amyloid persistence in decellularized liver: biochemical and histopathological characterization. Amyloid *23*, 1–7.

McClelland, R., Wauthier, E., Uronis, J., and Reid, L. (2008). Gradients in the liver's extracellular matrix chemistry from periportal to pericentral zones: Influence on human hepatic progenitors. Tissue Eng. - Part A *14*, 59–70.

Mclennan, C.E., and Rydell, A.H. (1965). Extent of Endometrial Shedding During Normal Menstruation. Obstet. Gynecol. *26*, 605.

Meng, C.-X., Andersson, K.L., Bentin-Ley, U., Gemzell-Danielsson, K., and Lalitkumar, P.G.L. (2009). Effect of levonorgestrel and mifepristone on endometrial receptivity markers in a three-dimensional human endometrial cell culture model. Fertil. Steril. *91*, 256–264.

Midwood, K.S., Chiquet, M., Tucker, R.P., and Orend, G. (2016). Tenascin-C at a glance. J Cell Sci *129*, 4321–4327.

Miner, J.H. (2011). Basement Membranes. In The Extracellular Matrix: An Overview, (Springer, Berlin, Heidelberg), pp. 117–145.

Miwa, I., Tamura, H., Takasaki, A., Yamagata, Y., Shimamura, K., and Sugino, N. (2009). Pathophysiologic features of "thin" endometrium. Fertil. Steril. *91*, 998–1004.

Miyauchi, Y., Yasuchika, K., Fukumitsu, K., Ishii, T., Ogiso, S., Minami, T., Kojima, H., Yamaoka, R., Katayama, H., Kawai, T., et al. (2017). A novel three-dimensional culture system maintaining the physiological extracellular matrix of fibrotic model livers accelerates progression of hepatocellular carcinoma cells. Sci. Rep. *7*, 9827.

Miyazaki, K., and Maruyama, T. (2014). Partial regeneration and reconstruction of the rat uterus through recellularization of a decellularized uterine matrix. Biomaterials *35*, 8791–8800.

Morris, S.A., Grewal, S., Barrios, F., Patankar, S.N., Strauss, B., Buttery, L., Alexander, M., Shakesheff, K.M., and Zernicka-Goetz, M. (2012). Dynamics of anterior–posterior axis formation in the developing mouse embryo. Nat. Commun. *3*, 673.

Naba, A., Clauser, K.R., Mani, D.R., Carr, S.A., and Hynes, R.O. (2017). Quantitative proteomic profiling of the extracellular matrix of pancreatic islets during the angiogenic switch and insulinoma progression. Sci. Rep. *7*.

Nair, L.S., and Laurencin, C.T. (2007). Biodegradable polymers as biomaterials. Prog. Polym. Sci. *32*, 762–798.

Nakayama, K.H., Batchelder, C.A., Lee, C.I., and Tarantal, A.F. (2010). Decellularized Rhesus Monkey Kidney as a Three-Dimensional Scaffold for Renal Tissue Engineering. Tissue Eng. Part A *16*, 2207–2216.

Nawroth, J., Rogal, J., Weiss, M., Brucker, S.Y., and Loskill, P. (2018). Organ-on-a-Chip Systems for Women's Health Applications. Adv. Healthc. Mater. *7*, 1700550.

Nelson, C.M., and Bissell, M.J. (2006). Of Extracellular Matrix, Scaffolds, and Signaling: Tissue Architecture Regulates Development, Homeostasis, and Cancer. Annu. Rev. Cell Dev. Biol. *22*, 287–309.

O'Brien, F.J. (2011). Biomaterials & scaffolds for tissue engineering. Mater. Today *14*, 88–95.

Oefner, C.M., Sharkey, A., Gardner, L., Critchley, H., Oyen, M., and Moffett, A. (2015). Collagen type IV at the fetal–maternal interface. Placenta *36*, 59–68.

Oh, H.H., Ko, Y.-G., Lu, H., Kawazoe, N., and Chen, G. (2012). Preparation of Porous Collagen Scaffolds with Micropatterned Structures. Adv. Mater. *24*, 4311–4316.

Okumura-Nakanishi, S., Saito, M., Niwa, H., and Ishikawa, F. (2005). Oct-3/4 and Sox2 regulate Oct-3/4 gene in embryonic stem cells. J. Biol. Chem. *280*, 5307–5317.

Olalekan, S.A., Burdette, J.E., Getsios, S., Woodruff, T.K., and Kim, J.J. (2017). Development of a novel human recellularized endometrium that responds to a 28-day hormone treatment. Biol. Reprod. *96*, 971–981.

Oliveira, A.C., Garzón, I., Ionescu, A.M., Carriel, V., Cardona, J. de la C., González-Andrades, M., Pérez, M. del M., Alaminos, M., and Campos, A. (2013). Evaluation of Small Intestine Grafts Decellularization Methods for Corneal Tissue Engineering. PLOS ONE *8*, e66538.

Ombelet, W., Cooke, I., Dyer, S., Serour, G., and Devroey, P. (2008). Infertility and the provision of infertility medical services in developing countries. Hum. Reprod. Update *14*, 605–621.

Ott, H.C., Matthiesen, T.S., Goh, S.-K., Black, L.D., Kren, S.M., Netoff, T.I., and Taylor, D.A. (2008). Perfusion-decellularized matrix: using nature's platform to engineer a bioartificial heart. Nat. Med. *14*, 213–221.

Ouni, E., Vertommen, D., Chiti, M.C., Dolmans, M.-M., and Amorim, C.A. (2018). A draft map of the human ovarian proteome for tissue engineering and clinical applications. Mol. Cell. Proteomics MCP.

Ozkan, O., Akar, M.E., Ozkan, O., Erdogan, O., Hadimioglu, N., Yilmaz, M., Gunseren, F., Cincik, M., Pestereli, E., Kocak, H., et al. (2013). Preliminary results of the first human uterus transplantation from a multiorgan donor. Fertil. Steril. *99*, 470–476.

Palasz, A.T., Rodriguez-Martinez, H., Beltran-Breña, P., Perez-Garnelo, S., Martinez, M.F., Gutierrez-Adan, A., and Fuente, J.D. la (2016). Effects of hyaluronan, BSA, and serum on bovine embryo in vitro development, ultrastructure, and gene expression patterns. Mol. Reprod. Dev. *73*, 1503–1511.

Parenteau-Bareil, R., Gauvin, R., and Berthod, F. (2010). Collagen-Based Biomaterials for Tissue Engineering Applications. Materials *3*, 1863–1887.

Park, D.W., Choi, D.S., Ryu, H.-S., Kwon, H.C., Joo, H., and Min, C.K. (2003). A well-defined in vitro three-dimensional culture of human endometrium and its applicability to endometrial cancer invasion. Cancer Lett. *195*, 185–192.

Parmar, T., Sachdeva, G., Savardekar, L., Katkam, R.R., Nimbkar-Joshi, S., Gadkar-Sable, S., Salvi, V., Manjramkar, D.D., Meherji, P., and Puri, C.P. (2008). Protein repertoire of human

uterine fluid during the mid-secretory phase of the menstrual cycle. Hum. Reprod. Oxf. Engl. *23*, 379–386.

Pashneh-Tala, S., MacNeil, S., and Claeyssens, F. (2016). The Tissue-Engineered Vascular Graft—Past, Present, and Future. Tissue Eng. Part B Rev. *22*, 68–100.

Patel, Z.S., and Mikos, A.G. (2004). Angiogenesis with biomaterial-based drug- and cell-delivery systems. J. Biomater. Sci. Polym. Ed. *15*, 701–726.

Pellegata, A.F., Tedeschi, A.M., and De Coppi, P. (2018). Whole Organ Tissue Vascularization: Engineering the Tree to Develop the Fruits. Front. Bioeng. Biotechnol. *6*, 56.

Peloso, A., Dhal, A., Zambon, J.P., Li, P., Orlando, G., Atala, A., and Soker, S. (2015). Current achievements and future perspectives in whole-organ bioengineering. Stem Cell Res. Ther. *6*.

Piccoli, M., D'Angelo, E., Crotti, S., Sensi, F., Urbani, L., Maghin, E., Burns, A., De Coppi, P., Fassan, M., Rugge, M., et al. (2018). Decellularized colorectal cancer matrix as bioactive microenvironment for in vitro 3D cancer research. J. Cell. Physiol. *233*, 5937–5948.

Pinto, M.L., Rios, E., Silva, A.C., Neves, S.C., Caires, H.R., Pinto, A.T., Durães, C., Carvalho, F.A., Cardoso, A.P., Santos, N.C., et al. (2017). Decellularized human colorectal cancer matrices polarize macrophages towards an anti-inflammatory phenotype promoting cancer cell invasion via CCL18. Biomaterials *124*, 211–224.

Place, E.S., George, J.H., Williams, C.K., and Stevens, M.M. (2009). Synthetic polymer scaffolds for tissue engineering. Chem. Soc. Rev. *38*, 1139–1151.

Poel, W.E. (1948). Preparation of Acellular Homogenates From Muscle Samples. Science *108*, 390–391.

Postlethwaite, A.E., Seyer, J.M., and Kang, A.H. (1978). Chemotactic attraction of human fibroblasts to type I, II, and III collagens and collagen-derived peptides. Proc. Natl. Acad. Sci. U. S. A. *75*, 871–875.

Pouliot, R.A., Link, P.A., Mikhaiel, N.S., Schneck, M.B., Valentine, M.S., Kamga Gninzeko, F.J., Herbert, J.A., Sakagami, M., and Heise, R.L. (2016). Development and characterization of a naturally derived lung extracellular matrix hydrogel. J. Biomed. Mater. Res. A *104*, 1922–1935.

Pridgen, B.C., Woon, C.Y.L., Kim, M., Thorfinn, J., Lindsey, D., Pham, H., and Chang, J. (2011). Flexor tendon tissue engineering: acellularization of human flexor tendons with preservation of biomechanical properties and biocompatibility. Tissue Eng. Part C Methods *17*, 819–828.

Quint, C., Kondo, Y., Manson, R.J., Lawson, J.H., Dardik, A., and Niklason, L.E. (2011). Decellularized tissue-engineered blood vessel as an arterial conduit. Proc. Natl. Acad. Sci. U. S. A. *108*, 9214–9219.

Ramírez-González, J.A., Vaamonde-Lemos, R., Cunha-Filho, J.S., Varghese, A.C., and Swanson, R.J. (2016). Overview of the Female Reproductive System. In Exercise and Human

Reproduction, D. Vaamonde, S.S. du Plessis, and A. Agarwal, eds. (New York, NY: Springer New York), pp. 19–46.

Rana, D., Zreiqat, H., Benkirane-Jessel, N., Ramakrishna, S., and Ramalingam, M. (2017). Development of decellularized scaffolds for stem cell-driven tissue engineering. J. Tissue Eng. Regen. Med. *11*, 942–965.

Raya-Rivera, A.M., Esquiliano, D., Fierro-Pastrana, R., López-Bayghen, E., Valencia, P., Ordorica-Flores, R., Soker, S., Yoo, J.J., and Atala, A. (2014). Tissue-engineered autologous vaginal organs in patients: a pilot cohort study. The Lancet *384*, 329–336.

Remuzzi, A., Figliuzzi, M., Bonandrini, B., Silvani, S., Azzollini, N., Nossa, R., Benigni, A., and Remuzzi, G. (2017). Experimental Evaluation of Kidney Regeneration by Organ Scaffold Recellularization. Sci. Rep. *7*, 43502.

Sabatier, L., Chen, D., Fagotto-Kaufmann, C., Hubmacher, D., McKee, M.D., Annis, D.S., Mosher, D.F., and Reinhardt, D.P. (2009). Fibrillin Assembly Requires Fibronectin. Mol. Biol. Cell *20*, 846–858.

Saldin, L.T., Cramer, M.C., Velankar, S.S., White, L.J., and Badylak, S.F. (2017). Extracellular matrix hydrogels from decellularized tissues: Structure and function. Acta Biomater. *49*, 1–15.

Salgado, R.M., Capelo, L.P., Favaro, R.R., Glazier, J.D., Aplin, J.D., and Zorn, T.M. (2009). Hormone-regulated expression and distribution of versican in mouse uterine tissues. Reprod. Biol. Endocrinol. RBE *7*, 60.

Sánchez, P.L., Fernández-Santos, M.E., Costanza, S., Climent, A.M., Moscoso, I., Gonzalez-Nicolas, M.A., Sanz-Ruiz, R., Rodríguez, H., Kren, S.M., Garrido, G., et al. (2015). Acellular human heart matrix: A critical step toward whole heart grafts. Biomaterials *61*, 279–289.

Santamaria, X., Cabanillas, S., Cervelló, I., Arbona, C., Raga, F., Ferro, J., Palmero, J., Remohí, J., Pellicer, A., and Simón, C. (2016). Autologous cell therapy with CD133+ bone marrow-derived stem cells for refractory Asherman's syndrome and endometrial atrophy: a pilot cohort study. Hum. Reprod. Oxf. Engl. *31*, 1087–1096.

Santoso, E.G., Yoshida, K., Hirota, Y., Aizawa, M., Yoshino, O., Kishida, A., Osuga, Y., Saito, S., Ushida, T., and Furukawa, K.S. (2014). Application of Detergents or High Hydrostatic Pressure as Decellularization Processes in Uterine Tissues and Their Subsequent Effects on In Vivo Uterine Regeneration in Murine Models. PLOS ONE *9*, e103201.

Sayegh, M.H., and Carpenter, C.B. (2004). Transplantation 50 years later--progress, challenges, and promises. N. Engl. J. Med. *351*, 2761–2766.

Schafer, W.R., Fischer, L., Roth, K., Jullig, A.K., Stuckenschneider, J.E., Schwartz, P., Weimer, M., Orlowska-Volk, M., Hanjalic-Beck, A., Kranz, I., et al. (2011). Critical evaluation of human endometrial explants as an ex vivo model system: a molecular approach. Mol. Hum. Reprod. *17*, 255–265.

Schultz, G.S., Davidson, J.M., Kirsner, R.S., Bornstein, P., and Herman, I.M. (2011). Dynamic Reciprocity in the Wound Microenvironment. Wound Repair Regen. Off. Publ. Wound Heal. Soc. Eur. Tissue Repair Soc. *19*, 134–148.

Schutte, S.C., and Taylor, R.N. (2012). A tissue engineered human endometrial stroma that responds to cues for secretory differentiation, decidualization and menstruation. Fertil. Steril. *97*, 997–1003.

Schutte, S.C., James, C.O., Sidell, N., and Taylor, R.N. (2015). Tissue-Engineered Endometrial Model for the Study of Cell–Cell Interactions. Reprod. Sci. *22*, 308–315.

Scolari, S.C., Pugliesi, G., Strefezzi, R. de F., Andrade, S.C. da S., Coutinho, L.L., and Binelli, M. (2017). Dynamic remodeling of endometrial extracellular matrix regulates embryo receptivity in cattle. Reproduction *153*, 49–61.

Seif-Naraghi, S.B., Horn, D., Schup-Magoffin, P.J., and Christman, K.L. (2012). Injectable extracellular matrix derived hydrogel provides a platform for enhanced retention and delivery of a heparin-binding growth factor. Acta Biomater. *8*, 3695–3703.

Seif-Naraghi, S.B., Singelyn, J.M., Salvatore, M.A., Osborn, K.G., Wang, J.J., Sampat, U., Kwan, O.L., Strachan, G.M., Wong, J., Schup-Magoffin, P.J., et al. (2013). Safety and efficacy of an injectable extracellular matrix hydrogel for treating myocardial infarction. Sci. Transl. Med. *5*.

Senturk, L.M., and Erel, C.T. (2008). Thin endometrium in assisted reproductive technology. Curr. Opin. Obstet. Gynecol. *20*, 221–228.

Shafiq, M.A., Gemeinhart, R.A., Yue, B.Y.J.T., and Djalilian, A.R. (2012). Decellularized human cornea for reconstructing the corneal epithelium and anterior stroma. Tissue Eng. Part C Methods *18*, 340–348.

Shenfield, F., Pennings, G., Cohen, J., Devroey, P., de Wert, G., and Tarlatzis, B. (2005). ESHRE Task Force on Ethics and Law 10: Surrogacy. Hum. Reprod. *20*, 2705–2707.

Shupe, T., Williams, M., Brown, A., Willenberg, B., and Petersen, B.E. (2010). Method for the decellularization of intact rat liver. Organogenesis *6*, 134–136.

Simões, I.N., Vale, P., Soker, S., Atala, A., Keller, D., Noiva, R., Carvalho, S., Peleteiro, C., Cabral, J.M.S., Eberli, D., et al. (2017). Acellular Urethra Bioscaffold: Decellularization of Whole Urethras for Tissue Engineering Applications. Sci. Rep. *7*, 41934.

Simon, A., and Laufer, N. (2012). Assessment and treatment of repeated implantation failure (RIF). J. Assist. Reprod. Genet. *29*, 1227–1239.

Simón, C., Horcajadas, J., Pellicer, A., and García-Velasco, J. (2009). El Endometrio Humano. B. Aires Argent. Editor. Panam.

Smith, G.D., Takayama, S., and Swain, J.E. (2012). Rethinking In Vitro Embryo Culture: New Developments in Culture Platforms and Potential to Improve Assisted Reproductive Technologies. Biol. Reprod. *86*.

Song, T., Zhao, X., Sun, H., Li, X., Lin, N., Ding, L., Dai, J., and Hu, Y. (2015). Regeneration of uterine horns in rats using collagen scaffolds loaded with human embryonic stem cell-derived endometrium-like cells. Tissue Eng. Part A *21*, 353–361.

Sood, D., Chwalek, K., Stuntz, E., Pouli, D., Du, C., Tang-Schomer, M., Georgakoudi, I., Black, L.D., and Kaplan, D.L. (2016). Fetal Brain Extracellular Matrix Boosts Neuronal

Network Formation in 3D Bioengineered Model of Cortical Brain Tissue. ACS Biomater. Sci. Eng. *2*, 131–140.

Speroff, L., and Fritz, M.A. (2005). Clinical gynecologic endocrinology and infertility (lippincott Williams & wilkins).

Strowitzki, T., Germeyer, A., Popovici, R., and Von Wolff, M. (2006). The human endometrium as a fertility-determining factor. Hum. Reprod. Update *12*, 617–630.

Sullivan, D.C., Mirmalek-Sani, S.-H., Deegan, D.B., Baptista, P.M., Aboushwareb, T., Atala, A., and Yoo, J.J. (2012). Decellularization methods of porcine kidneys for whole organ engineering using a high-throughput system. Biomaterials *33*, 7756–7764.

Sun, M., Chen, S., Adams, S.M., Florer, J.B., Liu, H., Kao, W.W.-Y., Wenstrup, R.J., and Birk, D.E. (2011). Collagen V is a dominant regulator of collagen fibrillogenesis: dysfunctional regulation of structure and function in a corneal-stroma-specific Col5a1-null mouse model. J. Cell Sci. *124*, 4096–4105.

Swain, J.E., and Smith, G.D. (2011). Advances in embryo culture platforms: novel approaches to improve preimplantation embryo development through modifications of the microenvironment. Hum. Reprod. Update *17*, 541–557.

Swain, J.E., Carrell, D., Cobo, A., Meseguer, M., Rubio, C., and Smith, G.D. (2016). Optimizing the culture environment and embryo manipulation to help maintain embryo developmental potential. Fertil. Steril. *105*, 571–587.

Swift, J., and Discher, D.E. (2014). The nuclear lamina is mechano-responsive to ECM elasticity in mature tissue. J Cell Sci *127*, 3005–3015.

Tan, O., Ornek, T., Seval, Y., Sati, L., and Arici, A. (2008). Tenascin is highly expressed in endometriosis and its expression is upregulated by estrogen. Fertil. Steril. *89*, 1082–1089.

Tapias, L.F., and Ott, H.C. (2014). Decellularized Scaffolds as a Platform for Bioengineered Organs. Curr. Opin. Organ Transplant. *19*, 145–152.

Taveau, J.W., Tartaglia, M., Buchannan, D., Smith, B., Koenig, G., Thomfohrde, K., Stouch, B., Jeck, S., and Greene, C.H. (2004). Regeneration of uterine horn using porcine small intestinal submucosa grafts in rabbits. J. Investig. Surg. Off. J. Acad. Surg. Res. *17*, 81–92.

Tawia, S.A., and Rogers, P. a. W. (1992). In vivo microscopy of the subepithelial capillary plexus of the endometrium of rats during embryo implantation. J. Reprod. Fertil. *96*, 673–680.

Thorne, J.T., Segal, T.R., Chang, S., Jorge, S., Segars, J.H., and Leppert, P.C. (2015). Dynamic Reciprocity Between Cells and Their Microenvironment in Reproduction. Biol. Reprod. *92*.

Tsang, K.Y., Cheung, M.C.H., Chan, D., and Cheah, K.S.E. (2010). The developmental roles of the extracellular matrix: beyond structure to regulation. Cell Tissue Res. *339*, 93.

Turco, M.Y., Gardner, L., Hughes, J., Cindrova-Davies, T., Gomez, M.J., Farrell, L., Hollinshead, M., Marsh, S.G.E., Brosens, J.J., Critchley, H.O., et al. (2017). Long-term, hormone-responsive organoid cultures of human endometrium in a chemically-defined medium. Nat. Cell Biol. *19*, 568–577.

Turner, N.J., and Badylak, S.F. (2013). Biologic scaffolds for musculotendinous tissue repair. Eur. Cell. Mater. *25*, 130–143.

Uludag, H., De Vos, P., and Tresco, P.A. (2000). Technology of mammalian cell encapsulation. Adv. Drug Deliv. Rev. *42*, 29–64.

Uriel, S., Huang, J.-J., Moya, M.L., Francis, M.E., Wang, R., Chang, S.-Y., Cheng, M.-H., and Brey, E.M. (2008). The role of adipose protein derived hydrogels in adipogenesis. Biomaterials *29*, 3712–3719.

Uygun, B.E., Soto-Gutierrez, A., Yagi, H., Izamis, M.-L., Guzzardi, M.A., Shulman, C., Milwid, J., Kobayashi, N., Tilles, A., Berthiaume, F., et al. (2010). Organ reengineering through development of a transplantable recellularized liver graft using decellularized liver matrix. Nat. Med. *16*, 814–820.

Valdez, J., Cook, C.D., Ahrens, C.C., Wang, A.J., Brown, A., Kumar, M., Stockdale, L., Rothenberg, D., Renggli, K., Gordon, E., et al. (2017). On-demand dissolution of modular, synthetic extracellular matrix reveals local epithelial-stromal communication networks. Biomaterials *130*, 90–103.

Varaprasad, K., Raghavendra, G.M., Jayaramudu, T., Yallapu, M.M., and Sadiku, R. (2017). A mini review on hydrogels classification and recent developments in miscellaneous applications. Mater. Sci. Eng. C *79*, 958–971.

Vico, L., Collet, P., Guignandon, A., Lafage-Proust, M.-H., Thomas, T., Rehailia, M., and Alexandre, C. (2000). Effects of long-term microgravity exposure on cancellous and cortical weight-bearing bones of cosmonauts. The Lancet *355*, 1607–1611.

Voytik-Harbin, S.L., Brightman, A.O., Waisner, B.Z., Robinson, J.P., and Lamar, C.H. (1998). Small Intestinal Submucosa: A Tissue-Derived Extracellular Matrix That Promotes Tissue-Specific Growth and Differentiation of Cells in Vitro. Tissue Eng. *4*, 157–174.

Vyas, D., Baptista, P.M., Brovold, M., Moran, E., Gaston, B., Booth, C., Samuel, M., Atala, A., and Soker, S. (2017). Self-assembled liver organoids recapitulate hepatobiliary organogenesis in vitro. Hepatol. Baltim. Md.

Wang, H., Pilla, F., Anderson, S., Martínez-Escribano, S., Herrer, I., Moreno-Moya, J.M., Musti, S., Bocca, S., Oehninger, S., and Horcajadas, J.A. (2012). A novel model of human implantation: 3D endometrium-like culture system to study attachment of human trophoblast (Jar) cell spheroids. MHR Basic Sci. Reprod. Med. *18*, 33–43.

Wang, H.-B., Lü, S.-H., Lin, Q.-X., Feng, L.-X., Li, D.-X., Duan, C.-M., Li, Y., and Wang, C.-Y. (2010). Reconstruction of endometrium in vitro via rabbit uterine endometrial cells expanded by sex steroid. Fertil. Steril. *93*, 2385–2395.

Wang, L., Johnson, J.A., Zhang, Q., and Beahm, E.K. (2013). Combining decellularized human adipose tissue extracellular matrix and adipose-derived stem cells for adipose tissue engineering. Acta Biomater. *9*, 8921–8931.

Watt, F.M., and Huck, W.T.S. (2013). Role of the extracellular matrix in regulating stem cell fate. Nat. Rev. Mol. Cell Biol. *14*, 467–473.

Wei, G., and Ma, P.X. (2004). Structure and properties of nano-hydroxyapatite/polymer composite scaffolds for bone tissue engineering. Biomaterials *25*, 4749–4757.

Weimar, C.H.E., Post Uiterweer, E.D., Teklenburg, G., Heijnen, C.J., and Macklon, N.S. (2013). In-vitro model systems for the study of human embryo–endometrium interactions. Reprod. Biomed. Online *27*, 673–688.

Weinberg, R.S. (2013). Chapter 81 - Overview of Cellular Therapy. In Transfusion Medicine and Hemostasis (Second Edition), B.H. Shaz, C.D. Hillyer, M. Roshal, and C.S. Abrams, eds. (San Diego: Elsevier), pp. 533–540.

Wichterle, O., and Lím, D. (1960). Hydrophilic Gels for Biological Use. Nature *185*, 117–118.

Willerth, S.M., and Sakiyama-Elbert, S.E. (2008). Combining stem cells and biomaterial scaffolds for constructing tissues and cell delivery. In StemBook, (Cambridge (MA): Harvard Stem Cell Institute), p.

Wilshaw, S.-P., Kearney, J.N., Fisher, J., and Ingham, E. (2006). Production of an acellular amniotic membrane matrix for use in tissue engineering. Tissue Eng. *12*, 2117–2129.

Wilshaw, S.-P., Kearney, J., Fisher, J., and Ingham, E. (2008). Biocompatibility and potential of acellular human amniotic membrane to support the attachment and proliferation of allogeneic cells. Tissue Eng. Part A *14*, 463–472.

Wobma, H., and Vunjak-Novakovic, G. (2016). Tissue Engineering and Regenerative Medicine 2015: A Year in Review. Tissue Eng. Part B Rev. *22*, 101–113.

Wolf, M.T., Daly, K.A., Brennan-Pierce, E.P., Johnson, S.A., Carruthers, C., D'Amore, A., Nagarkar, S.P., Velankar, S.S., and Badylak, S.F. (2012). A Hydrogel Derived From Decellularized Dermal Extracellular Matrix. Biomaterials *33*, 7028–7038.

Wong, M.L., Wong, J.L., Vapniarsky, N., and Griffiths, L.G. (2016). In vivo xenogeneic scaffold fate is determined by residual antigenicity and extracellular matrix preservation. Biomaterials *92*, 1–12.

Xiao, S., Coppeta, J.R., Rogers, H.B., Isenberg, B.C., Zhu, J., Olalekan, S.A., McKinnon, K.E., Dokic, D., Rashedi, A.S., Haisenleder, D.J., et al. (2017). A microfluidic culture model of the human reproductive tract and 28-day menstrual cycle. Nat. Commun. *8*, 14584.

Xu, L., Ding, L., Wang, L., Cao, Y., Zhu, H., Lu, J., Li, X., Song, T., Hu, Y., and Dai, J. (2017). Umbilical cord-derived mesenchymal stem cells on scaffolds facilitate collagen degradation via upregulation of MMP-9 in rat uterine scars. Stem Cell Res. Ther. *8*.

Yamanaka, M., Taga, M., and Minaguchi, H. (1996). Immunohistological localization of tenascin in the human endometrium. Gynecol. Obstet. Invest. *41*, 247–252.

Yang, H., Wu, S., Feng, R., Huang, J., Liu, L., Liu, F., and Chen, Y. (2017). Vitamin C plus hydrogel facilitates bone marrow stromal cell-mediated endometrium regeneration in rats. Stem Cell Res. Ther. *8*, 267.

Yang, J.-A., Yeom, J., Hwang, B.W., Hoffman, A.S., and Hahn, S.K. (2014). In situ-forming injectable hydrogels for regenerative medicine. Prog. Polym. Sci. *39*, 1973–1986.

Yap, K.H., Murphy, R., Devbhandari, M., and Venkateswaran, R. (2013). Aortic valve replacement: is porcine or bovine valve better? Interact. Cardiovasc. Thorac. Surg. *16*, 361–373.

Young, R.C., and Goloman, G. (2013). Allo- and Xeno-Reassembly of Human and Rat Myometrium from Cells and Scaffolds. Tissue Eng. Part A *19*, 2112–2119.

Young, D.A., Choi, Y.S., Engler, A.J., and Christman, K.L. (2013). Stimulation of adipogenesis of adult adipose-derived stem cells using substrates that mimic the stiffness of adipose tissue. Biomaterials *34*, 8581–8588.

Young, R.C., Schumann, R., and Zhang, P. (2003). Three-Dimensional Culture of Human Uterine Smooth Muscle Myocytes on a Resorbable Scaffolding. Tissue Eng. *9*, 451–459.

Youngstrom, D.W., Barrett, J.G., Jose, R.R., and Kaplan, D.L. (2013). Functional Characterization of Detergent-Decellularized Equine Tendon Extracellular Matrix for Tissue Engineering Applications. PLoS ONE *8*, e64151.

Zegers-Hochschild, F., Adamson, G.D., de Mouzon, J., Ishihara, O., Mansour, R., Nygren, K., Sullivan, E., and van der Poel, S. (2009). The International Committee for Monitoring Assisted Reproductive Technology (ICMART) and the World Health Organization (WHO) Revised Glossary on ART Terminology, 2009. Hum. Reprod. *24*, 2683–2687.

Zhang, X., and Dong, J. (2015). Direct comparison of different coating matrix on the hepatic differentiation from adipose-derived stem cells. Biochem. Biophys. Res. Commun. *456*, 938–944.

Zhang, Y., He, Y., Bharadwaj, S., Hammam, N., Carnagey, K., Myers, R., Atala, A., and Van Dyke, M. (2009). Tissue-specific extracellular matrix coatings for the promotion of cell proliferation and maintenance of cell phenotype. Biomaterials *30*, 4021–4028.

APPENDIX

APPENDIX A. Bayesian parameters

Table 1. Bayesian parameters of in vitro development rate.

Embryo Diameter (µm)	D_{A-B} [1]	$HPD_{95\%}$ [2]		P [3]
A= Control; B= FBS+	-0.0243	-0.0435 ,	-0.0033	0.99
A= Control; B= M	0.0212	-0.0030 ,	0.0464	0.95
A= Control; B= NS	-0.0078	-0.0299 ,	0.0117	0.78
A= Control; B= ES	-0.0173	-0.0373 ,	0.0026	0.96
A= FBS+; B= M	0.0455	0.0206 ,	0.0703	1.00
A= FBS+; B= NS	0.0165	-0.0046 ,	0.0370	0.94
A= FBS+; B= ES	0.0071	-0.0130 ,	0.0264	0.75
A= M; B= NS	-0.0290	-0.0532 ,	-0.0027	0.99
A= M; B= ES	-0.0384	-0.0633 ,	-0.0146	1.00
A= NS; B= ES	-0.0094	-0.0292 ,	0.0106	0.82

[1] D_{A-B} = Median of the difference (median of the marginal posterior distribution of the difference between the experimental groups).
[2] $HPD_{95\%}$ = The highest posterior density region at 95% of probability.
[3] P = Probability of the difference being greater than 0 when $D_{A-B} > 0$ or lower than 0 when $D_{A-B} < 0$.

Table 2. Bayesian parameters of the three core pluripotency factors (OCT4, Nanog and SOX2).

Trait	D_{A-B} [1]	$HPD_{95\%}$ [2]		P [3]
NANOG (a.u.)				
A= FBS-; B= FBS+	0.1444	-1.1957 ,	1.4422	0.60
A= FBS-; B= M	0.2745	-0.9477 ,	1.4169	0.70
A= FBS-; B= NS	0.1125	-1.0341 ,	1.3213	0.59
A= FBS-; B= ES	0.0637	-1.0928 ,	1.1995	0.56
A= FBS+; B= M	0.1301	-1.2674 ,	1.3932	0.60
A= FBS+; B= NS	-0.0319	-1.2795 ,	1.3219	0.53
A= FBS+; B= ES	-0.0807	-1.3743 ,	1.2079	0.55
A= M; B= NS	-0.1620	-1.3360 ,	0.9879	0.62
A= M; B= ES	-0.2108	-1.3092 ,	1.0648	0.66
A= NS; B= ES	-0.0488	-1.2289 ,	1.1033	0.54
OCT4 (a.u.)				
A= FBS-; B= FBS+	-0.0427	-0.6488 ,	0.5851	0.56
A= FBS-; B= M	-0.1573	-0.7139 ,	0.4014	0.74
A= FBS-; B= NS	-0.2566	-0.8423 ,	0.2734	0.84
A= FBS-; B= ES	-0.1543	-0.7043 ,	0.4151	0.74
A= FBS+; B= M	-0.1146	-0.7291 ,	0.4936	0.67
A= FBS+; B= NS	-0.2139	-0.8337 ,	0.3922	0.77
A= FBS+; B= ES	-0.1116	-0.6888 ,	0.5048	0.67
A= M; B= NS	-0.0993	-0.6611 ,	0.4337	0.66
A= M; B= ES	0.0030	-0.5439 ,	0.5263	0.51
A= NS; B= ES	0.1023	-0.4311 ,	0.6410	0.66

Trait	D_{A-B} [1]	$HPD_{95\%}$ [2]		P [3]
SOX2 (a.u.)				
A= FBS-; B= FBS+	-0.4048	-1.3695 ,	0.5073	0.83
A= FBS-; B= M	-0.0885	-0.9833 ,	0.7414	0.59
A= FBS-; B= NS	-0.5506	-1.4396 ,	0.3120	0.91
A= FBS-; B= ES	-0.4107	-1.2923 ,	0.4143	0.85
A= FBS+; B= M	0.3164	-0.6383 ,	1.2680	0.80
A= FBS+; B= NS	-0.1458	-1.1484 ,	0.7635	0.62
A= FBS+; B= ES	-0.0059	-0.9524 ,	0.9552	0.50
A= M; B= NS	-0.4621	-1.3446 ,	0.3923	0.88
A= M; B= ES	-0.3223	-1.1426 ,	0.5582	0.80
A= NS; B= ES	0.1398	-0.7238 ,	0.9842	0.64

[1] D_{A-B} = Median of the difference (median of the marginal posterior distribution of the difference between the experimental groups).
[2] $HPD_{95\%}$ = The highest posterior density region at 95% of probability.
[3] P = Probability of the difference being greater than 0 when $D_{A-B} > 0$ or lower than 0 when $D_{A-B} < 0$.

APPENDIX B. Scientific production PhD student

1. International scientific publications

- **Campo, Hannes**, Pedro M. Baptista, Nuria López-Pérez, Amparo Faus, Irene Cervelló, and Carlos Simón. "De- and Recellularization of the Pig Uterus: A Bioengineering Pilot Study." *Biology of Reproduction* 96, no. 1 (01 2017): 34–45. https://doi.org/10.1095/biolreprod.116.143396.
- **Campo, Hannes**, Irene Cervelló, and Carlos Simón. "Bioengineering the Uterus: An Overview of Recent Advances and Future Perspectives in Reproductive Medicine." *Annals of Biomedical Engineering* 45, no. 7 (July 2017): 1710–17. https://doi.org/10.1007/s10439-016-1783-3.

2. Book Chapters

- **Campo H**, Santamaría X, Cervelló I, Simón C. Handbook of Tissue Engineering Scaffolds Volume 2 Part 8: Scaffolds for reproductive system. 42. scaffold for the bioengineered uterus. 2018- Manuscript status: Under preproduction.

3. Works submitted to national or international conferences

3.1. Oral presentations

- "The Added Value of Regenerative Medicine in Reproductive Medicine: (where) can Tissue Engineering Make a Difference?" Name of the conference: ESGE 26th Annual Congress. City of event: Antalya, Turkey. Date of event: 18/10/2017. End date: 21/10/2017. Organising entity: European Society for Gynaecological Endoscopy. **Hannes Campo**; Irene Cervelló;Antonio Pellicer, Irene Cervelló, and Carlos Simón.
- "Bioengineering the uterus: current progress and future perspectives." Conference: Congreso Nacional Biomedicina Jóvenes Investigadores en Valencia. City of event: Valencia, Valencian Community, Spain. Dates: 28-29/11/2016. **Hannes Campo**; Nuria López Pérez; Amparo Faus; Pedro Baptista; Nicolás Garrido; Jose Remohí; Antonio Pellicer; Carlos Simón; Irene Cervelló.
- "The artificial uterus: Fiction or reality?" Conference: ESGE 25th Annual Congress (ESGE) City of event: Brussels, Belgium. Dates: 02/10/2016 End date: 05/12/2016 Organising entity: European Society for Gynaecological Endoscopy **Hannes Campo**; Irene Cervelló; Nuria López Pérez; Amparo Faus; Pedro Baptista; Carlos Simón.

- "Artificial uterus: an option?" Name of the conference: Congrès Annuel Saint-Luc UCL Bruxelles: L'endomètre dans tous ses états. City of event: Brussels, Belgium. Dates: 26-28/11/2015 Organising entity: Université catholique de Louvain. City of event: Brussels, Belgium. **Hannes Campo**; Nuria López Pérez; Amparo Faus; Pedro Baptista; Irene Cervelló; Carlos Simón.

3.2. Posters

- "Endometrial Specific Hydrogels as New Platform for 3D *in vitro* Models and Future Treatments." Conference: Congreso II Nacional Biomedicina Jóvenes Investigadores City: Valencia, Valencian Community, Spain. Dates: 28-29/11/2016 **Hannes Campo**; Irene Cervelló.
- "Decellularization of rabbit uterus: is it possible to cryopreserve uterine extracellular matrix" Conference: Congreso Nacional Biomedicina Jóvenes Investigadores en Valencia City of event: Valencia, Valencian Community, Spain Dates: 28-29/11/2016 Ximo Garcia Dominguez; **Hannes Campo**; Jose S Vincente; Francisco Marco Jiménez; Irene Cervelló.
- "De- and Recellularization of the Pig Uterus: a Pilot Study in Uterus Bioengineering." Name of the conference: SRI's 63rd Annual Scientific Meeting. City of event: Montreal, Canada. Dates: 16-19/03/2016 Organising entity: Society for Reproductive Investigation (SRI). **Hannes Campo**; Pedro Baptista; Nuria Lopez-Perez; Amparo Faus; Irene cervelló; Carlos Simon.
- "Human endometrial reconstitution using W5C5+, ICAM1+ cells and Side Population cell lines in a xenograft model". Name of the conference: SRI's 65th Annual Scientific Meeting. City of event: Orlando, Florida, Canada. year: 2017 Organising entity: Society for Reproductive Investigation (SRI). Nuria López-Pérez, Claudia Gil-Sanchis, Amparo Faus, Ana Díaz, **Hannes Campo**, Nicolás Garrido, Jose Remohí, Antonio Pellicer, Irene Cervelló and Carlos Simón. -
- "Proof of Concept of Endometrial Somatic Stem Cell Markers" Conference: Congreso Nacional Biomedicina Jóvenes Investigadores en Valencia. City of event: Valencia, Valencian Community, Spain. Dates: 28-29/11/2016. Nuria López-Pérez, Claudia Gil-Sanchis, Amparo Faus, Ana Díaz, **Hannes Campo**, Nicolás Garrido, Jose Remohí, Antonio Pellicer, Irene Cervelló and Carlos Simón. -